5-2015

Role of Ataxia Telangiectasia Mutated Kinase in the Healing Process of the Heart Following Myocardial Infarction

Laura L. Daniel
East Tennessee State University

Role of Ataxia Telangiectasia Mutated Kinase in the Healing Process of the Heart Following Myocardial Infarction

---

A dissertation

presented to

the faculty of the Department of Biomedical Sciences

East Tennessee State University

In partial fulfillment

of the requirements for the degree

Doctor of Philosophy in Biomedical Sciences

---

by

Laura Lynn Daniel

May 2015

Krishna Singh, PhD, Chair

Chuanfu Li, MD

Mahipal Singh, PhD

Phillip Musich, PhD

Tom Ecay, PhD

William Joyner, PhD

Keywords: ATM, heart, fibrosis, myocardial ischemia, remodeling

ABSTRACT

Role of Ataxia Telangiectasia Mutated Kinase in the Healing Process of the Heart Following Myocardial Infarction

by

Laura Lynn Daniel

Ataxia telangiectasia (AT), caused by mutations in the gene encoding ataxia telangiectasia mutated kinase (ATM), is a rare autosomal recessive disorder. AT individuals exhibit neuronal degeneration and are predisposed to cancer. Carriers of this disorder are predisposed to cancer and ischemic heart disease. Heart disease, mostly due to myocardial infarction (MI), is a leading cause of death in the US. Following MI, release of catecholamines in the heart stimulates β-adrenergic receptors (β-AR). Our lab has shown that β-AR stimulation increases ATM expression in the heart and myocytes, and ATM plays an important role in β-AR-stimulated myocardial remodeling with effects on function, fibrosis and apoptosis. Using wild-type (WT) and ATM heterozygous knockout (hKO) mice, this study investigated the role of ATM in the inflammatory, proliferative and maturation phases of infarct healing post-MI. During the inflammatory phase, 1 and 3 days post-MI, a deficiency of ATM resulted in decreased left ventricular dilation as measured by echocardiography. It decreased the number of neutrophils and macrophages in the heart 1 day post-MI. Myocardial fibrosis, expression of alpha-smooth muscle actin (α-sma) and apoptosis were higher in the infarct region of ATM deficient hearts. Akt activation (anti-apoptotic) was lower, while Bax expression (pro-apoptotic) was higher in the infarct region of ATM deficient hearts. During the proliferative phase, 7 days post-MI, ATM

deficiency attenuated cardiac dysfunction as measured by echocardiography. ATM deficient hearts exhibited increased fibrosis and expression of α-sma in the infarct region with increased myocyte apoptosis in the border area. During the maturation phase, 14 and 28 days post-MI, ATM deficiency resulted in exaggerated cardiac function. It associated with increased fibrosis, expression of α-sma and decreased cardiac cell apoptosis in the infarct region 28 days post-MI. Myocyte hypertrophy was greater in the non-infarct region during ATM deficiency. ATM deficiency decreased expression of p16 (marker of cell senescence) and activation of pro-apoptotic protein, GSK-3β. Thus, ATM modulates the remodeling processes of the heart including function, fibrosis, apoptosis and hypertrophy post-MI. ATM (1) delays the inflammatory response post-MI, (2) decreases dilative remodeling during inflammatory and proliferative phases and (3) exaggerates dysfunction during the maturation phase.

DEDICATION

To my loving husband, J. Neal Daniel: words cannot express how much I appreciate the support you have given me through the process of obtaining my degree. You were my strength when I had none left to give. You will always be my Sunshine on sunny and rainy days. Thank you.

To my wonderful parents, Lisa Moody and Rick Moody: Both of you have been great role models growing up. If not for your encouragement throughout the years I don't believe I would be at this point in my life. Thank you.

ACKNOWLEDGEMENTS

To my advisor Dr. Krishna Singh: For being a never ending source of encouragement and support. You have taught me so much about being a good scientist. I will always be grateful to you. It was a pleasure to be a student in your lab. You are a great mentor and I hope that one day I may be as successful a scientist as you are.

To my committee: Drs. Tom Ecay, William Joyner, Chuanfu Li, Phillip Musich and Mahipal Singh. Thank you for all your time and your advice. I am very honored that each of you would serve on my committee. I could not have asked for a better committee.

To my lab members and friends: Dr. Cerrone Foster, it has been my pleasure to work with you and share ideas. I appreciate your help getting me started in the lab and on the project. Sonu, Stephanie and Chris: Thank you all for your friendship and support. I could not have picked better lab mates. Bobbie, thank you for all the work you do to make the lab run smoothly. You take such good care of all of us.

TABLE OF CONTENTS

Page

LIST OF TABLES

LIST OF FIGURES

CHAPTER 1

INTRODUCTION

Heart Disease and Myocardial Infarction

According to the Global Burden of Disease Study 2010, heart disease is one of the leading causes of death worldwide (Lozano et al. 2012). It is currently considered the leading cause of death in the US. An estimated 83.6 million American adults have had at least one type of cardiovascular disease; this includes high blood pressure, myocardial infarction, stroke and heart failure. It is estimated that the direct and indirect (loss of productivity) cost of cardiovascular diseases is in upwards of $300 billion per year. It is projected that by 2030 the costs will rise to over $900 billion (Go et al. 2014). Myocardial infarction (MI) is a large contributor to this burden. In 2006, it was estimated that MI occurs in approximately 865,000 people annually, and is responsible for nearly half of all deaths due to cardiovascular diseases (Turpie 2006).

MI and Cardiac Myocyte Death

Cardiac myocytes are responsible for the contractile function of the heart. MI is an ischemic event that leads to death of cardiac myocytes resulting in a decline in cardiac function (Alpert et al. 2000). Cardiac myocyte death occurs via apoptosis and necrosis (Fliss and Gattinger 1996; James 1998). Myocytes are terminally differentiated and have limited regenerative capacity (Frangogiannis 2008). Following extensive myocyte loss, such as is the case during MI, the remaining myocytes usually aren't adequate enough to maintain cardiac function which leads to cardiac dysfunction and, then, heart failure. Therefore, the extent of

myocyte death can be used as a predictor of heart failure (Olivetti et al. 1997; Nakayama et al. 2007).

Apoptosis is a controlled cell death that can occur in response to irreparable DNA damage. During apoptosis there is chromatin condensation, cellular shrinkage and cellular fragmentation into apoptotic bodies (Ouyang et al. 2012). These apoptotic bodies are surrounded by a plasma membrane in order to prevent the release of the intracellular contents (Krysko et al. 2006). This process minimizes the inflammatory response and damage to the surrounding tissue (Ouyang et al. 2012). Following MI, there is an increase in sympathetic nerve activity caused by an increase in catecholamines (Schömig 1990). Accumulation of catecholamines is suggested as a contributing factor leading to heart failure (Downing and Chen 1985). This is in part due to the fact that catecholamines are shown to induce cardiac myocyte apoptosis, both *in vitro* and *in vivo* (Shizukuda et al. 1998; Colucci et al. 2000; Singh et al. 2001). Specific β_1-adgernergic receptor (β_1-AR) blockers such as metoprolol and non-specific β-AR-blockers such as carvedilol have been shown to decrease myocyte apoptosis (Kawai et al. 2004; Ahmet et al. 2008).

Necrosis was originally thought to be “accidental" cell death that was uncontrolled. Since then, mediators of necrotic death such as receptor-interacting protein kinases (RIP) and poly (ADP ribose) polymerase (PARP) have been discovered and the idea that necrosis is another form of programmed cell death, like apoptosis, has been gaining acceptance. Increased oxidative stress due to MI can induce myocyte necrosis. Necrosis associates with loss of membrane integrity resulting in the intracellular material being released into the extracellular space (Ouyang et al. 2012). Loss of membrane integrity is a result of cellular swelling. On the other hand, apoptosis results in cell shrinkage followed by complete engulfment of the apoptotic cell by phagocytes. The necrotic cellular contents are internalized by a macropinocytotic mechanism.

During this process only parts of the cell are taken up by phagocytes (Krysko et al. 2006). The cellular contents that remain in the extracellular environment are thought to act as "danger signals" and elicit an inflammatory response (Proskuryakov et al. 2003). However, this idea is controversial since studies have shown that exposure of necrotic cells, like apoptotic cells, to macrophages is not sufficient to alter macrophage expression of pro-inflammatory cytokines (Cocco and Ucker 2001; Brouckaert et al. 2004). Necrotic cells, but not apoptotic cells, trigger an increase in the secretion of pro-inflammatory cytokines from independently-activated macrophages (Cocco and Ucker 2001). It is possible that release of cytokines or other factors from necrotic cells also may be critical for the induction of an inflammatory response. Cells that die as a result of necrosis, but not apoptosis, upregulate and secrete the pro-inflammatory cytokine interleukin-6 (IL-6) (Vanden Berghe et al. 2006).

Infarct Healing Post-MI

Since the heart has limited regenerative capacity, the damaged heart is repaired and replaced by a collagen-based scar. The repair process induces structural and functional changes in the infarct as well as non-infarct regions of the heart. This cardiac remodeling process associates with left ventricle (LV) chamber dilation, myocyte hypertrophy and formation of an infarct scar. The infarct healing or reparative process can be divided into these overlapping phases: (a) Inflammatory; (b) Proliferative and (c) Maturation (Frangogiannis 2008).

Inflammatory Phase. Inflammation following MI is activated by a number of pathways. As a result of necrosis, the complement cascade can be activated (Pinckard et al. 1975). This leads to leukocyte recruitment (Hill and Ward 1971). There is also an increase in "damage associated molecular patterns" (DAMPs). DAMPs act as signaling molecules further activating the innate inflammatory response. These signaling molecules can be released by necrotic cells.

Damaged extracellular matrix proteins are also considered to be DAMPs. Other examples of DAMPs include heat shock protein (HSPs), high-mobility group box-1 (HMGB1), low molecular weight hyaluronic acid and fibronectin fragments (Timmers et al. 2012). Activation of the innate immune response via DAMPs is in part due to the activation of toll like receptors (TLR-2 and -4) (Termeer et al. 2002; Jiang et al. 2005).

Following MI, the generation of oxygen-related free radicals exceeds the heart's capacity for removal, resulting in increases in reactive oxygen species (ROS). This increase in ROS can cause impairments in mitochondrial function by increasing lipid peroxidation, enhancing mitochondrial DNA damage as well as inducing inactivation of the electron transport chain (ETC) proteins and antioxidant enzymes (Chen and Zweier 2014). An increase in ROS also can trigger an inflammatory response which is in part due to the fact that oxidative stress activates NF-κB (Kabe et al. 2005). NF-κB is a transcription factor that regulates gene expression involved in the inflammatory response, cell adhesion, growth control and cell death. NF-κB can be activated by a variety of other stimuli including cytokines such as tumor necrosis factor-α (TNF-α) and interleukin-1β (IL-1β) (Stancovski and Baltimore 1997).

During the inflammatory phase, chemokines, cytokines and adhesion molecules are upregulated leading to the recruitment of leukocytes into the wound with neutrophils being among the first (Frangogiannis 2008). The inflammatory phase in humans usually begins 6 hours after infarction and can last up to 4 days (Cleutjens, Blankesteijn, Daemen, & Smits, 1999), whereas, in rodents the inflammatory response last approximately 1-48 hours post-MI (Dobaczewski et al. 2010). The increase in pro-inflammatory cytokines and chemokines results in the activation of endothelial cells thus priming them to "capture" neutrophils. The adherence of neutrophils to the endothelium of post capillary venules is mediated by members of the

selectin family. The L-selectins of neutrophils bind to P and/or E selectin in the endothelials. This attachment triggers activation of integrins via a G protein-coupled receptor (GPCR). The integrin responsible for this attachment is β2-integrin which is expressed exclusively on cells of leukocyte origin. β2-integrins can attach to intercellular adhesion molecules (ICAM-1) expressed in the endothelium. This results in a transition from leukocyte rolling (via selectins) to firm adhesion. Following this, leukocytes transmigrate into the infarct region through interactions that involve a wide variety of adherent molecules including platelet endothelial cell adhesion molecule (PECAM)-1, ICAM-1, vascular-endothelial (VE)-cadherin and members of the junctional adhesion molecule (JAM) family. This occurs both at endothelial cell junctions and at non-junctional locations (Williams et al. 2011).

Following neutrophil recruitment, there is an infiltration of monocytes and lymphocytes into the wound. Monocytes eventually differentiate into macrophages in part due to the upregulation of macrophage-colony stimulating factor (MCSF). MCSF appears to be important for the survival of macrophages since its upregulation associates with macrophage proliferation (Frangogiannis et al. 2003). Macrophages appear in the infarcted heart two days post-MI to aid in clearing the wound of dead cells, including neutrophils, and matrix debris (Matsui et al. 2010). They release anti-inflammatory cytokines and growth factors which aid in formation of highly-vascularized granulation tissue. In addition, the release of cytokines and growth factors results in the suppression of pro-inflammatory mediators and the proliferation of fibroblasts and endothelial cells. Macrophages also aid in wound repair by secreting matrix metalloproteinases (MMPs) as well as their inhibitors (Frangogiannis 2008).

The extracellular matrix (ECM) is an important structural component of the myocardium with the majority of structural integrity coming from type I and III fibrillar collagen. The ECM

provides support for myocytes and blood vessels, helps maintain cardiac shape, and aids in coordinating the delivery of force that is generated by myocytes to the ventricular chamber. The ECM is an important determinate of diastolic and systolic myocardial stiffness. Alterations in ECM organization can result in changes to cardiac function (Weber 1989). MMPs are proteins that can degrade the ECM. Following MI, there is an initial increase in ECM degradation. Type I collagen fragments can be found in the serum of pigs 15-30 minutes after coronary artery occlusion (Villarreal et al. 2004). The initial increase in cardiac ECM degradation comes from activation of latent MMPs as opposed to production of new MMPs (Etoh et al. 2001). Increased degradation of the ECM post-MI is thought to be responsible for myocyte slippage, sarcomere overdistension, wall thinning and cardiac rupture following MI (Cleutjens, Kandala, et al. 1995). Following degradation of the original matrix, there is a formation of fibrin-based provisional matrix. This provisional matrix can serve as a scaffold for the migration and proliferation of inflammatory cells, endothelial cells and fibroblasts. However, this provisional matrix is lysed by proteolytic enzymes that are produced by granulation tissue cells as the wound heals. A cell-derived matrix containing cellular fibronectin and hyaluronan replaces the provisional matrix. Cellular fibronectin is secreted by fibroblasts and macrophages (Dobaczewski et al. 2010).

Proliferative Phase. Following the inflammatory phase of wound healing is the proliferative phase. During this phase, there is a suppression of the inflammatory response by "stop signals" such as IL-10 and transforming growth factor (TGF)-β1 as well as an increase in proliferation of myofibroblasts and endothelial cells. In rodents, the proliferative phase begins approximately 48 hours post-MI and lasts up to 5 days post-MI (Dobaczewski et al. 2010). In higher mammals, the proliferative phase begins 7 days post-MI and can last up to 14 days post-MI (Cleutjens et al. 1999; Virag and Murry 2003).

Myofibroblasts are not generally found in the healthy heart. However, they are present in the infarct region following MI and play an important role in wound healing. Myofibroblasts aid in wound closure and are the main source of collagen production during infarct healing (Cleutjens, Verluyten, et al. 1995). Myofibroblasts isolated from infarct regions exhibit a higher rate of proliferation and collagen synthesis when compared to fibroblasts isolated from non-infarct regions or sham operated hearts. Interestingly, the myofibroblasts exhibited a decrease in migration that was attributed to increased adhesion to some the ECM proteins (Squires et al. 2005). Myofibroblasts can come from a variety of sources such as epithelial cells, endothelial cells, mesenchymal stem cells, bone marrow-derived circulating progenitor cells, smooth muscle cells and pericytes (Turner and Porter 2013). Resident fibroblasts are transformed into myofibroblasts in a two-step process. During the first step, fibroblasts respond to increased mechanical tension and transform into proto-myofibroblasts which are characterized by the formation of stress fibers containing β- and γ-cytoplasmic actins. During the second step, the proto-myofibroblasts are exposed to additional signals such as active TGF-β and ED-A (a splice variant of cellular fibronectin) resulting in their conversion into myofibroblasts (Serini et al. 1998; Hinz et al. 2001; Tomasek et al. 2002). Normally TGF-β requires proteolytic cleavage to become active, but it has been shown that mechanical strain can result in TGF-β activation in the absence of protease activity (Buscemi et al. 2011). Once the proto-myofibroblast express α-sma they are referred to as myofibroblasts. The acquisition of α-sma is thought to aid in the contraction of the heart following injury (Dobaczewski et al. 2010).

Following MI, there is an increase in collagen production with type I and type III procollagen increasing several fold in the infarct region. Type III procollagen mRNA levels have been shown to increase in the infarct region as early as 2 days post-MI and can remain elevated

for up to 21 days post-MI, while type I procollagen increased in the infarct region 4 days post-MI and remained elevated up to 90 days post-MI. While most of the increases in collagen production occur in the infarct region, there can also be an increase in collagen production in the non-infarct region of the right ventricle as well as the non-infarcted septum. However, the increase in collagen production in the non-infarct region is less than that seen in the infarcted LV region. When examining the phenotype of the cells responsible for collagen production, it appears that the collagen being produced in the infarcted region comes from myofibroblasts, while the collagen produced in the non-infarcted region originates from non-transformed fibroblasts (Cleutjens, Verluyten, et al. 1995).

Part of the wound healing process is the formation of a new vasculature. Fibroblasts move into the wound in order to create a matrix necessary for structural support. There is also growth of new blood vessels, in the infarct region, which provides the area with oxygen and nutrients (Tonnesen et al. 2000). Angiogenesis is a process in which new microvessels are formed from pre-existing capillaries. Endothelial cells become activated in response to a variety of signals such as hypoxia, growth factors and nitric oxide. Once activated, the endothelial cells begin to proliferate forming a new vessel lumen which is later covered by mural cells to ensure neovessel stability (Cochain et al. 2013).

Maturation Phase. In humans, the maturation phase usually begins 2-3 weeks post-MI and can last for several months (Cleutjens et al. 1999). While, in rodents the maturation phase occurs from approximately day 14 until 2 months post-MI (Dobaczewski et al. 2010). During the maturation phase of healing, fibroblasts and vascular cells undergo apoptosis (Frangogiannis 2008). Cross-linking of the collagen matrix is carried out by enzymes such as lysyl-oxidase which imparts tensile strength to the matrix (Eyre 1980). However, cross-linking also leads to

increases in passive stiffness resulting in diastolic dysfunction (Kato et al. 1995; Badenhorst et al. 2003).

During the maturation phase, there is a decrease in myofibroblast density in the newly-formed scar. In humans, myofibroblasts can persist for years. The reduction in myofibroblasts is thought to occur as a combination of myofibroblast senescence and apoptosis. (Turner and Porter 2013). While short-term inhibition of myofibroblast apoptosis may be beneficial early post-MI, the persistence presence of myofibroblasts usually results in excessive scaring leading to ventricular wall stiffening and cardiac dysfunction (Brown et al. 2005).

Ataxia Telangiectasia.

Ataxia telangiectasia (AT) is a rare autosomal recessive disorder caused by mutations in the gene encoding for ataxia telangiectasia mutated kinase (ATM). It affects approximately 1:40,000 – 1:300,000 children (Sandoval et al. 1999). Although, mutations in the ATM gene that result in AT are varied and do not occur at a particular location within the gene, the mutations generally lead to protein instability and lack of a functional protein (McKinnon 2004). On the other hand, some mutations result in decreased amounts of the functional protein or cause a decrease in its kinase activity. These mutations result in a less severe phenotype than do the mutations that cause the complete absence of a functional protein (Stewart et al. 2001). The most notable sign of AT is loss of cerebella function, progressive dysarthria and choreoathetosis (McKinnon 2004). MRI scans show that there is cerebellar atrophy with involvement of the vermis (Farina et al. 1994; Tavani et al. 2003). Affected individuals usually have ataxia of the limbs at a very early age resulting from neuronal degeneration causing them to be wheelchair bound prior to adolescence. As AT individuals age, there is an increased risk of aspiration (Lefton-Greif et al. 2000). These individuals also suffer from thymic degeneration, immune

deficiency, retarded somatic growth, premature aging, telangiectasia of the eyes and skin, gonadal dysgenesis and sensitivity to ionizing radiation (Rotman 1998). The immunodeficiencies usually present in the form of decreased Ig subtypes and lymphopenia. Upper and lower respiratory tract infections are frequent, although it should be pointed out that systemic bacterial, severe viral and opportunistic infections are rare (Nowak-Wegrzyn et al. 2004). There is also a cancer predisposition that usually presents in the form of leukemia or lymphoma (Gumy-Pause et al. 2004).

Carriers of a mutated *Atm* allele make up approximately 1.4-2.0% of the general population. One functional copy of the gene coding for ATM is able to compensate to a large extent for the missing gene; however, individuals with only one copy do exhibit some abnormalities. Carriers of a mutated allele have a significantly increased risk of death when compared to non-carriers. On average, these individuals die 7 to 8 years earlier than non-carriers with cancer being the predominant cause followed by ischemic heart disease as the second major cause of death resulting in premature death approximately 11 years earlier than the non-carriers (Su and Swift 2000). Carriers also exhibit increased susceptibility to metabolic diseases such as hypertension, diabetes and impaired glucose metabolism (Stracker et al. 2013).

ATM, DNA repair and oxidative stress

ATM is a large serine-threonine protein kinase with a molecular weight of approximately 350 kDa. It contains 66 exons and its mRNA length is approximately 12 kb. The most widely known cellular function of ATM is to aid the in repair of DNA double-stranded breaks (DSB). These breaks can occur as a result of meiosis, immune system maturation, and telomere maintenance (McKinnon 2004). Following DSB, ATM initiates the repair process beginning with autophosphorylation, which results in ATM activation (Bakkenist and Kastan 2003).

Inactive ATM exists as a dimer. ATM autophosphorylates several residues following DNA damage, including S367, S1893, S1981 and S2996, which results in its activation. This activation of ATM is MRN complex (MRE11–RAD50–NBS1) dependent, and results in ATM becoming a monomer and beginning its kinase activity (Bakkenist and Kastan 2003; Kozlov et al. 2006; Kozlov et al. 2011). In response to DNA damage, activation of ATM can induce cell cycle arrest during G1/S, G2/M, and S phases in order to prevent replication of the damaged DNA. (Rotman 1998). ATM can activate and stabilize p53, a regulator of the G1/S checkpoint and in some cases is an initiator of apoptosis. ATM accomplishes this not only by directly phosphorylating p53, but also by phosphorylating Chk2 kinase and Mdm2. Chk2 phosphorylates p53 at a site different from ATM also resulting in its activation. Phosphorylation of Mdm2, on the other hand, inhibits Mdm2 from signaling for the degradation of p53 (Barzilai et al. 2002). ATM can also phosphorylate BRCA1, resulting in cell cycle arrest at intra-S-phase and G2-M check points. Besides phosphorylating cell cycle arrest proteins, ATM also phosphorylates a variety of proteins that result in DNA repair. Among them are proteins in the MRN complex. Following DNA damage the MRN complex rapidly forms foci at the site of DNA damage in order to repair the damaged DNA (Rotman 1998). The MRN complex is the primary sensor of DSB and ATM's recruitment to this complex appears necessary for full activation of ATM (Berkovich et al. 2007).

While ATM does take part in DNA repair, there is a built-in redundancy within the cell. DNA-dependent protein kinases (DNA-PKs) also respond to DSB. In fact, ATM responds to only approximately 10% of DSB, most of which are in regions of heterochromatin. ATM and DNA-PK redundancy may explain the fact the global DSB repair capability of ATM deficient cells is only partially attenuated (Goodarzi et al. 2008). However, AT patients still have a

hypersensitivity to radiation and are predisposed to cancer. While there are no gross abnormalities in either recombination or V(D)J rearrangements, AT individuals are often immunocompromised (Lavin et al. 2007).

ATM is predominantly located in the nucleus and is activated in response to DNA damage. However, ATM also has a presence and function in the cytoplasm that is unrelated to DNA damage (Shiloh and Ziv 2013). ATM that is activated in response to oxidative stress can exist as a dimer and is MRN independent (Guo et al. 2010). ATM may play a part in redox balance by regulation of an important antioxidant cofactor, NADH. ATM is shown to enhance the pentose phosphate pathway (PPP), a major source of NADH, in response to genotoxic stress. This is accomplished by inducing glucose-6-phosphate dehydrogenase (G6PD) activity, the rate limiting enzyme in the PPP (Cosentino et al. 2011). Increasing autophagy also provides a protective mechanism against ROS. ATM can enhance autophagy by phosphorylating tuberous sclerosis complex 2 (TSC2), a negative regulator of mammalian target of rapamycin (mTORC1), which removes the repression of autophagy by mTORC1 (Shiloh and Ziv 2013).

Lack of ATM is suggested to result in increased levels of ROS and signs of oxidative stress. ATM knockout (KO) mice have differing levels of activity of thioredoxin, catalase and manganese superoxide dismutase (SOD). Alterations in these compounds are thought to keep neurons at an increased state of oxidative stress causing the neuronal degeneration seen in AT patients (Kamsler et al. 2001). The increased levels of ROS in the brain appear to be located in the cerebellum and striatum, but not in the cortex (Quick and Dugan 2001). In addition to AT cells having increased levels of ROS, fibroblast isolated from AT patients have increased susceptibility to oxidative stress when compared with fibroblasts from non-affected individuals (Yi et al. 1990; Ward et al. 1994). Mitochondria are major sites of ROS production (Cadenas

and Davies 2000). ATM KO mice exhibit mitochondrial dysfunction in thymocytes; there is an increase in mitochondrial size as well as mitochondrial ROS production. The increase in mitochondria size is thought to be due to a decrease in mitochondrial mitophagy as opposed to an increase in mitochondrial biogenesis (Valentin-Vega et al. 2012).

ATM and the heart

As discussed previously, increases in sympathetic nerve activity are a major factor post-MI. Increases in sympathetic activity result in an accumulation of catecholamines, such as norepinephrine, in the interstitial space. Stimulation of β-AR in response to norepinephrine induces cardiac myocyte apoptosis *in vivo* and *in vitro* (Shizukuda et al. 1998; Colucci et al. 2000; Singh et al. 2001). A major project in our lab investigates the molecular signals involved in cardiac myocyte apoptosis in response to β-AR stimulation. To identify differential expression of apoptosis-related genes in response to β-AR stimulation our lab used a Gene-Array technique. For this, mice were infused with isoproterenol (a β-AR agonist) for 7 days. Total RNA, isolated from the LV, was reverse-transcribed and radio-labeled. The resultant cDNAs, from vehicle-infused and isoproterenol-infused heart, were simultaneously hybridized with two Gene-Array membranes containing 96 apoptosis-related genes. This analysis revealed increased expression of ATM in the hearts in response to β-AR stimulation. RT-PCR confirmed increased expression of ATM in the heart and in adult cardiac myocytes (Foster et al. 2011). To investigate the role of ATM in myocyte apoptosis and myocardial remodeling, our lab used ATM heterozygous knockout (hKO) mice. Homozygous knockout (KO) mice are infertile and they die around the age of 2 months due to thymic lymphomas. Therefore, we breed hKO mice which provides us with KO mice. We found that at basal levels body weights (BW) and heart weights (HW) are lower in KO mice when compared to the age-matched wild-type (WT) mice. However, there

was no difference in HW/BW ratio, an indicating no cardiac hypertrophy. KO mice also exhibited increased myocardial fibrosis and myocyte hypertrophy. Measurement of structural and functional parameters of the heart using echocardiography showed that while the KO hearts did not display differences in percent fractional shortening (%FS) or ejection fraction (EF) they did have reduced septal wall thickness and LV cavity diameter. Expression of fibrosis-related genes (connective tissue growth factor, CTGF; plasminogen activator inhibitor, PAI-1; and MMP-2) and hypertrophy-related genes (atrial natriuretic peptide, ANP) were higher in KO hearts. Using WT and ATM KO mice, we examined the role of ATM in cardiac remodeling following 24 hours of β-AR stimulation using isoproterenol. β-AR stimulation resulted in an increase in myocyte size in both genotypes with no significant differences between the two genotypes. Apoptosis was increased in both genotypes following β-AR stimulation, with no differences in apoptosis between the two genotypes. Interestingly, β-AR stimulation resulted in distinct differences in the activation of apoptosis-related proteins, when comparing the two genotypes. Phosphorylation of p53 and activation of JNKs were absent in KO hearts, but present in WT hearts. In addition, Akt activation was also lower in KO hearts when compared to WT hearts. These results led us to suggest that β-AR-stimulated apoptosis in the WT hearts was a result of p53- and JNKs-dependent mechanisms, while decreased Akt activity appears to play a role in increased myocyte apoptosis in the absence of ATM (Foster et al. 2012).

Using WT and hKO mice our lab also examined the effects of ATM deficiency in cardiac myocyte apoptosis and cardiac remodeling following 28 days of β-AR stimulation. In this study, β-AR stimulation increased the functional parameters of the heart as analyzed by increased %FS and EF; however, the increase in %FS and EF was blunted in ATM deficient hearts. β-AR stimulation resulted in a significant increase in fibrosis as well as apoptosis in both groups

although the increase in fibrosis and myocyte apoptosis was higher in ATM deficient hearts. β-AR stimulation increased phosphorylation of p53 and expression of p53 and Bax to a similar extent in both groups; however, there was a differential expression of fibrosis-related proteins; e.g. MMPs, TIMP-2, and β1- integrins. These studies suggested a protective role for ATM in myocardial remodeling following β-AR stimulation (Foster et al. 2011).

Specific Aims

The overall goal of this project was to understand the role of ATM in cardiac myocyte apoptosis and myocardial remodeling following MI. Based on the observations in our β-AR stimulation model, we hypothesized that ATM deficiency would affect cardiac remodeling following MI, specifically with regard to apoptosis, fibrosis and function, early and late post-MI. As discussed previously, the myocardial remodeling (infarct healing) process can be divided into three overlapping phases: inflammatory, proliferative and maturation. The overall goal of this project was to examine how ATM deficiency affects each stage of the infarct healing process. The specific aims of this study were: (1) investigate how ATM deficiency affects cardiac remodeling during the inflammatory phase using 1 and 3 days post-MI time points; (2) examine how ATM deficiency alters cardiac remodeling during the proliferative phase of infarct healing using a 7 day post-MI time point and (3) determine how ATM deficiency alters the maturation phase of the infarct healing using a 28 days post-MI time point.

.

CHAPTER 2

DEFICIENCY OF ATAXIA TELANGIECTASI MUTATED KINASE DELAYS INFLAMMATORY RESPONSE IN THE HEART FOLLOWING MYOCARDIAL INFARCTION

Laura L. Daniel, B.S[1]; Christopher R. Daniels, B.S.[1]; Saghar Harirforoosh[1], Cerrone R. Foster[1,2], Ph.D.; Mahipal Singh, Ph.D.[1] and Krishna Singh, Ph.D.[1,3]*

[1]Department of Biomedical Sciences, James H Quillen College of Medicine
[2]Department of Biological Sciences
[3]James H Quillen Veterans Affairs Medical Center
East Tennessee State University
Johnson City, TN 37614

Running title: ATM and myocardial infarction

Total number of figures: 10

Number of Tables: 2

*__Correspondence__: Krishna Singh, Ph.D.
Department of Biomedical Sciences
James H Quillen College of Medicine
East Tennessee State University
PO Box 70582, Johnson City, TN 37614
Ph: 423-439-2049
Fax: 423-439-2052
E-mail: singhk@etsu.edu

Abstract

Background: Ataxia-telangiectasia results from mutations in Ataxia Telangiectasia Mutated Kinase (ATM) gene. We recently reported that ATM deficiency attenuates left ventricular (LV) dysfunction and dilatation 7 days after myocardial infarction (MI) with increased apoptosis and fibrosis. Here we investigated the role of ATM in the induction of inflammatory response, and activation of survival signaling molecules in the heart acute post-MI. **Methods and Results:** LV structure, function, inflammatory response and biochemical parameters were measured in wild-type (WT) and ATM heterozygous knockout (hKO) mice 1 and 3 days post-MI. ATM deficiency had no effect on infarct size. MI-induced decline in heart function, as measured by changes in % fractional shortening, ejection fraction and LV end systolic and diastolic volumes, was lower in hKO-MI versus WT-MI (n=10-12). The number of neutrophils and macrophages was significantly lower in the infarct LV region of hKO versus WT 1 day post-MI. Fibrosis and expression of α-smooth muscle actin (myofibroblast marker) were higher in hKO-MI, while active TGF-β1 levels were higher in the WT-MI 3 days post-MI. Myocyte cross-sectional area was higher in hKO-sham with no difference between the two MI groups. MMP-9 protein levels were similarly increased in the infarct LV region of both MI groups. Apoptosis was significantly higher in the infarct LV region of hKO at both time points. Akt activation was lower, while Bax expression was higher in hKO-MI infarct. **Conclusion:** ATM deficiency results in decreased dilative remodeling and delays inflammatory response acute post-MI. However, it associates with increased fibrosis and apoptosis.

Keywords: ATM, apoptosis, cardiac remodeling, fibrosis, myocardial infarction, inflammation

Introduction

Ataxia–telangiectasia (A-T) is a rare autosomal recessive genetic disorder that causes neurological degeneration. It is caused by mutations in the gene encoding for ataxia telangiectasia mutated kinase (ATM) [1]. This disease affects approximately 1 in 40,000 births in the US [2]. A-T individuals are predisposed to the development of cancer, usually lymphoid cancer. In addition, these individuals suffer from immunological problems resulting in frequent sino-pulmonary infections [2]. Both humoral and cell-mediated immunity are affected, the later showing itself in the form of lymphopenia [3]. Individuals that are recessive for this mutation usually die 7 to 8 years earlier than non-carrier as a result of either cancer or ischemic heart disease [4].

ATM, a ~370 kDa protein kinase, is a member of the phosphatidylinositol 3-kinase-like protein kinase (PIKK) family. Genotoxic stress, oxidative stress and growth factors affect ATM gene expression in various cell types [5;6]. ATM is activated in response to DNA double-strand breaks caused by ionizing radiation and V(D)J recombination in B and T lymphocyte development [3]. It is also shown to be activated in cells exposed to hypoxia, insulin, and reactive oxygen species independent of DNA damage. ATM activation affects cell cycle check points, apoptotic signaling, senescence, and DNA repair [7].

Myocardial infarction (MI) induces cardiac cell death due to apoptosis and necrosis, thereby initiating the inflammatory process. Neutrophils are the first inflammatory cells recruited to the infarct area [8]. Infiltration of neutrophils occurs within hours and peaks 1-3 days post-MI [9]. Neutrophils facilitate the post-MI repair process by phagocytosing dead cells and tissue debris [8]. During the inflammatory process cytokines such as TNF-α, IL-1β, and IL-6 are induced [10;11]. Neutrophils then undergo apoptosis generating annexin A1 and lactoferrin which inhibits

neutrophil recruitment and attracts phagocytic macrophages to remove neutrophils. Once the macrophages have engulfed the neutrophils, they activate the anti-inflammatory pathway by producing molecules such as IL-10 and TGF-β marking the end of the inflammatory phase of infarct healing and the beginning of the proliferative phase of healing [12]. During the proliferative phase, activated fibroblast (myofibroblast) produce extracellular matrix proteins aiding in the scar formation [8]. Our previous work examined the role of ATM in myocardial remodeling post-MI during the proliferative phase of infarct healing. We reported that ATM deficiency attenuates LV dysfunction and dilatation 7 days post-MI. In addition, we provided evidence that ATM deficiency results in increased cardiac fibrosis and expression of α-smooth muscle actin (α-SMA, a marker for myofibroblasts) in the infarct region 7 days post-MI [13]. The objective of this study was to investigate the role of ATM deficiency in cardiac remodeling during the inflammatory phase of infarct healing. A major finding of this study is that deficiency of ATM associates with decreased inflammatory response and dilative remodeling early post-MI without affecting infarct size. ATM deficiency also affects apoptosis, fibrosis, expression of proteins involved in fibrosis and inflammation, and activation of apoptosis-related kinases.

Methods

Vertebrate Animals

This investigation conforms to the *Guide for the Care and Use of Laboratory Animals* published by the US National Institutes of Health (NIH Publication No. 85-23, revised 1996). All of the experiments were performed in accordance with the protocols approved by the East Tennessee State University Animal Care and Use Committee. ATM transgenic mice (129xblack Swiss hybrid background) were purchased from Jackson Laboratory. Aged-matched (~4 month old) male and female mice were used for the study. The study used heterozygous knockout (hKO) mice since homozygous knockout (KO) mice die at ~2 months of age mainly due to thymic lymphomas [14]. Genotyping was performed by PCR using primers suggested by the Jackson Laboratory.

Myocardial infarction

Myocardial infarction (MI) was performed as previously described [13]. Briefly, mice were anesthetized using a mixture of isoflurane (2%) and oxygen (0.5 l/min), and maintained under anesthesia using isoflurane (1%) and oxygen (0.5 l/min). The mice were ventilated using a rodent ventilator. Body temperature was maintained at ~37^{0}C using a heating pad. Heart was exposed by a left thoracotomy followed by the ligation of left anterior descending artery (LAD) using 7-0 polypropylene suture. Mice in the sham group underwent the same procedure without the ligation of LAD. At the end of the study period, 1 or 3 days post-MI, isolated hearts were used for either histology or for molecular analyses.

Echocardiography

Transthoracic two-dimensional m-mode echocardiography was performed using a Toshiba Aplio 80 Imaging System (Tochigi, Japan) equipped with a 12 MHz linear transducer as previously described [15]. An individual blinded to the experimental groups recorded the cardiac structural parameters. A second individual read the recordings and calculated the functional parameters of the heart.

Morphometric analyses

Following MI, hearts were removed and arrested in diastole using KCl (30 mmol/L). After fixing with 10% buffered formalin, hearts were cut into 3 transverse sections (base, mid-LV and apex) and embedded in paraffin. Cross-sections (4μm think) were stained using Masson's Trichrome stain in order to determine infarct size 3 days post-MI. Infarct size was calculated as the percentage of LV circumference occupied by infarct scar [13]. Infarct size 1 day post-MI was calculated using TTC stained hearts as previously described [16]. Masson's Trichrome stained sections were also used to quantify percent fibrosis.

Myocyte cross-sectional area

To measure myocyte cross-sectional area, cross-sections (4μm thick) of the heart were stained with FITC-labeled wheat germ agglutinin (WGA). The sections were visualized using fluorescent microscopy (20X; Nikon) and images were recorded using Retiga 1300 color-cooled camera. Suitable area of the section was defined as the one with nearly circular capillary profiles and nuclei. Myocyte cross-sectional areas were measured using Bioquant Image analysis software (Nashville, TN) as described [15].

Terminal deoxynucleotidyl transferase nick end labeling (TUNEL staining) assay

TUNEL staining was carried out according to manufacturer's instruction (Cell death detection assay; Roche) [13]. Sections were counterstained with Hoechst 33258 (Sigma) to identify nuclei. The index of apoptosis was calculated as the percentage of apoptotic nuclei/total number of nuclei.

Immunohistochemistry

Cross-sections of the heart (4μm thick) were deparaffinized and immunostained for neutrophils and macrophages using anti-neutrophil (1:100, Santa Cruz) and anti-F4/80 (macrophage; 1:200; Santa Cruz) antibodies, respectively. Detection was performed using ABC staining system (Santa Cruz). Sections were counterstained with 1% eosin. Expression of α-SMA serves as a marker for the differentiation of fibroblasts into myofibroblasts [17]. To examine expression of α-SMA, heart sections were immunostained using anti-α-SMA antibodies (Sigma) as described [13]. Images were acquired using Nikon TE-2000 microscope equipped with a Regita-1300 color-cooled camera. Quantitative analysis was carried using Bioquant Image analysis software (Nashville, TN). At least five different images within the infarct area from each heart were used for quantitative purposes. Images acquired from the septal wall represented non-infarct LV region. Images from the sham group were acquired from various regions around the LV.

Western blot analyses

LV lysates were prepared in RIPA buffer, separated by SDS-PAGE and transferred to PVDF membranes. The membranes were blocked using either 5% non-fat dry milk or 5% BSA in TBST. The membranes were then incubated overnight with antibodies against ATM, TGF-β, Bax (Santa Cruz), MMP-9 (Millipore), Bcl-2, p-Akt (ser-473) or p-GSK-3β (ser-9) (Cell

Signaling). GAPDH (Santa Cruz) immunostaining or Ponceau-S staining was used as protein loading control. Band intensities were quantified using Kodak photo documentation system (Eastman Kodak Co.).

MMP activity

Gelatin in-gel zymography was used to determine activity of MMP-9 as previously described [18]. Clear digested bands were quantified using Kodak photo documentation system (Eastman Kodak Co.).

Statistical analyses

Data are presented as mean ± SEM: Shapiro-Wilk test was used to assess the normality of the data. One-way analysis of variance (ANOVA) or Kruskal-Wallis was used for multiple comparisons. Pairwise comparisons were carried out using either student's t-test or Mann-Whitney U test (two-sample). When comparing BW before and after surgery, a two-tailed paired t-test was used. Survival between the two genotypes was analyzed using Kaplan-Meier survival analysis. Probability (p) values of <0.05 were considered to be significant.

Results

ATM expression in the heart post-MI

To investigate expression of ATM in the heart post-MI, left ventricular (LV) lysates were prepared from the infarct and non-infarct LV regions of WT and hKO 1 and 3 days post-MI. LV lysate prepared from ATM KO heart served as a negative control. Western blot analysis using anti-ATM antibodies showed complete absence of ATM protein (~370 kDa) in the LV lysate prepared from the KO heart (Fig 2.1A; lane 1). A faint signal for ATM was observed in WT-sham sample (data not shown). However, clear signal for ATM protein was observed in the non-infarct and infarct LV regions of WT and hKO hearts 1 and 3 days post-MI (Fig 2.1A & B). ATM protein levels were higher in the infarct LV regions when compared to the non-infarct LV regions. Overall, ATM protein levels were lower (~50%) in non-infarct and infarct LV regions of hKO when compared to the WT counterparts.

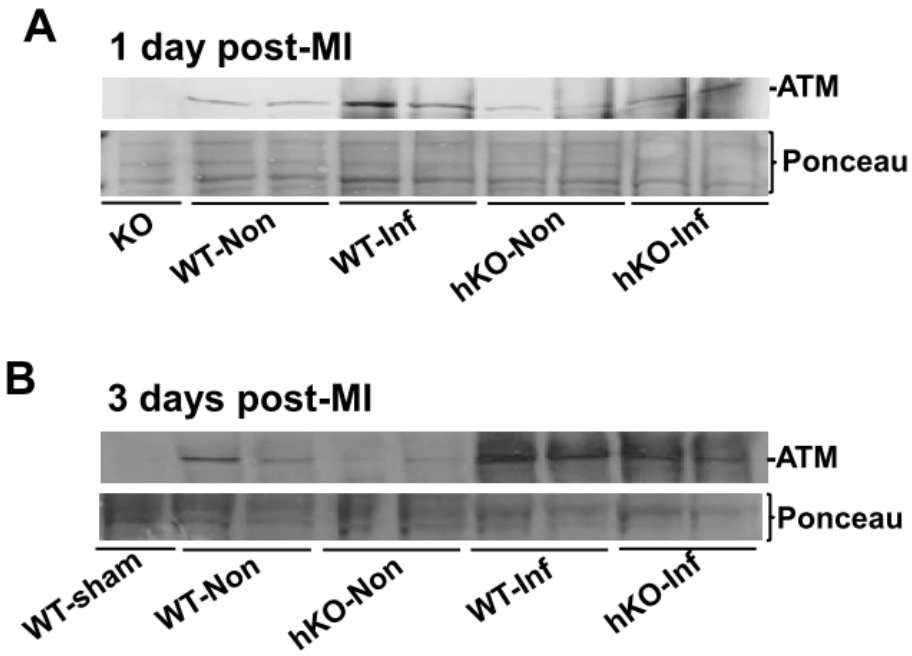

Figure 2.1. MI increases ATM expression in the heart. LV lysates prepared from WT-sham, ATM KO, and non-infarct (Non) and infarct (Inf) LV regions of WT and hKO 1 and 3 days post-MI were analyzed by western blot using anti-ATM antibodies. A. 1 day post-MI; B. 3 days post-MI. Protein loading is indicated by Ponceau-S staining.

Morphological analyses

No significant difference in morphometric parameters was observed between 1 and 3 day sham groups; therefore, 1 and 3 day sham groups were pooled. Surgery (sham or MI) significantly decreased body weights (BW) when compared to the pre-surgery BW with no significant differences between the two genotypes. MI increased heart weights (HW) 3 days post-MI in both genotypes with no significant difference between the two genotypes. HW/BW ratios were significantly higher 1 and 3 days post-MI when compared to their respective sham with no significant differences between the two genotypes (Table 2.1). Infarct sizes between the two genotypes were not different at either 1 day or 3 days post-MI (Table 2.2). The survival rate for both genotypes 1 day post-MI was 100%, while it was 98.4% for WT and 86.2% for hKO 3 days post-MI with no significant difference between the two groups.

Table 2.1. Morphometric Measurements 1 and 3 Days Post-MI

		Pre-BW	BW	HW	HW/BW
Sham	WT (n=11)	26.87 ± 0.82	23.96 ± 1.11$^{@}$	124.46 ± 4.02	4.73 ± 0.11
	hKO (n=11)	26.49 ± 0.68	22.78 ± 0.77$^{@}$	121.03 ± 4.78	4.96 ± 0.21
1 Day post-MI	WT-MI (n=17)	28.38 ± 1.04	24.21 ± 1.06$^{@}$	135.53 ± 6.98	5.17 ± 0.23$^{\#}$
	hKO-MI (n=11)	26.5 ± 1.07	24.69 ± 2.43 $^{@}$	134.01 ± 5.12	5.61 ± 0.14$^{\#}$
3 Days post-MI	WT-MI (n=15)	24.93 ± 0.89	22.28 ± 0.80$^{@}$	143.90 ± 4.91$^{\#}$	6.43 ± 0.24$^{\#}$
	hKO-MI (n=20)	25.39 ± 0.68	23.07 ± 0.61$^{@}$	140.17 ± 7.51$^{\#}$	6.07 ± 0.27$^{\#}$

Values are mean ± SEM. $^{@}p<0.001$ vs pre-BW; $^{\#}p<0.05$ vs Sham; BW, body weight; HW, heart weight

Table 2.2. Infarct size and Myocyte Cross-sectional Area

		Percent infarct	Cross sectional area (mm^2)
Sham	WT (n=8)	NA	185.06 ± 5.08
	hKO (n=7-8)	NA	203.72 ± 6.64*
1 Day Post-MI	WT-MI (n=4-7)	32.64 ± 4.07	213.23 ± 9.0$^{\#}$
	hKO-MI (n=4-6)	35.13 ± 6.08	203.92 ± 6.19
3 Days Post-MI	WT-MI (n=5-6)	50.41± 2.41	211.36 ± 7.29$^{\#}$
	hKO-MI (n=5-7)	51.09 ± 5.78	204.50 ± 8.19

Values are mean ± SEM. $^{\#}p<0.05$ vs Sham, *$p<0.05$ vs WT-Sham

Echocardiographic studies

Figure 2.2A exhibits M-mode echocardiography images obtained from sham and MI (1 day post-MI) groups. No significant difference in echocardiographic parameters was observed between 1 and 3 day sham groups. Therefore, 1 and 3 day sham groups were pooled. A significant decrease ($p<0.05$) in heart function, as evidenced by a decrease in percent fractional shortening (%FS) and ejection fraction (EF), was observed at 1 and 3 day post-MI in both genotypes when compared to

their respective sham groups. However, the decrease in %FS and EF was significantly lower in hKO-MI versus WT-MI 1 day post-MI. No significant differences in %FS and EF were observed between the two genotypes 3 days post-MI (Fig 2.2B and 2.2C). Increased LV end-systolic volume (LVESV) is considered as a predictor of mortality post-MI [19]. WT-MI group exhibited a significant increase in LVESV and LV end-diastolic volume (LVEDV) 1 and 3 days post-MI when compared to WT-sham. In hKO-MI, a significant increase in LVESV and LVEDV was observed 1 day, not 3 days, post-MI when compared to hKO-sham. Interestingly, LVESV and LVEDV were significantly higher in WT-MI versus hKO-MI at both time points (Fig 2.2D and 2.2E).

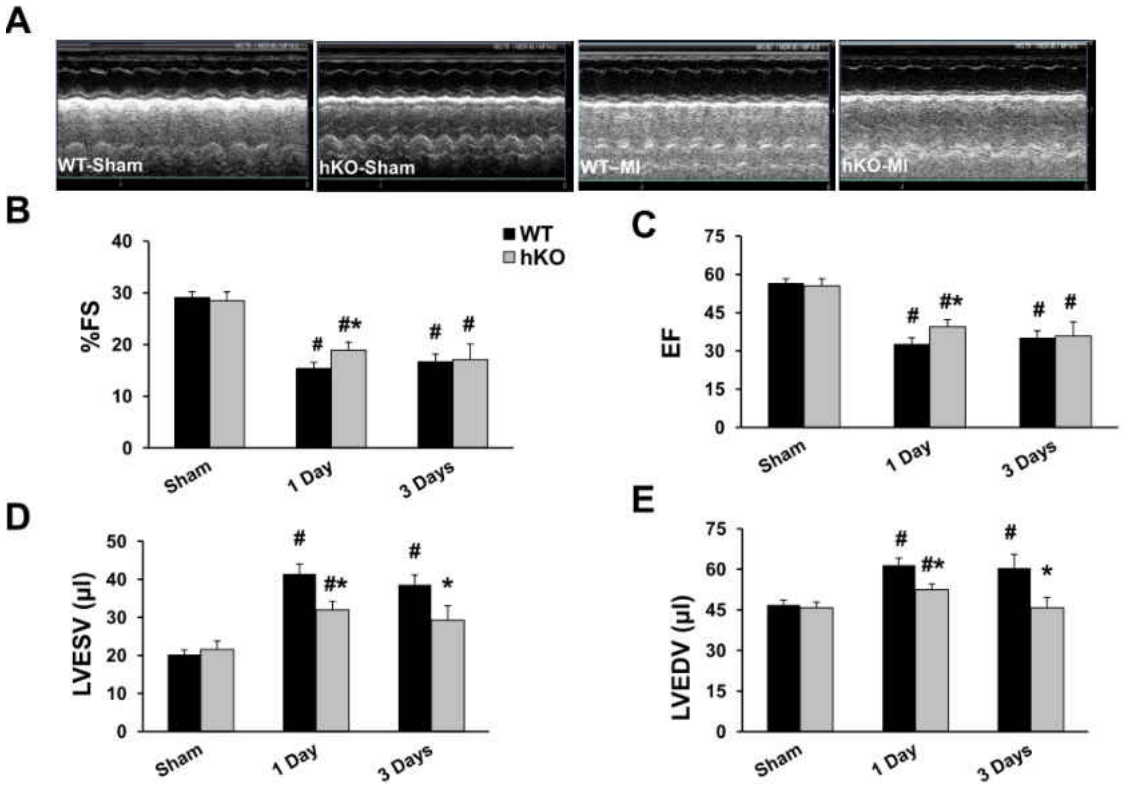

Figure 2.2. ATM deficiency improves LV function. MI was performed in WT and hKO mice. Panel A shows M-mode echocardiographic images obtained from sham and 1 day post-MI groups. Indices of cardiac function (percent fractional shortening, %FS; ejection fraction, EF) and volume (LV end systolic volume, LVESV; LV end diastolic volume, LVEDV) were calculated using echocardiographic images 1 and 3 days post-MI. $^{\#}p<0.005$ vs Sham, $^{*}p<0.05$ vs WT-MI; n= 10-12.

Inflammatory cell infiltration

Sham groups exhibited the presence of only a few neutrophils in the heart with no significant difference between the two genotypes. MI increased the number of neutrophils in the infarct LV regions of both genotypes at both time points when compared to their respective sham groups (Fig 2.3A and B). A significant increase in neutrophil number was also observed in the non-infarct LV region of WT group 1 day post-MI versus WT-sham (Fig 2.3A). Interestingly, the number of neutrophils was significantly lower in the infarct and non-infarct LV regions of hKO-MI when compared to WT-MI 1 day post-MI (Fig 2.3A). The number of neutrophils in the infarct LV region decreased significantly in both MI groups 3 days post-MI. However, the number stayed higher in the infarct LV regions when compared to the sham groups and non-infarct LV regions in both genotypes. There was no significant difference in the number of neutrophils between the two genotypes 3 days post-MI, although the number of neutrophils in the non-infarct LV region of hKO-MI was significantly higher when compared to hKO-sham (Fig 2.3B).

Sham groups exhibited the presence of a few macrophages in the heart with no significant difference between the two genotypes. MI increased the number of macrophages in the infarct and non-infarct LV regions of both genotypes when compared to their respective sham groups. However, the number of macrophages was significantly lower ($p<0.05$) in the infarct LV region of hKO-MI versus WT-MI 1 day post-MI (Fig 2.3C). Three days post-MI, the number of macrophages was still higher in the infarct LV regions of both genotypes when compared to their respective sham groups, however, there was no significant difference between the two genotypes. In addition, the number of macrophages in the non-infarct LV region of hKO-MI was significantly higher when compared to hKO-sham (Fig 2.3D).

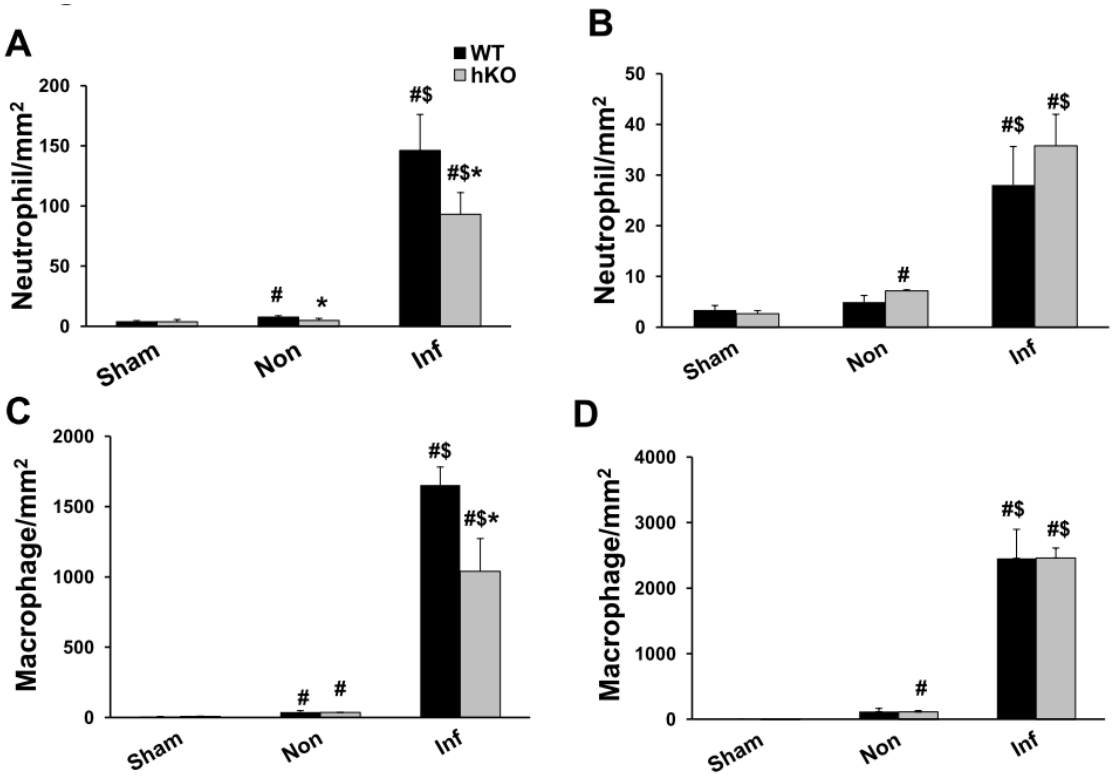

Figure 2.3. ATM deficiency results in decreased inflammatory cells in the infarct LV region 1 day post-MI. Cross-sections of the heart post-MI were immunostained using anti-neutrophil (A&B) and anti-F4/80 (macrophage; C&D) antibodies. The number of immune-positive cells was quantified using Bioquant Image analysis software. Quantitative analyses of neutrophils 1 (A) and 3 (B) days post-MI. Quantitative analyses of macrophages 1 (C) and 3 (D) days post-MI. $^{\#}p<0.05$ vs Sham, $^{\$}p<0.05$ vs Non, $^{*}p<0.05$ vs WT; n=4-6.

Fibrosis, apoptosis, and myocyte cross-sectional area

Quantitative analysis of fibrosis using Masson's Trichrome-stained sections revealed no change in fibrosis between 1 and 3 day sham groups, therefore the sham groups were pooled. The amount of fibrosis was significantly higher in hKO-sham versus WT-sham. MI increased fibrosis in the infarct LV region of both groups 3 days post-MI. However, the amount of fibrosis was significantly higher in hKO-MI versus WT-MI (Fig 2.4).

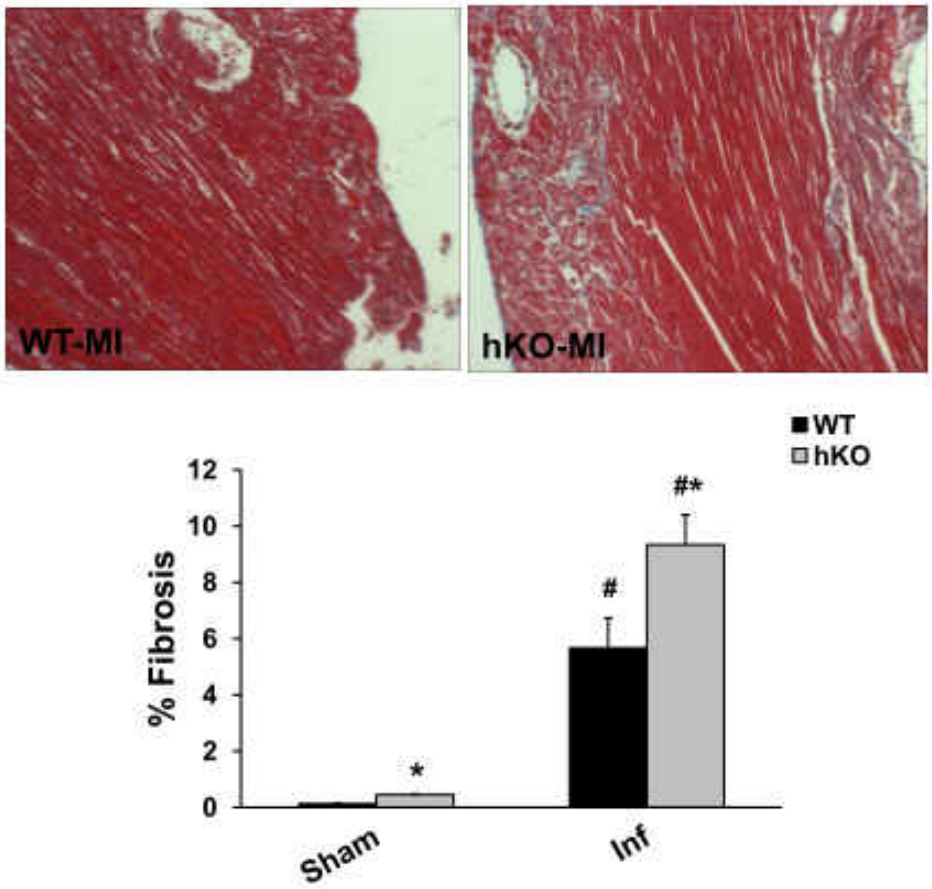

Figure 2.4. ATM deficiency results in increased fibrosis. Masson's trichrome stained sections of the heart were used for quantitative measurement of fibrosis. Upper panel depicts Masson's trichrome-stained sections exhibiting fibrosis in WT and hKO hearts 3 days post-MI. Lower panel exhibits quantitative analysis of fibrosis. $^{\#}p<0.05$ vs Sham, *$p<0.05$ vs WT-MI; n=5-6.

Only a few apoptotic cells were detected in the sham and non-infarct LV regions of WT-MI and hKO-MI 1 day post-MI. MI significantly increased the number of apoptotic cells in the infarct LV region of both genotypes 1 day post-MI (Fig 2.5A). However, the number of apoptotic cells was significantly greater in the hKO-MI ($p<0.05$) versus WT-MI. Three days post-MI, the level of apoptosis in the infarct LV regions decreased in both genotypes versus 1 day post-MI. However, it remained higher when compared to their respective sham groups and non-infarct LV regions (Fig 2.5B). Interestingly, hKO-MI continued to have significantly higher number of apoptotic cells ($p<0.05$) in the infarct LV region versus WT-MI. hKO-MI also

exhibited a significant increase ($p<0.05$) in apoptosis in the non-infarct LV region when compared to hKO-sham and non-infarct WT-MI.

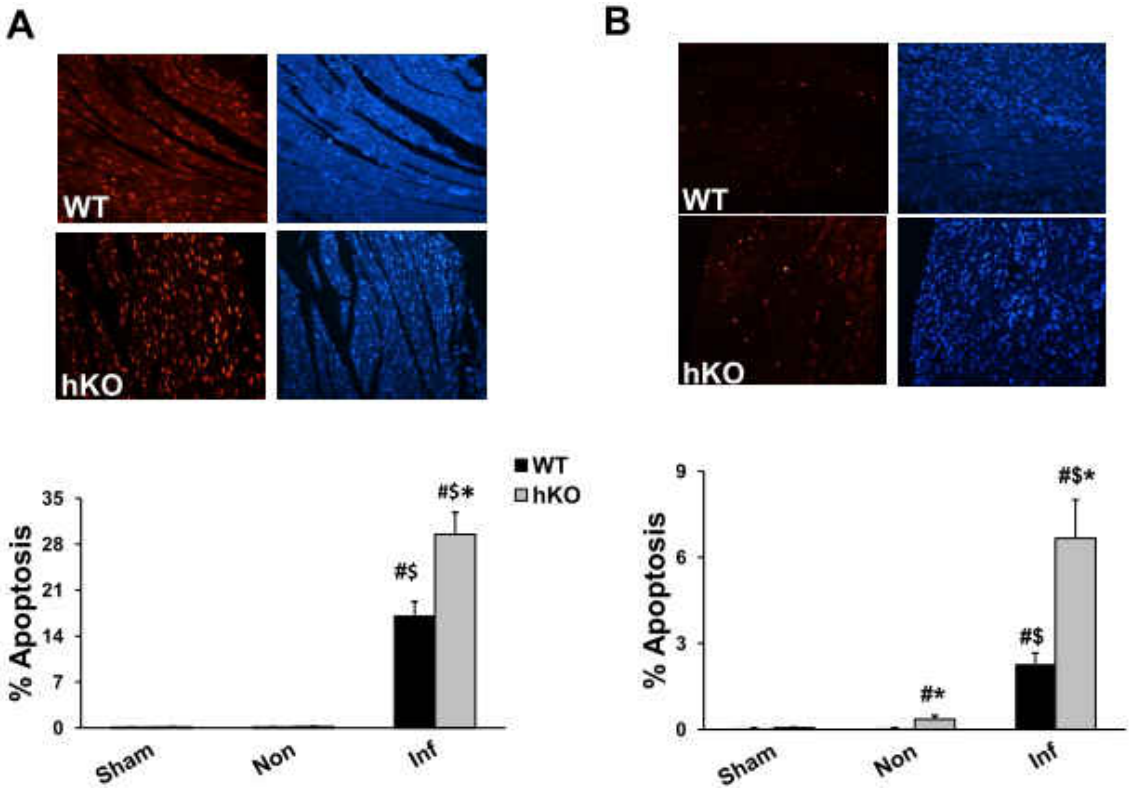

Figure 2.5. ATM deficiency results in enhanced apoptosis post-MI. Quantitative analysis of cardiac cell apoptosis in the non-infarct (Non) and infarct (Inf) LV regions 1 (A) and 3 (B) days post-MI. Upper panels depict TUNEL-stained and Hoechst-stained images obtained from WT and hKO hearts 1 and 3 days post-MI. Red fluorescent staining indicates TUNEL-positive (apoptotic) nuclei, while blue fluorescent staining indicates total number of nuclei. The lower panels exhibit quantitative analysis. $^{\#}p<0.05$ vs Sham *$p<0.05$ vs WT, $^{\$}p<0.05$ vs Non; n=4-6.

Myocyte cross-sectional area was significantly higher in hKO-sham group versus WT-sham. Myocyte cross-sectional area in the non-infarct LV region remained unchanged in the hKO-MI group 1 and 3 days post-MI. However, a significant increase in myocyte cross-sectional area was observed in WT-MI group when compared to WT-sham 1 and 3 days post-MI (Table 2.2).

Expression of TGF-β1

The anti-inflammatory cytokine TGF-β1 plays an important role in myocardial remodeling post-MI via its involvement in the differentiation of fibroblasts into myofibroblasts and ECM deposition [8]. One source of TGF-β1 is macrophages as they phagocytose apoptotic neutrophils [12]. Western blot analysis showed no presence of active TGF-β1 protein (23 kDa band) in the sham groups, non-infarct or infarct LV regions 1 day post-MI (data not shown). Presence of active TGF-β1 band was only observed in the infarct LV regions of both genotypes 3 days post-MI. However, the levels of active TGF-β1 were significantly higher in the WT-MI versus hKO-MI (Fig 2.6).

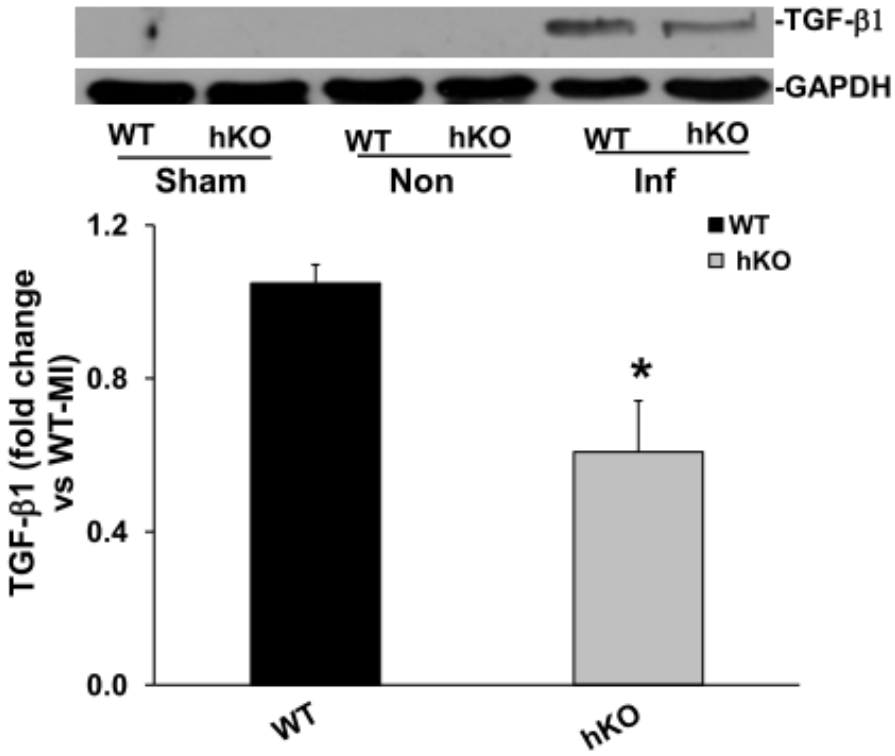

Figure 2.6. Expression of TGF-β1. Total LV lysates, prepared from sham and non-infarct (Non) and infarct (Inf) LV regions 3 days post-MI, were analyzed by western blot using anti-TGF-β1 antibodies. The upper panel depicts autoradiogram indicating immunostaining for active TGF-β1 (~26 kDa band) and GAPDH. The lower panel exhibits quantitative analysis of TGF- β1 in the Inf LV regions of WT and hKO groups normalized to GAPDH. *p<0.05 vs WT-Inf; n=8-9.

Expression of α-smooth muscle actin (α-SMA)

Increased α-SMA expression is considered as a marker for the differentiation of fibroblasts into myofibroblast [20]. One day post-MI, little to no expression of α-SMA expression was observed in the infarct LV regions of either group (data not shown). Three days post-MI, a significant increase in α-SMA expression was observed in the infarct LV region of both genotypes when compared to their respective sham groups. However, the increase in α-SMA expression was significantly higher ($p<0.05$) in hKO-MI versus WT-MI (Fig 2.7).

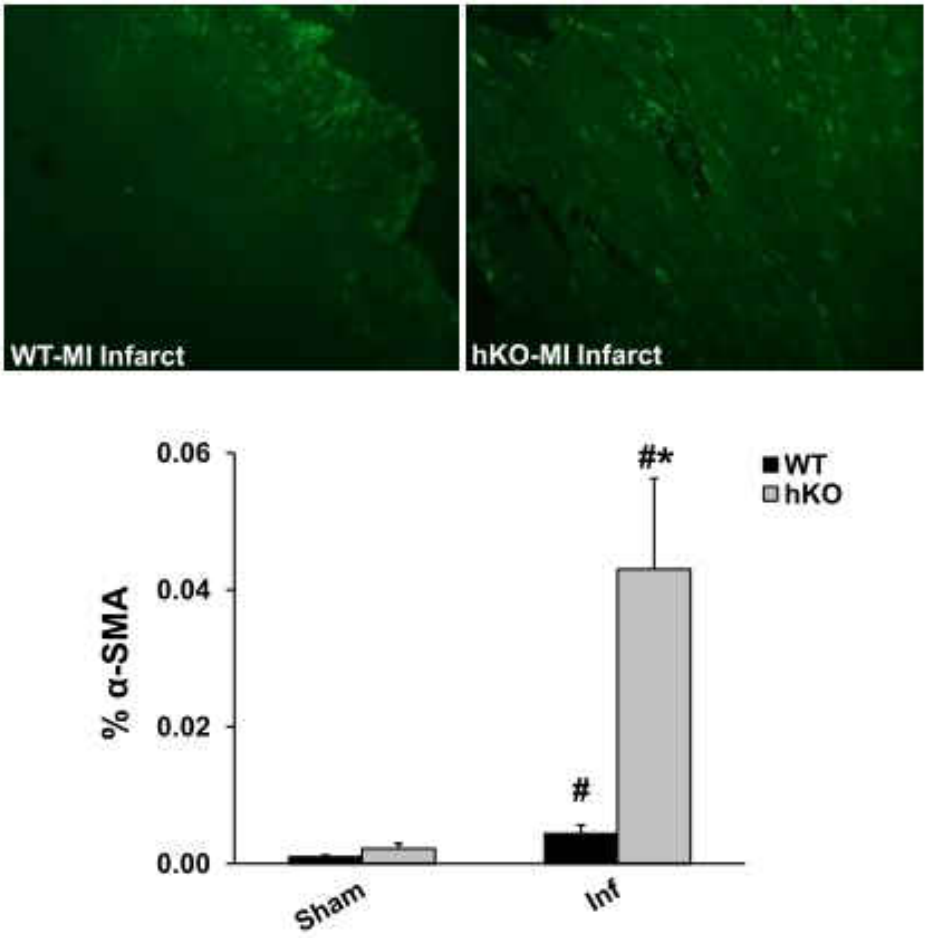

Figure 2.7. Quantitative analysis of α-smooth muscle actin (α-SMA) expression. Cross-sections of the heart were immunostained using anti-α-SMA antibodies. Upper panel depicts α-SMA-stained images from the infarct (Inf) LV regions of WT and hKO hearts 3 days post-MI. Lower panel exhibits quantitative immunocytochemical analysis of α-SMA in sham and Inf LV regions 3 days post-MI. $^{\#}p<0.05$ vs Sham, $*p<0.05$ vs WT-Inf; n=4-5.

Expression and activity of MMP-9

MMP-9 regulates the remodeling processes of the heart that involves inflammation and fibrosis [21]. MMP-9 levels in the ischemic region of the heart increase within minutes after MI and stay higher during the first few days in animal models [21;22]. Western blot analysis revealed increased MMP-9 protein levels in the infarct LV regions of both genotypes 1 day post-MI when compared to their respective sham groups. However, no significant differences were observed between the two genotypes (Fig 2.8A). MMP-9 expression remained higher in the infarct LV regions of both genotypes 3 days post-MI with no significant difference between the two genotypes (Fig 2.8B). In-gel zymography revealed increased MMP-9 activity in the infarct LV regions of both genotypes (data not shown).

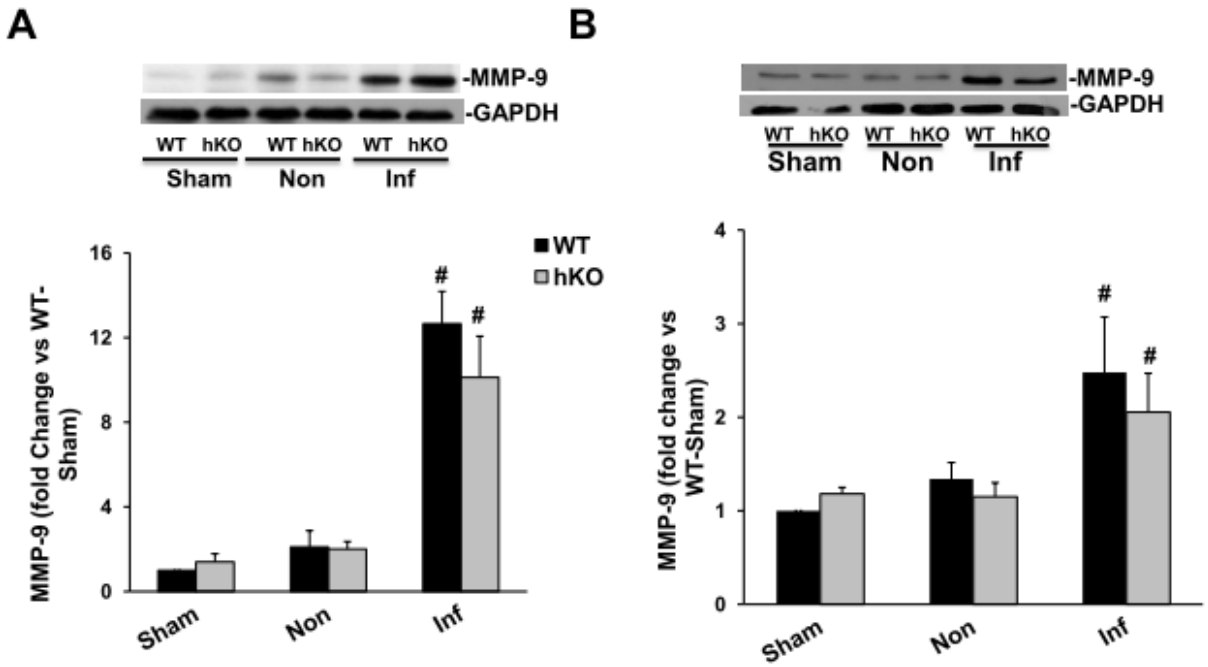

Figure 2.8. Expression of MMP-9. Total LV lysates, prepared from sham, non-infarct (Non) and infarct (Inf) LV regions 1 and 3 day post-MI, were analyzed by western blot using anti-MMP-9 antibodies. The upper panels depict autoradiograms indicating immunostaining for MMP-9 and GAPDH. The lower panels exhibit quantitative analyses of MMP-9 normalized to GAPDH. A. MMP-9 protein levels 1 day post-MI (n=6). B. MMP-9 protein levels 3 days post-MI (n=5) $^{\#}p<0.05$ vs sham.

Activation and expression of apoptosis-related proteins

Increased phosphorylation (activation) of Akt is generally considered as an anti-apoptotic signal [23]. Phosphorylation of Akt remained unchanged in the WT-MI 1 day post-MI. However, Akt phosphorylation was significantly lower in the non-infarct and infarct LV regions of hKO-MI versus hKO-sham. In addition, Akt phosphorylation was significantly lower in the hKO-MI infarct LV region versus WT-MI infarct LV region (Fig 2.9A). No significant change in Akt phosphorylation was observed among the groups 3 days post-MI (data not shown).

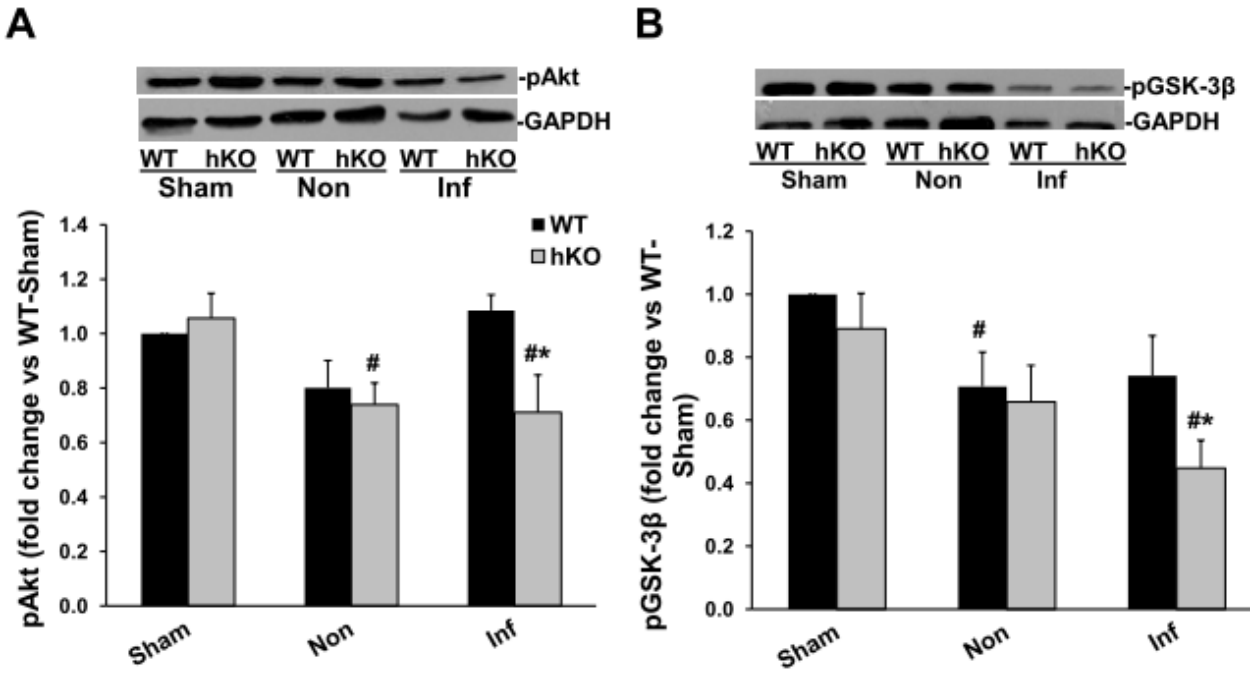

Figure 2.9. Phosphorylation of Akt and GSK-3β. Total LV lysates, prepared from sham, non-infarct (Non) and infarct (Inf) LV regions 1 day post-MI, were analyzed by western blot using phospho-specific antibodies for Akt (ser-473) and GSK-3β (ser-9). The upper panels depict autoradiograms indicating immunostaining for p-Akt, p-GSK-3β and GAPDH. The lower panels exhibit quantitative analyses of p-Akt (A) and p-GSK-3β (B) normalized to GAPDH. $^{\#}p<0.05$ vs Sham; *$p<0.05$ vs WT-Inf; n=6.

Activation of GSK-3β plays a pro-apoptotic role in β-adrenergic receptor-stimulated apoptosis [24]. Phosphorylation of N-terminal serine-9 inactivates GSK-3β [25]. GSK-3β phosphorylation (serine-9) was lower in the non-infarct LV region of WT-MI versus WT-sham 1 day post-MI. In the infarct LV region, hKO-MI exhibited a significant decrease in GSK-3β phosphorylation when compared to hKO-sham and WT-MI infarct LV region (Fig 2.9B). Three days post-MI, GSK-3β phosphorylation was significantly lower ($p<0.05$) in infarct and non-infarct region of both WT and hKO mice when compared to their respective sham groups with no significant difference between the two MI groups (data not shown).

Bax, a pro-apoptotic protein, is a transmembrane protein located in the outer mitochondrial membrane. Homodimerization of Bax increases cytochrome c release resulting in the induction of apoptosis. Bcl-2 can inhibit Bax induced apoptosis by forming a heterodimer with Bax [26]. Western blot analyses showed no difference in Bax or Bcl-2 protein levels between the two genotypes in the infarct LV regions 1 day post-MI (data not shown). Bax expression was significantly higher in the infarct LV region of hKO when compared to WT group 3 days post-MI. However, there was no significant difference in Bcl2 expression between the two genotypes 3 days post-MI (Fig 2.10).

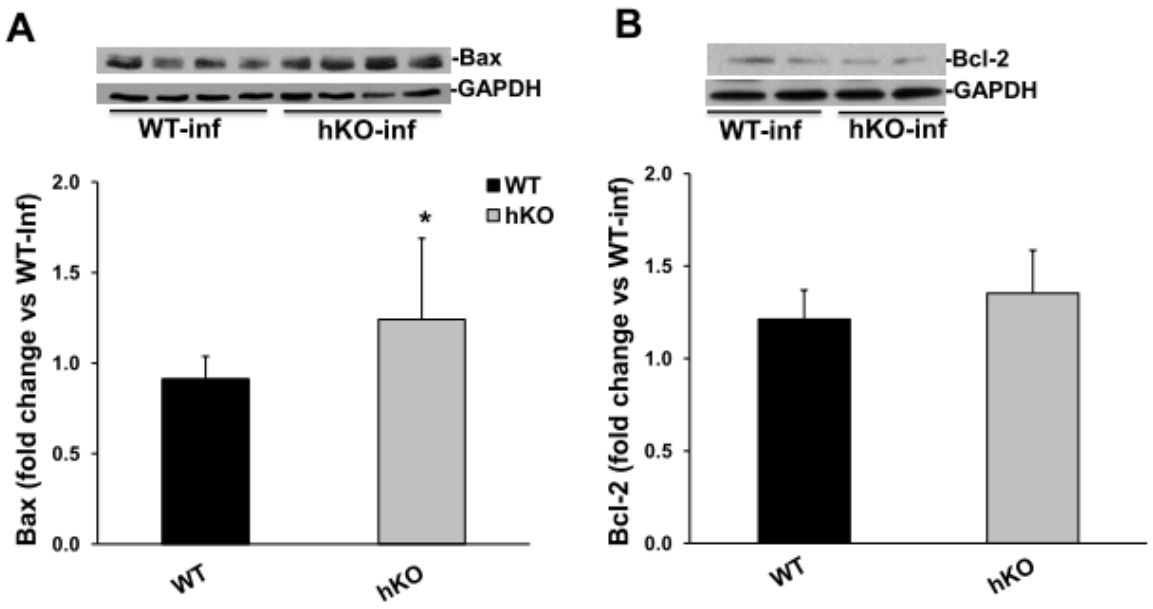

Figure 2.10. Expression of Bax and Bcl-2. Total LV lysates, prepared from infarct LV regions 3 days post-MI, were analyzed by western blot using anti-Bax and anti-Bcl-2 antibodies. The upper panels depict autoradiograms indicating immunostaining for Bax (A), Bcl-2 (B) and GAPDH. The lower panels exhibit quantitative analyses of Bax (A) and Bcl-2 (B) normalized to GAPDH. *$p<0.05$ vs WT-MI; n=6-8.

Discussion

Previously we provided evidence that ATM deficiency results in improved heart function and decreased LV dilatation 7 days post-MI. A major finding of this study is that ATM deficiency associates with delayed inflammatory response post-MI. This is evidenced by the decreased number of neutrophils and macrophages 1 day post-MI, and decreased expression of TGF-β1 in the infarct area 3 days post-MI. ATM deficiency also associated with increased apoptosis, fibrosis and expression of α-SMA in the heart post-MI. Activation of pro-survival kinase, Akt, was lower, while activation of pro-apoptotic kinase, GSK-3β, was higher in ATM deficient hearts 1 day post-MI. The data presented here support our previous findings [13], and suggest multifaceted role of ATM in myocardial remodeling post-MI.

ATM normally becomes activated in response to DNA damage, particularly due to the formation of DNA double-strand breaks. This activation occurs due to its autophosphorylation on Ser1981 [27]. Genotoxic agents, oxidative stress and growth factors also increase ATM expression in certain cell types [5;6]. In peripheral blood mononuclear cells, maximum increase in ATM expression in response to mitogenic stimuli was observed 3-4 days after exposure [6]. Previously, we have shown that β-AR stimulation increases ATM expression in adult rat ventricular myocytes and heart [28]. This study provides evidence that MI increases ATM expression in the heart. The increase in ATM could be a result of either increased sympathetic nerve activity and/or increased oxidative stress, both of which increase in the heart following MI [29;30].

MI usually leads to increased chamber diameter which results in increased loading capacity of the heart represented by increased LVESV and LVEDV. Increased LVESV is suggested as one of the major determinants of survival post-MI [19]. Previously, we provided

evidence that deficiency of ATM attenuates LV dysfunction and dilatation 7 days post-MI [13]. The data presented here suggest that the attenuation of LV dysfunction and dilation during ATM deficiency can be observed as early as 1 day post-MI. ATM deficient mice exhibit a lesser degree of impairment in systolic parameters as evidenced by higher %FS and EF 1 day post-MI. It was interesting to note that %FS and EF were not different between the two genotypes 3 days post-MI, although LVESV and LVEDV were significantly lower in ATM deficient hearts at both time points. The better LV function 1 day post-MI during ATM deficiency did not correlate with infarct size since infarct sizes remained unchanged between the two genotypes 1 and 3 days post-MI. Other factors such as infarct thickness, myocardial fibrosis, and myocyte hypertrophy also influence heart function post-MI [31]. ATM deficient hearts exhibited increased infarct thickness, increased fibrosis and increased α-SMA expression 7 days post-MI [13]. While increased levels of fibrosis late post-MI is a predictor of heart failure, early fibrosis may play a protective role in the healing process by preventing infarct expansion [32]. Infarct thickness remained unchanged between the two genotypes 1 and 3 days post-MI. Expression of α-SMA was higher in ATM deficient hearts 3 days post-MI. Therefore, slightly better function exhibited by ATM deficient hearts 1 day post-MI cannot be explained by infarct thickness or expression of α-SMA. ATM deficiency associates with increased myocyte cross-sectional area and fibrosis at basal levels, and results in delayed inflammatory response post-MI. Therefore, myocyte hypertrophy, myocardial fibrosis and delayed inflammatory response may help explain better function during ATM deficiency 1 day post-MI.

Neutrophils begin to infiltrate into the infarcted myocardium within hours of the ischemic event peaking 24 hours post-MI [9]. Neutrophil infiltration activates resident monocytes to differentiate into macrophage in the infarct LV region shortly after MI. Macrophage number

stays relatively stable from 1 - 7 days post-MI [12]. Macrophages play a number of roles in post-MI healing process. They phagocytose dead cells, tissue debris and apoptotic neutrophils. In addition, they secret MMPs and their inhibitors to aid in extracellular matrix reorganization [12]. Consistent with these data, we observed increased number of neutrophils and macrophages in the myocardium of both genotypes at both time points. Interestingly, the number of inflammatory cells was significantly lower in ATM deficient hearts 1 day post-MI. Three days post-MI, the number of neutrophils decreased, while the number of macrophages increased in the infarct LV regions of both genotypes. However, the number of neutrophils and macrophages was not significantly different between the two genotypes. These data suggest a delayed inflammatory response during ATM deficiency early post-MI. Neutrophils are recruited to the site of inflammation via chemokines and cytokines [8]. However, signals such as lactoferrin and annexin 1 released by apoptotic cells can inhibit recruitment of neutrophils to the site of the injury [33;34]. ATM deficient hearts exhibit increased apoptotic response when compared with their WT counterparts. This increase in apoptosis during ATM deficiency can have an inhibitory effect on neutrophil migration. A decrease in inflammatory receptors (selectins, integrins and adhesion receptors) may also influence neutrophil recruitment [35]. Further investigations are required to investigate the involvement of these molecular signals in the inflammatory response in the heart post-MI during ATM deficiency.

Phagocytosis of neutrophils by macrophages initiates the release of anti-inflammatory signal involved in resolution of inflammation [12]. Suppression of inflammatory response may involve a variety of signals, including a secreted protein TGF-β. TGF-β1, an anti-inflammatory signal, can affect infarct healing by modulating the release of cytokines and chemokines, synthesis of ECM proteins and transdifferentiation of fibroblasts into myofibroblasts [36]. In rat MI

model, increased expression of TGF-β1 mRNA was observed 3 days post-MI [37]. Here we observed increased levels of active TGF-β1 in the heart 3 days post-MI. ATM deficiency associated with decreased macrophage count 1 day post-MI and decreased active TGF-β1 levels 3 days post-MI. This is consistent with the fact that macrophages are a major producer of TGF-β post-MI [8]. It is interesting to note that ATM deficiency also associates with increased expression of α-SMA and fibrosis 3 days post-MI. While TGF-β is a known activator of fibroblast differentiation, TGF-β alone does not trigger fibroblast differentiation. Myofibroblast transformation also requires specialized ECM proteins like the ED-A splice variant of fibronectin as well as increased mechanical stress. Under normal conditions, fibroblasts are protected against mechanical stress via cross-linkage of the ECM. During injury, the ECM begins remodeling itself leading to the activation of myofibroblast [38]. Therefore, it is possible that the enhanced apoptosis in the heart during ATM deficiency increases mechanical stress leading to enhanced myofibroblast activation.

Extracellular matrix (ECM) plays a critical role in the restructuring of the heart post-MI. Changes in MMP abundance and activity is shown to be associated with changes in ECM deposition and myocardial remodeling post-MI [21]. MMP-9 levels increase in the heart within minutes and remain elevated during the first few days post-MI [22;39]. Previously, we have shown that ATM deficiency associates with higher MMP-9 protein levels and activity in the infarct LV region 7 days post-MI when compared to WT [13]. Neutrophils are identified as a source of MMP-9 during acute ischemia/reperfusion myocardial injury [40]. This expression of MMP-9 was suggested to aid in the migration of neutrophils. Here, we observed increased MMP-9 protein levels in both genotypes at both time points. However, MMP-9 protein levels were not different between the two MI groups. Furthermore, reduced neutrophil numbers did not result in reduced

MMP-9 expression during ATM deficiency, suggesting other cell types of the heart post-MI may participate in MMP-9 expression [21]. Of note, neutrophils isolated from MMP-9 null mice show no defect in transendothelial migration under flow in vitro [41].

The extent of cardiac myocyte death is a major determinant of myocardial remodeling post-MI. Myocyte death can occur due to necrosis and apoptosis in the ischemic zone. During the inflammatory phase, infiltrated neutrophils also die due to apoptosis as part of the healing process [36]. Cardiac cell apoptosis was significantly higher in ATM deficient hearts 1 and 3 days post-MI. Although not investigated, this number most likely includes apoptotic neutrophils and macrophages. Mitochondria play a crucial role in determination of cell fate with respect to cell survival and apoptosis [42]. Bcl2 family proteins, Bcl2 and Bax, modulate mitochondrial membrane potential and activation of caspases [26]. ATM deficiency resulted in enhanced expression of Bax in the infarct LV region. Although there was no change in Bcl2 expression, the increase in Bax may induce loss of mitochondrial membrane potential and apoptosis. The increase in apoptotic cells during ATM deficiency also associated with decreased activation of anti-apoptotic kinase, Akt and enhanced activation of pro-apoptotic kinase, GSK-3β 1 day post-MI. In fact, Akt exerts its anti-apoptotic effect, in part, through inactivation of GSK-3β [43]. Previously, we have shown decreased activation of Akt in the myocardium of mice lacking ATM in response to β-AR stimulation [15]. However, β-AR stimulation had no effect on GSK-3β activation during ATM deficiency. Collectively, these data suggest activation of Akt, via ATM, as a common signaling event during myocardial stress. Activation of GSK-3β appears to be modulated differentially in response to different myocardial stress during ATM deficiency.

In summary, ATM deficiency results in improved heart function as determined by a decrease in dilative remodeling and inflammatory response acute post-MI. However, it also associates with negative remodeling as determined by increased apoptosis and decreased activation of anti-apoptotic kinase, Akt. In addition, ATM deficiency results in an increase in fibrosis and expression of α-SMA. These studies, together with our previous findings [13], suggest that ATM has the potential to modulate the remodeling processes of the heart post-MI. Further investigations are needed to define the long-term impact of ATM deficiency in the healing processes of the heart post-MI.

Funding

This work was supported by a Merit Review award (number BX000640) from the Biomedical Laboratory Research and Development Service of the Veterans Affairs Office of Research and Development, grants from The National Heart, Lung, and Blood Institute (Grant numbers R21HL-091405 and R21HL-092459), and funds from Institutional Research and Improvement account (KS).

Acknowledgement

Technical help received from Barbara A. Connelly is appreciated.

Conflict of Interest/Disclosure: None

References

1. Taylor AM, Byrd PJ. Molecular pathology of ataxia telangiectasia. J. Clin. Pathol. 2005;58:1009-15.

2. Chun HH, Gatti RA. Ataxia-telangiectasia, an evolving phenotype. DNA Repair (Amst) 2004;3:1187-96.

3. Nowak-Wegrzyn A, Crawford TO, Winkelstein JA, Carson KA, Lederman HM. Immunodeficiency and infections in ataxia-telangiectasia. J. Pediatr. 2004;144:505-11.

4. Su Y, Swift M. Mortality rates among carriers of ataxia-telangiectasia mutant alleles. Ann. Intern. Med. 2000;133:770-78.

5. Fang ZM, Lee CS, Sarris M, Kearsley JH, Murrell D, Lavin MF *et al.* Rapid radiation-induction of ATM protein levels in situ. Pathology 2001;33:30-36.

6. Fukao T, Kaneko H, Birrell G, Gatei M, Tashita H, Yoshida T *et al.* ATM is upregulated during the mitogenic response in peripheral blood mononuclear cells. Blood 1999;94:1998-2006.

7. Ditch S, Paull TT. The ATM protein kinase and cellular redox signaling: beyond the DNA damage response. Trends Biochem.Sci. 2012;37:15-22.

8. Frangogiannis NG. The immune system and cardiac repair. Pharmacol. Res. 2008;58:88-111.

9. Ma Y, Yabluchanskiy A, Lindsey ML. Neutrophil roles in left ventricular remodeling following myocardial infarction. Fibrogenesis Tissue Repair 2013;6:11.

10. Deten A, Volz HC, Briest W, Zimmer HG. Cardiac cytokine expression is upregulated in the acute phase after myocardial infarction. Experimental studies in rats. Cardiovasc. Res. 2002;55:329-40.

11. Nah DY, Rhee MY. The inflammatory response and cardiac repair after myocardial infarction. Korean Circ. J. 2009;39:393-98.

12. Frangogiannis NG. Regulation of the inflammatory response in cardiac repair. Circ. Res. 2012;110:159-73.

13. Foster CR, Daniel LL, Daniels CR, Dalal S, Singh M, Singh K. Deficiency of ataxia telangiectasia mutated kinase modulates cardiac remodeling following myocardial infarction: involvement in fibrosis and apoptosis. PLoS. One. 2013;8:e83513.

14. Barlow C, Hirotsune S, Paylor R, Liyanage M, Eckhaus M, Collins F *et al.* Atm-deficient mice: a paradigm of ataxia telangiectasia. Cell 1996;86:159-71.

15. Foster CR, Zha Q, Daniel LL, Singh M, Singh K. Lack of ataxia telangiectasia mutated kinase induces structural and functional changes in the heart: role in beta-adrenergic receptor-stimulated apoptosis. Exp. Physiol 2012;97:506-15.

16. Liu Z, Kastis GA, Stevenson GD, Barrett HH, Furenlid LR, Kupinski MA *et al.* Quantitative analysis of acute myocardial infarct in rat hearts with ischemia-reperfusion using a high-resolution stationary SPECT system. J. Nucl. Med. 2002;43:933-39.

17. Desmouliere A, Geinoz A, Gabbiani F, Gabbiani G. Transforming growth factor-beta 1 induces alpha-smooth muscle actin expression in granulation tissue myofibroblasts and in quiescent and growing cultured fibroblasts. J. Cell Biol. 1993;122:103-11.

18. Xie Z, Singh M, Singh K. Differential regulation of matrix metalloproteinase-2 and -9 expression and activity in adult rat cardiac fibroblasts in response to interleukin-1beta. J. Biol. Chem. 2004;279:39513-19.

19. White HD, Norris RM, Brown MA, Brandt PW, Whitlock RM, Wild CJ. Left ventricular end-systolic volume as the major determinant of survival after recovery from myocardial infarction. Circulation 1987;76:44-51.

20. Eddy RJ, Petro JA, Tomasek JJ. Evidence for the nonmuscle nature of the "myofibroblast" of granulation tissue and hypertropic scar. An immunofluorescence study. Am. J. Pathol. 1988;130:252-60.

21. Halade GV, Jin YF, Lindsey ML. Matrix metalloproteinase (MMP)-9: a proximal biomarker for cardiac remodeling and a distal biomarker for inflammation. Pharmacol. Ther. 2013;139:32-40.

22. Etoh T, Joffs C, Deschamps AM, Davis J, Dowdy K, Hendrick J *et al.* Myocardial and interstitial matrix metalloproteinase activity after acute myocardial infarction in pigs. Am. J. Physiol Heart Circ. Physiol 2001;281:H987-H994.

23. Nishida K, Kaziro Y, Satoh T. Anti-apoptotic function of Rac in hematopoietic cells. Oncogene 1999;18:407-15.

24. Menon B, Johnson JN, Ross RS, Singh M, Singh K. Glycogen synthase kinase-3beta plays a pro-apoptotic role in beta-adrenergic receptor-stimulated apoptosis in adult rat ventricular myocytes: Role of beta1 integrins. J. Mol. Cell Cardiol. 2007;42:653-61.

25. Stambolic V, Woodgett JR. Mitogen inactivation of glycogen synthase kinase-3 beta in intact cells via serine 9 phosphorylation. Biochem. J. 1994;303 (Pt 3):701-04.

26. Abbate A, Biondi-Zoccai GG, Baldi A. Pathophysiologic role of myocardial apoptosis in post-infarction left ventricular remodeling. J. Cell Physiol 2002;193:145-53.

27. Tanaka T, Huang X, Halicka HD, Zhao H, Traganos F, Albino AP *et al.* Cytometry of ATM activation and histone H2AX phosphorylation to estimate extent of DNA damage induced by exogenous agents. Cytometry A 2007;71:648-61.

28. Foster CR, Singh M, Subramanian V, Singh K. Ataxia telangiectasia mutated kinase plays a protective role in beta-adrenergic receptor-stimulated cardiac myocyte apoptosis and myocardial remodeling. Mol. Cell Biochem. 2011;353:13-22.

29. Jardine DL, Charles CJ, Ashton RK, Bennett SI, Whitehead M, Frampton CM *et al.* Increased cardiac sympathetic nerve activity following acute myocardial infarction in a sheep model. J. Physiol 2005;565:325-33.

30. Ide T, Tsutsui H, Kinugawa S, Utsumi H, Kang D, Hattori N *et al.* Mitochondrial electron transport complex I is a potential source of oxygen free radicals in the failing myocardium. Circ. Res. 1999;85:357-63.

31. French BA, Kramer CM. Mechanisms of Post-Infarct Left Ventricular Remodeling. Drug Discov. Today Dis. Mech. 2007;4:185-96.

32. See F, Watanabe M, Kompa AR, Wang BH, Boyle AJ, Kelly DJ *et al.* Early and Delayed Tranilast Treatment Reduces Pathological Fibrosis Following Myocardial Infarction. Heart Lung Circ. 2012.

33. Bournazou I, Pound JD, Duffin R, Bournazos S, Melville LA, Brown SB *et al.* Apoptotic human cells inhibit migration of granulocytes via release of lactoferrin. J. Clin. Invest 2009;119:20-32.

34. Hayhoe RP, Kamal AM, Solito E, Flower RJ, Cooper D, Perretti M. Annexin 1 and its bioactive peptide inhibit neutrophil-endothelium interactions under flow: indication of distinct receptor involvement. Blood 2006;107:2123-30.

35. Choi EY, Santoso S, Chavakis T. Mechanisms of neutrophil transendothelial migration. Front Biosci. (Landmark.Ed) 2009;14:1596-605.

36. Chen W, Frangogiannis NG. Fibroblasts in post-infarction inflammation and cardiac repair. Biochim. Biophys. Acta 2013;1833:945-53.

37. Deten A, Holzl A, Leicht M, Barth W, Zimmer HG. Changes in extracellular matrix and in transforming growth factor beta isoforms after coronary artery ligation in rats. J. Mol. Cell Cardiol. 2001;33:1191-207.

38. Goldsmith EC, Bradshaw AD, Spinale FG. Cellular mechanisms of tissue fibrosis. 2. Contributory pathways leading to myocardial fibrosis: moving beyond collagen expression. Am. J. Physiol Cell Physiol 2013;304:C393-C402.

39. Romson JL, Hook BG, Kunkel SL, Abrams GD, Schork MA, Lucchesi BR. Reduction of the extent of ischemic myocardial injury by neutrophil depletion in the dog. Circulation 1983;67:1016-23.

40. Romanic AM, Harrison SM, Bao W, Burns-Kurtis CL, Pickering S, Gu J *et al.* Myocardial protection from ischemia/reperfusion injury by targeted deletion of matrix metalloproteinase-9. Cardiovasc. Res. 2002;54:549-58.

41. Allport JR, Lim YC, Shipley JM, Senior RM, Shapiro SD, Matsuyoshi N *et al.* Neutrophils from MMP-9- or neutrophil elastase-deficient mice show no defect in transendothelial migration under flow in vitro. J. Leukoc. Biol. 2002;71:821-28.

42. Chen L, Knowlton AA. Mitochondria and heart failure: new insights into an energetic problem. Minerva Cardioangiol. 2010;58:213-29.

43. Jope RS, Johnson GV. The glamour and gloom of glycogen synthase kinase-3. Trends Biochem. Sci. 2004;29:95-102.

CHAPTER 3

DEFICIENCY OF ATAXIA TELANGIECTASIA MUTATED KINASE MODULATES CARDIAC REMODELING FOLLOWING MYOCARDIAL INFARCTION: INVOLVEMENT IN FIBROSIS AND APOPTOSIS.

Cerrone R. Foster, Laura L. Daniel, Christopher R. Daniels, Suman Dalal, Mahipal Singh, and Krishna Singh*

Department of Biomedical Sciences, James H Quillen College of Medicine
James H Quillen Veterans Affairs Medical Center
East Tennessee State University
Johnson City, TN 37614

Total number of figures: 9

Number of Tables: 1

Keywords: ATM, apoptosis, myocardial remodeling, fibrosis, myocardial infarction

*__Correspondence__: Krishna Singh, Ph.D.
Dept of Biomedical Sciences
James H Quillen College of Medicine
East Tennessee State University
PO Box 70582, Johnson City, TN 37614
Ph: 423-439-2049
Fax: 423-439-2052
E-mail: singhk@etsu.edu

Abstract

Ataxia telangiectasia mutated kinase (ATM) is a cell cycle checkpoint protein activated in response to DNA damage. We recently reported that ATM plays a protective role in myocardial remodeling following β-adrenergic receptor stimulation. Here we investigated the role of ATM in cardiac remodeling using myocardial infarction (MI) as a model. **Methods and Results:** Left ventricular (LV) structure, function, apoptosis, fibrosis, and protein levels of apoptosis- and fibrosis-related proteins were examined in wild-type (WT) and ATM heterozygous knockout (hKO) mice 7 days post-MI. Infarct sizes were similar in both MI groups. However, infarct thickness was higher in hKO-MI group. Two dimensional M-mode echocardiography revealed decreased percent fractional shortening (%FS) and ejection fraction (EF) in both MI groups when compared to their respective sham groups. However, the decrease in %FS and EF was significantly greater in WT-MI vs hKO-MI. LV end systolic and diastolic diameters were greater in WT-MI vs hKO-MI. Fibrosis, apoptosis, and α-smooth muscle actin staining was significantly higher in hKO-MI vs WT-MI. MMP-2 protein levels and activity were increased to a similar extent in the infarct regions of both groups. MMP-9 protein levels were increased in the non-infarct region of WT-MI vs WT-sham. MMP-9 protein levels and activity were significantly lower in the infarct region of WT vs hKO. TIMP-2 protein levels similarly increased in both MI groups, whereas TIMP-4 protein levels were significantly lower in the infarct region of hKO group. Phosphorylation of p53 protein was higher, while protein levels of manganese superoxide dismutase were significantly lower in the infarct region of hKO vs WT. In vitro, inhibition of ATM using KU-55933 increased oxidative stress and apoptosis in cardiac myocytes. **Conclusion:** Deficiency of ATM improves heart function 7 days post-MI. However, it has adverse effect on myocardial remodeling with increased apoptosis and fibrosis.

Introduction

Myocardial infarction (MI) induces a series of molecular and structural changes in the left ventricle leading to a progressive decline in LV performance [1–3]. The limited capacity for regeneration of myocytes in the adult heart suggests that cardiac myocyte loss due to apoptosis may contribute to the progression of heart failure. Dynamic synthesis and breakdown of extracellular matrix also plays a significant role in myocardial remodeling post-MI [4,5]. Therefore elucidation of events involved in the repair of the heart is an important clinical determinant of survival post-MI [6].

Ataxia telangiectasia mutated kinase (ATM) is a multifunctional kinase that affects multiple downstream targets in response to cellular stress or damage. Mutation or deficiency of ATM causes a hereditary multi-systemic disease called Ataxia telangiectasia (A-T). Individuals with mutations in both copies of the ATM gene suffer from increased susceptibility to ionizing radiation, predisposition to cancer, insulin resistance, immune deficiency, and premature aging. Carriers of one mutated allele at the A-T locus make up ~1.4 to 2% of the general population. These individuals with an ATM mutation in one allele are spared from most of the symptoms of A-T, but are more susceptible to cancer and ischemic heart disease [7–9].

Previously, a search to identify novel apoptosis-related genes using Super-Array technique followed by RT-PCR analyses revealed that β-adrenergic receptor (β-AR) stimulation increases expression of ATM in the heart and in adult cardiac myocytes [10]. Using ATM heterozygous knockout (hKO) mice and chronic β-AR stimulation as a model of myocardial remodeling, we provided evidence that ATM plays an important role in β-AR-stimulated myocardial remodeling with effects on ventricular function, apoptosis and fibrosis [10]. Recently, using ATM-/- mice, we have shown that lack of ATM induces structural and functional changes

in the heart with enhanced myocardial fibrosis and myocyte hypertrophy. β-AR-stimulated apoptosis in WT hearts associated with p53- and JNKs-dependent mechanism, while decreased Akt activity may play a role in increased myocyte apoptosis in the absence of ATM [11]. The objective of this study was to investigate the role of ATM in myocardial remodeling 7 days post-MI. The data presented here show that deficiency of ATM affects heart function, infarct thickness, fibrosis, apoptosis and expression of fibrosis- and apoptosis-related proteins.

Methods

Vertebrate animals

Age-matched (~ 4 months old) male and female ATM deficient mice were used as previously described [10]. Heterozygous knockout (hKO) and wild type (WT) ATM mice, purchased from the Jackson Laboratory, were of 129xblack Swiss hybrid background. Genotyping was performed by polymerase chain reaction (PCR) using primers suggested by the Jackson Laboratory. The absence of both ATM alleles produces a lethal phenotype at ~2 months of age mainly due to thymic lymphomas [12,13].

Ethics statement

The investigation conforms to the *Guide for the Care and Use of Laboratory Animals* published by the US National Institutes of Health (NIH Publication No. 85-23, revised 1996). All of the experiments were performed in accordance with the protocols approved by the East Tennessee State University Animal Care and Use Committee.

Myocardial infarction

MI and measurements were performed as previously described [14–16]. The left anterior descending coronary artery was occluded using a 7-0 mm silk suture. Sham animals underwent the same surgery without ligation of the coronary artery.

Echocardiography

Transthoracic two-dimensional M-mode echocardiography was performed as previously described [10,11]. All echocardiographic assessments and measurements were performed by the same investigator. A second person also performed measurements on a separate occasion using the same recordings with no significant differences in interobserver variability.

Morphometric analyses

Following MI, hearts were removed and arrested in diastole using KCl (30 mmol/L) followed by perfusion fixation with 10% buffered formalin. Infarct size was measured using Masson's trichrome stained sections as previously described [14,16]. Infarct size was calculated as the percentage of LV circumference occupied by infarct scar. Infarct thickness was calculated using mid-myocardial slides, averaging three equally spaced measurements along the infarct wall. Cross sections (4μm thick) were stained with Masson's trichrome for the measurement of fibrosis using Bioquant image analysis software (Nashville,TN).

Apoptosis

To detect apoptosis, TUNEL-staining was carried out as previously described [10,11]. Hoechst 33258 (10 μM; Sigma) staining was used to count the total number of nuclei. Apoptosis was calculated as the percentage of apoptotic cardiac cell nuclei / total number of nuclei. To identify apoptosis associated with cardiac myocytes, the sections were immunostained using α-sarcomeric actin antibodies (1:50, 5C5 clone; Sigma, St. Louis, MO). TUNEL-positive nuclei that were clearly seen within cardiac myocytes were counted. The number of apoptotic myocyte nuclei was counted, and index of apoptosis was calculated as the percentage of apoptotic myocyte nuclei/total number of nuclei. In isolated cells, the percentage of TUNEL-positive cells (relative to total myocytes) was determined by counting ~200 cells in 10 randomly chosen fields per coverslip for each experiment.

Immunohistochemistry

Sections (4μm thick) were deparrafinized and stained with anti-α-smooth muscle actin (α-SMA) as described [11]. The sections were visualized using fluorescent microscopy (Nikon) and images

were acquired using Retiga 1300 color-cooled camera. Images were quantitatively analyzed using Bioquant Image analysis software (Nashville, TN).

Western blot analysis

LV lysates were prepared in RIPA buffer as previously described [17]. Protein lysates (50 μg) were separated by SDS-PAGE (10%) and transferred to a PVDF membrane (240 mA, 2.5 h). The membranes were incubated with antibodies against p-p53 (serine-15; Cell Signaling), MMP-9 and MMP-2 (Millipore), TIMP-2 and TIMP-4 (Chemicon), and SOD-2 (Santa Cruz). Membranes were stripped and probed with GAPDH (Santa Cruz) as a protein loading control. Band intensities were quantified using Kodak photodocumentation system (Eastman Kodak Co.). The data are presented as fold change vs WT-sham.

In-gel zymography

In gel zymography was performed on 50 μg of LV lysates from WT-MI and hKO-MI hearts as previously described [18]. Clear and digested regions representing MMP-2 and MMP-9 activity were quantified using a Kodak documentation system.

Cell isolation, culture and treatment

Adult rat ventricular myocytes (ARVMs) were isolated as previously described [19]. ARVMs were plated in Dulbecco's modified Eagle's medium (DMEM; Mediatech) supplemented with HEPES (25 mM), BSA (0.2%), creatine (5 mM), L-carnitine (2 mM), taurine (5 mM) and 0.1% penicillin-streptomycin at a density of 30–50 cells/mm^2 on coverslips precoated with laminin (1μg/cm^2). ARVMs cultured for 24 h were treated with KU-55933 (KU), a specific inhibitor of ATM [20], for 24 h. Apoptosis was measured using TUNEL-assay as described above.

Detection of oxidative stress

To detect oxidative stress, ARVMs were treated with KU (0.1 μM and 1 μM) for 3h. Cells were then stained using total reactive oxygen species (ROS)/superoxide detection kit (Enzo Life Sciences) and visualized using fluorescent microscopy. The number of ROS-positive cells (relative to total myocytes) was determined by counting ~100 cells in 10 randomly chosen fields per coverslip for each experiment.

Statistical analyses

Data are represented as mean ± SEM. Data were analyzed using student's t test or one-way analysis of variance (ANOVA) and a post hoc Tukey's test. Probability (p) values of <0.05 were considered to be significant.

Results

Morphometric studies and mortality

Body weights remained unchanged among the sham and MI groups. Heart weight (HW) and HW to body weight ratios were increased in both MI groups ($p<0.001$ vs sham; n=6-12; Table 3.1) with no significant difference between the two MI groups. The mortality rates 7 days post-MI were 35% and 18% in WT and hKO mice, respectively. Masson's trichrome staining of the mid-LV sections is shown in figure 1A. Infarct size measured as a percentage of the LV circumference occupied by scar tissue was not different between the WT-MI and hKO-MI groups (p=NS, Fig 3.1B). However, infarct thickness measured from mid-myocardial sections was significantly greater in hKO-MI group versus WT-MI (Fig 3.1C).

Table 3.1. Morphometric Measurements 7 Days Post-MI

	WT-Sham (n=6)	hKO-Sham (n=7)	WT-MI (n=10)	hKO-MI (n=12)	p
BW	24.41 ± 0.96	26.49 ± 1.71	23.89 ± 0.76	23.43 ± 0.61	
HW	125.22 ± 7.74	139.08 ± 12.40	153.93 ± 5.27*	158.50 ± 5.93*	<0.001
HW/BW	5.11 ± 0.12	5.25 ± 0.04	6.48 ± 0.33*	6.86 ± 0.43*	<0.001

Values are mean ± SEM; *comparison between sham and MI group.

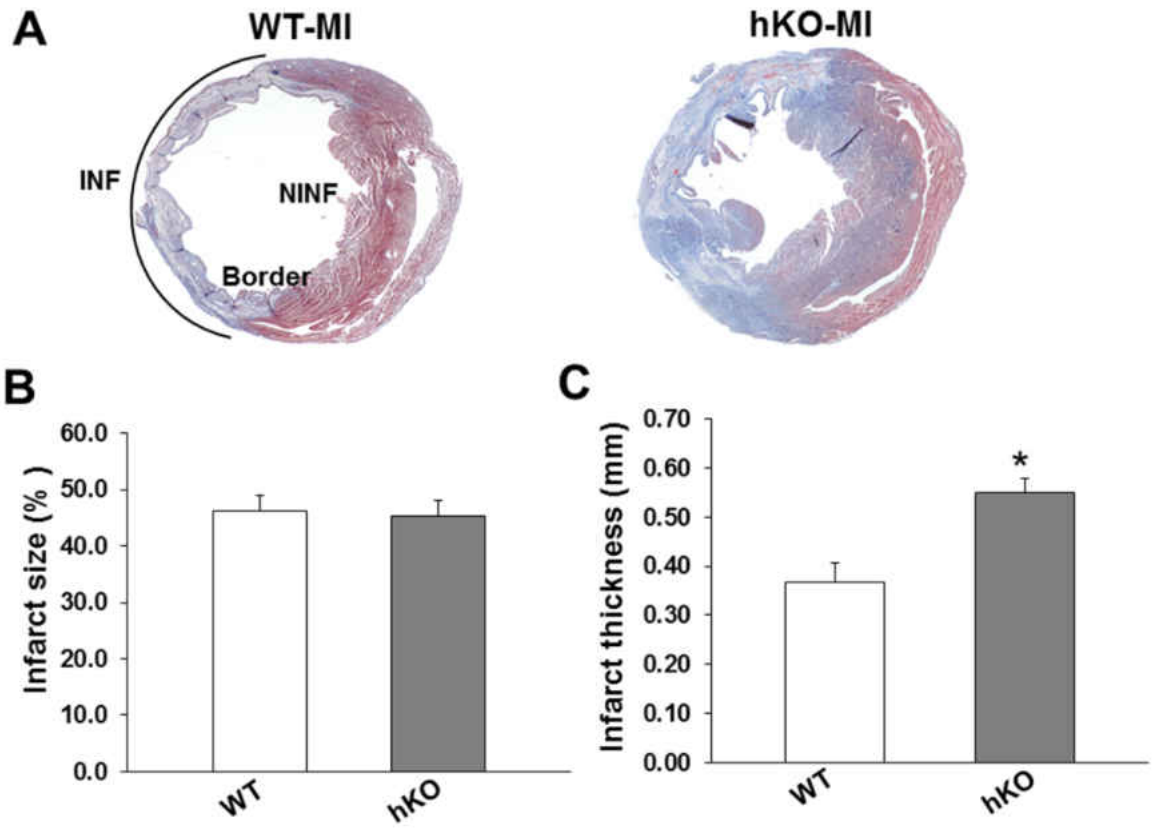

Figure 3.1. Infarct size and thickness. Masson's trichrome stained sections from WT and hKO hearts were analyzed for the measurement of infarct size and thickness. A. Transverse sections of the mid-myocardium from WT and hKO hearts post-MI. Quantitative analysis of infarct size (B) and thickness (C) as measured from trichrome stained hearts; *$p<0.05$ vs WT; n=5-7.

Echocardiographic studies

No significant differences in the echocardiographic parameters were observed between the two sham groups. M-mode echocardiography revealed a significant decrease in percent fractional shortening (%FS) and ejection fraction (EF) in both MI groups when compared to their respective sham groups. However, the decrease in %FS and EF was significantly greater in the WT-MI group when compared to hKO-MI ($^{\#}p<0.05$ vs WT-MI; Fig 3.2A & B). MI increased LV end systolic (LVESD) and diastolic (LVEDD) diameters in both MI groups. However, the

increase in LVEDD and LVESD was significantly lower in hKO-MI when compared to the WT-MI group ($^{\#}p<0.05$ vs WT-MI; Fig 3.2C & D).

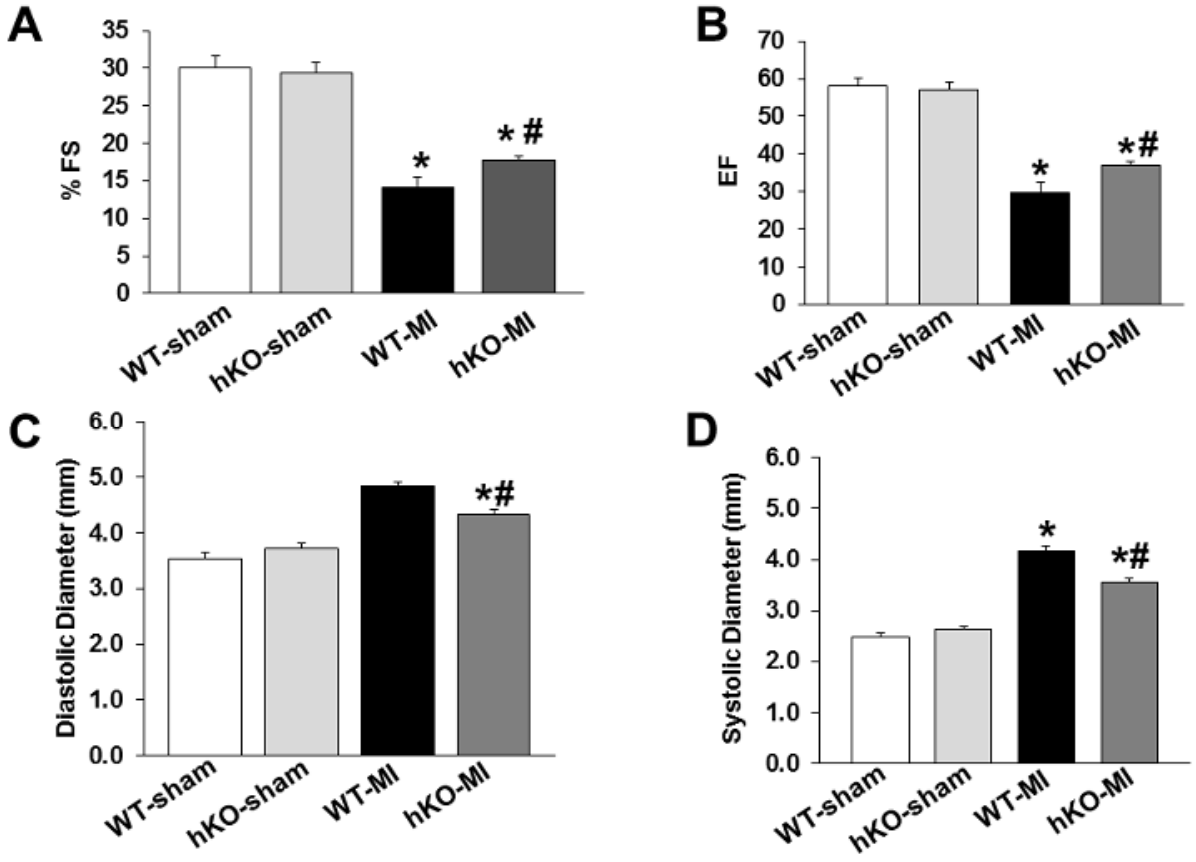

Figure 3.2. ATM deficiency improves LV function 7 days post-MI. MI was performed in WT (n=10) and ATM hKO (n=12) mice. Indices of cardiac function (percent fractional shortening, %FS; ejection fraction, EF) and structure (LV end diastolic diameter, LVEDD; LV end systolic diameter, LVESD) were measured using echocardiography 7 days after MI. A. %FS; B. EF; C, LVEDD; D. LVESD; *p<0.05 vs sham; $^{\#}p<0.05$ vs WT-MI; n=10-12.

Fibrosis and Apoptosis

Quantitative analysis of fibrosis using trichrome stained sections revealed increased fibrosis in hKO-sham group vs WT-Sham. MI increased fibrosis in the border and infarct LV regions of both groups when compared to their respective non-infarct LV regions. Interestingly, the level

of fibrosis was greater in the border and infarct regions of hKO-MI group when compared to the WT-MI (Fig 3.3 A&B).

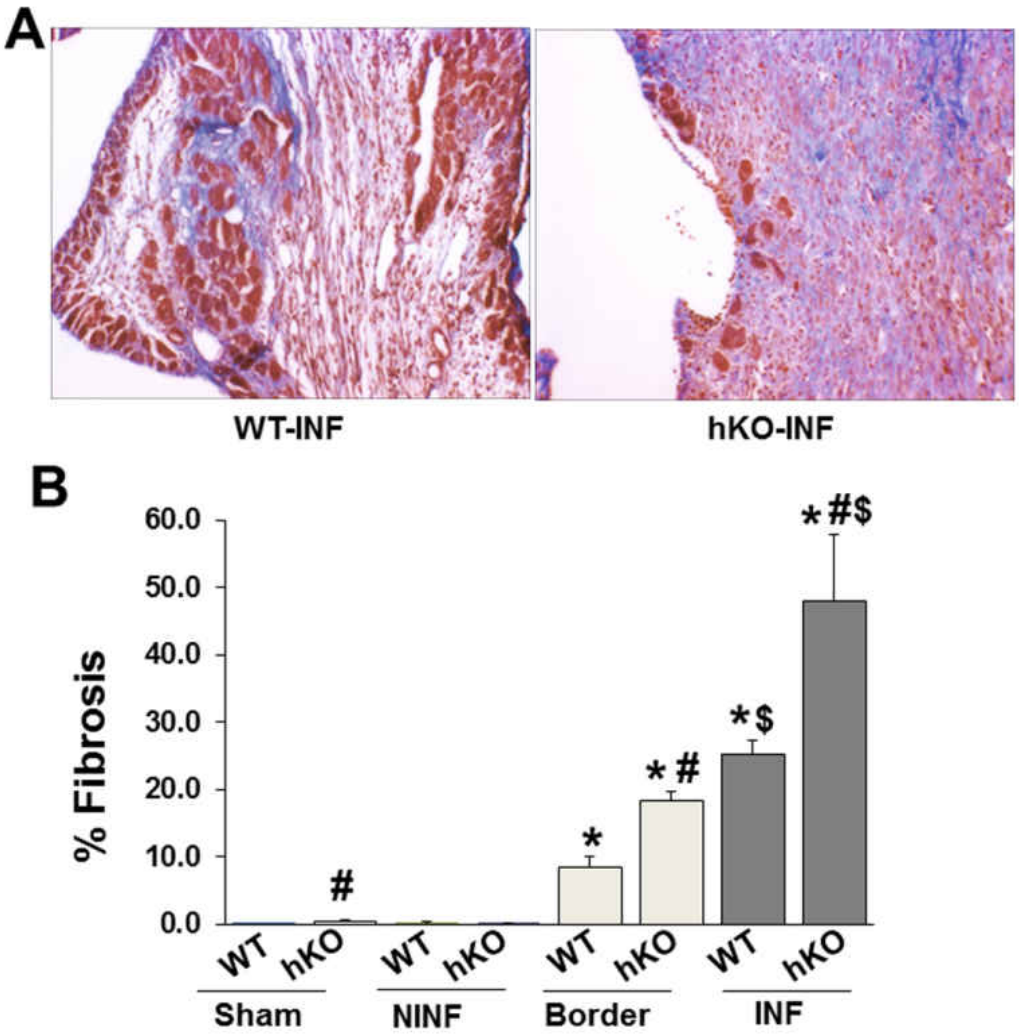

Figure 3.3. Analysis of fibrosis. Masson's trichrome stained sections of the heart were used for quantitative measurement of fibrosis. A. Masson's trichrome-stained sections demonstrating fibrosis in WT and hKO mice 7 days post-MI. B. Quantitative analysis of fibrosis. NINF, non-infarct LV region; INF, infarct; *p<0.05 vs sham; #p<0.05 comparisons between WT and hKO groups; $^{\$}$p<0.05 vs border; n=6-7.

Analysis of apoptosis using TUNEL-staining assay revealed increased apoptosis in the hKO-sham vs the WT-sham group. The number of apoptotic cells and myocytes remained unchanged in the non-infarct LV regions when compared to the sham groups (Fig 3.4 B&C). MI increased the number of apoptotic cells in the border and infarct LV regions of both groups when compared to the sham and non-infarct LV regions (Fig 3.4 A&B). In the border area, the number of apoptotic cells as well as myocytes was significantly higher in hKO vs WT group. In the infarct LV region, the number of apoptotic cells was significantly lower in hKO vs WT group (Fig 3.4B), while the number apoptotic myocytes remained unchanged between WT and hKO (Fig 3.4C).

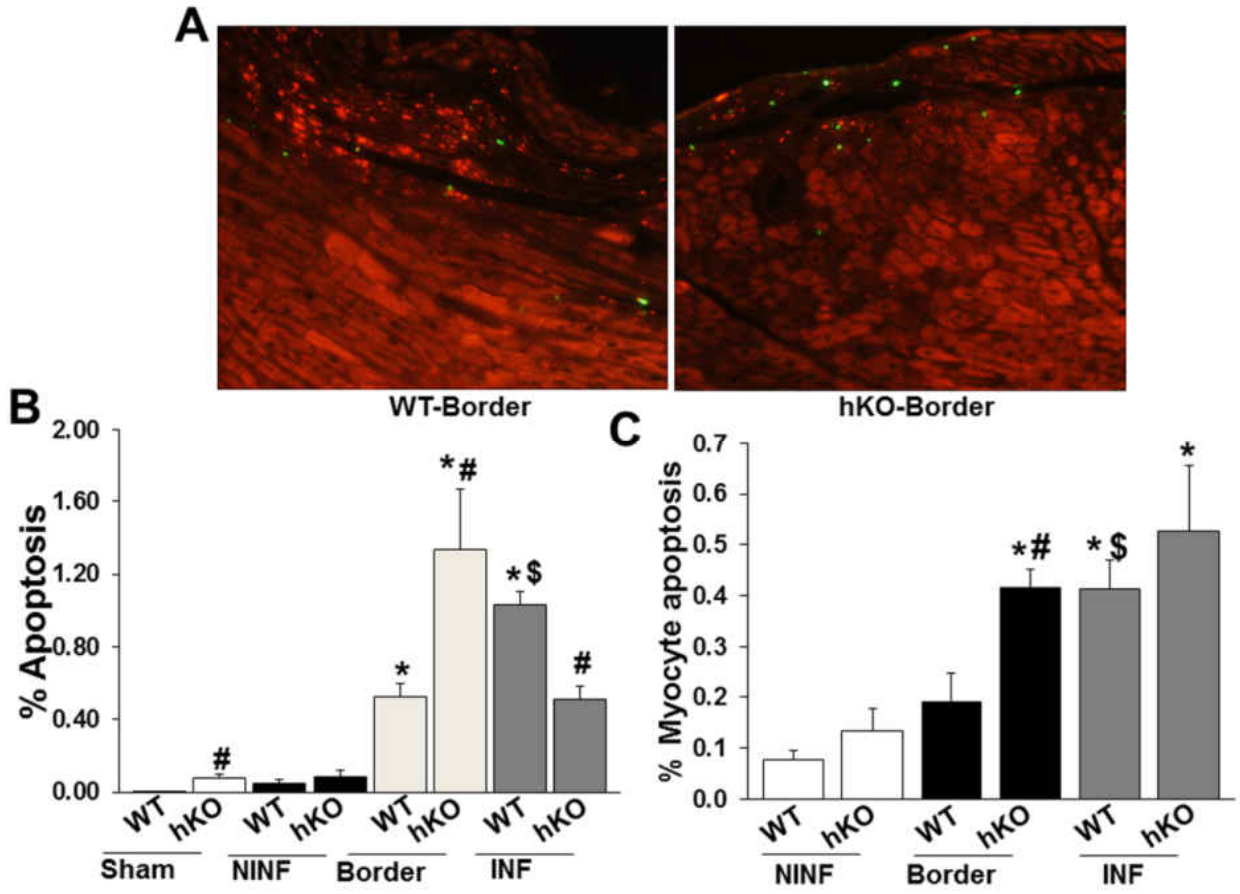

Figure 3.4. Analysis of apoptosis. A. TUNEL-stained images from the border regions of WT and hKO hearts post-MI. B. Quantitative analysis of cardiac cell apoptosis in the non-infarcted (NINF), border and infarct (INF) regions of WT and hKO mice 7 days post-MI. C. Quantitative analysis of myocyte apoptosis in the NINF, border and INF regions of WT and hKO mice 7 days post-MI. *p<0.05 vs sham; #p<0.05 comparisons between WT and hKO groups; $^{\$}$p<0.05 vs border; n=4.

Expression of α-smooth muscle actin (α-SMA)

Expression of α-SMA serves as a marker for the differentiation of fibroblasts into myofibroblasts [21–23]. MI increased α-SMA expression in the infarct LV regions of both groups (Fig 3.5A). Quantitative immunohistochemical analysis of heart sections revealed increased α-SMA expression in the infarct LV region of hKO when compared to the WT group (Fig 3.5B).

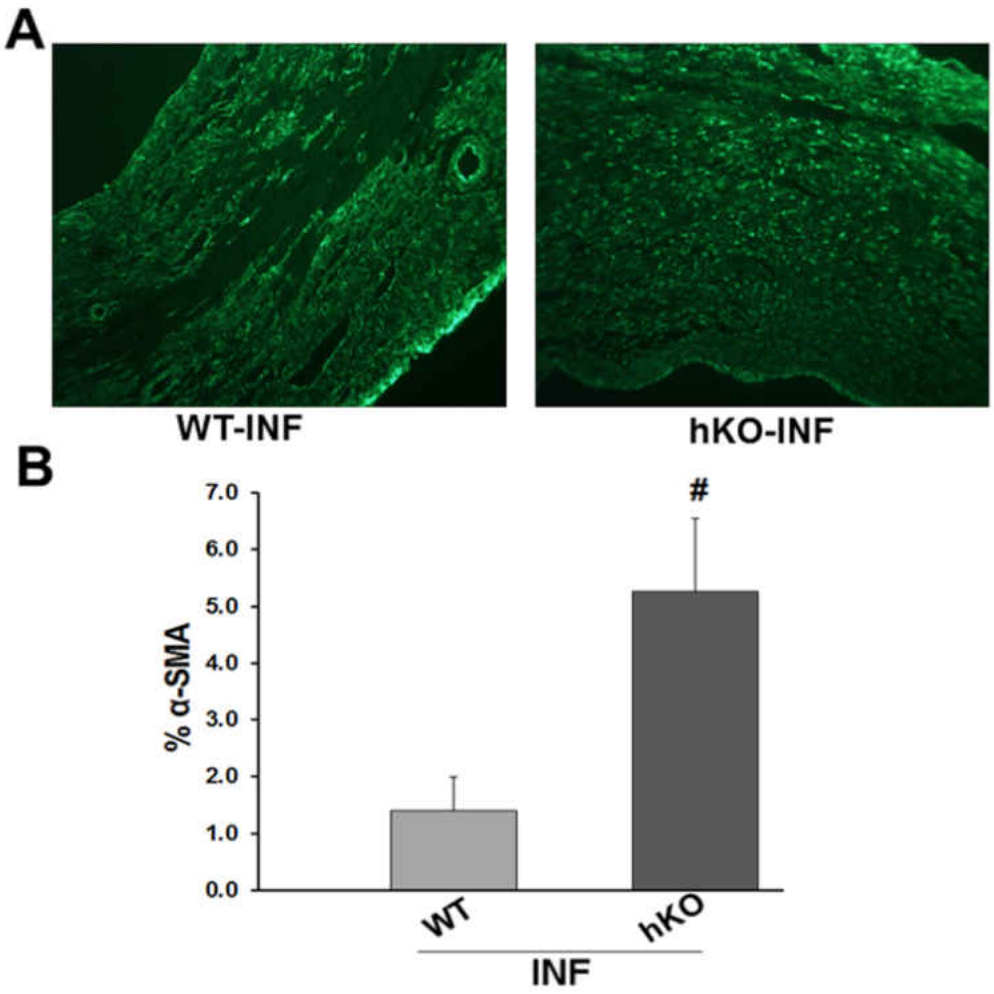

Figure 3.5. Expression of α-smooth muscle actin (α-SMA). A. α-SMA-stained images from the infarct LV regions of WT and hKO hearts post-MI. B. Quantitative immunohistological analysis of α-SMA expression in the infarct (INF) region of WT and hKO mice 7 days post-MI. #$p<0.05$ vs WT-INF; n=4.

Expression of matrix metalloproteinases (MMPs) and tissue inhibitors of MMPs (TIMPs)

Western blot analyses of LV lysates revealed no significant increase in MMP-2 protein levels in the non-infarct LV regions of both MI groups when compared to sham. MMP-2 protein levels were significantly higher in the infarct region of both MI groups when compared to sham. In the hKO group, the increase in MMP-2 protein levels was significantly greater in the infarct region when compared to the non-infarct region (Fig 3.6A). MMP-9 protein levels were increased in the

non-infarct region and decreased in the infarct region of the WT group when compared to sham. No such changes in MMP-9 protein levels were observed in the hKO group. In the infarct region, MMP-9 protein levels were significantly greater in the hKO group when compared to the WT (Fig 3.6B). Analysis of MMPs activity using in-gel zymography showed no difference in MMP-2 activity the infarct LV regions between the two MI groups (Fig 3.6C). However, MMP-9 activity in the hKO was significantly higher in the hKO group when compared to WT (Fig 3.6D).

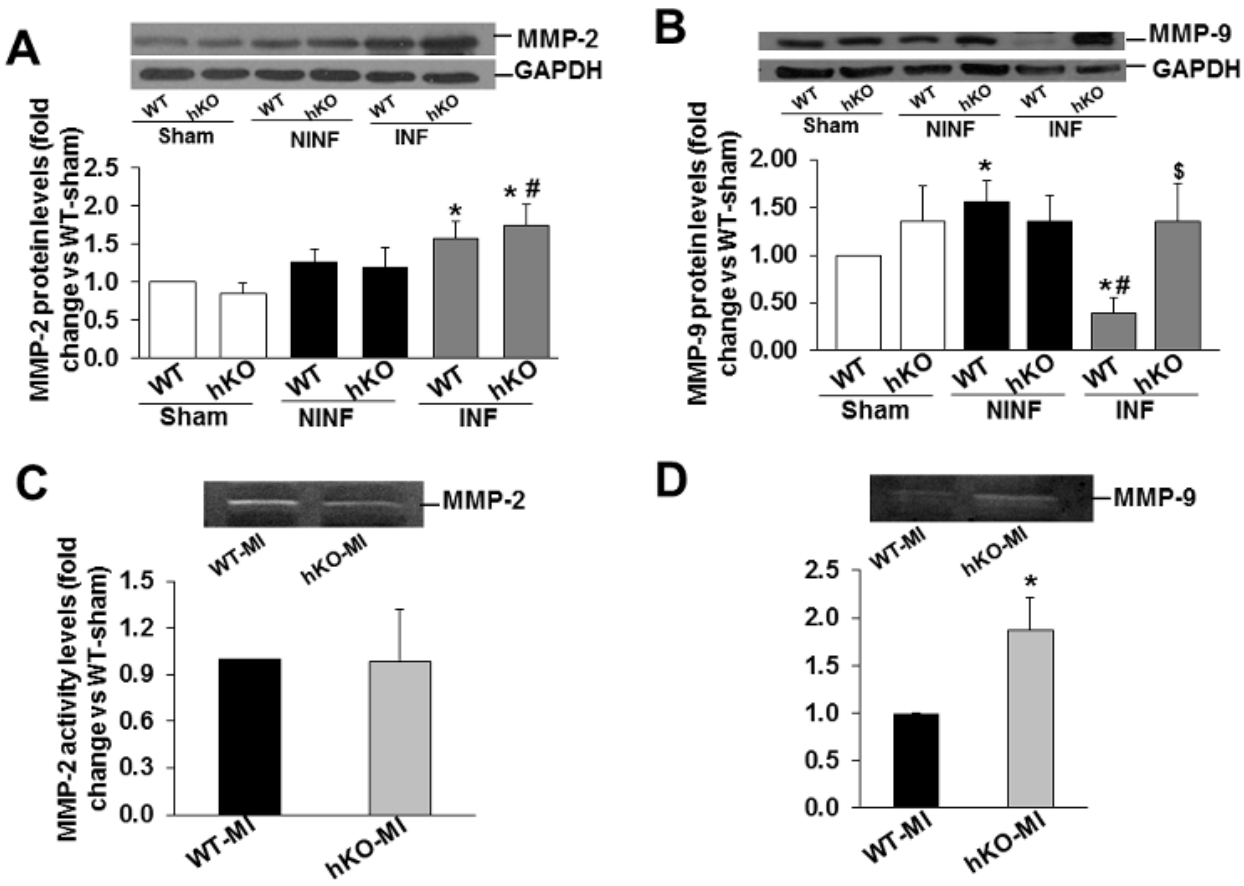

Figure 3.6. Expression and activity of MMPs. A & B. Total LV lysates (50 µg), prepared from sham and non-infarct (NINF) and infarct (INF) LV regions, were analyzed by western blot using anti-MMP-2 (A) and anti-MMP-9 (B) antibodies. The upper panels show autoradiograms indicating immunostaining for MMP-2, MMP-9, and GAPDH. The lower panels exhibit quantitative analyses of MMP-2, MMP-9 normalized to GAPDH. *$p<0.05$ vs sham; $^{\#}p<0.05$ vs NINF; $^{\$}p<0.05$ vs WT-INF; n=7. C&D. Total LV lysates (50 µg), prepared from the infarct LV regions were analyzed by in-gel zymography. C. MMP-2 activity. D. MMP-9 activity. *$p<0.05$ vs WT-MI; n=3.

TIMP-2 is suggested to inhibit MMP-2 activity [4], while TIMP-4 is predominantly expressed in the heart [24] . Western blot analyses showed no immunostaining for TIMP-2 in the sham groups. MI increased TIMP-2 protein levels in the non-infarct and infarct regions of the heart in both groups. However, TIMP-2 protein levels were significantly greater in the infarct region when compared to the non-infarct LV region with no significant difference between the

WT and hKO groups (Fig 3.7A). On the contrary, TIMP-4 protein levels were clearly present in both the sham groups. MI decreased TIMP-4 protein levels in the infarct LV region of both groups. TIMP-4 protein levels were significantly lower in hKO group when compared to WT (Fig 3.7B).

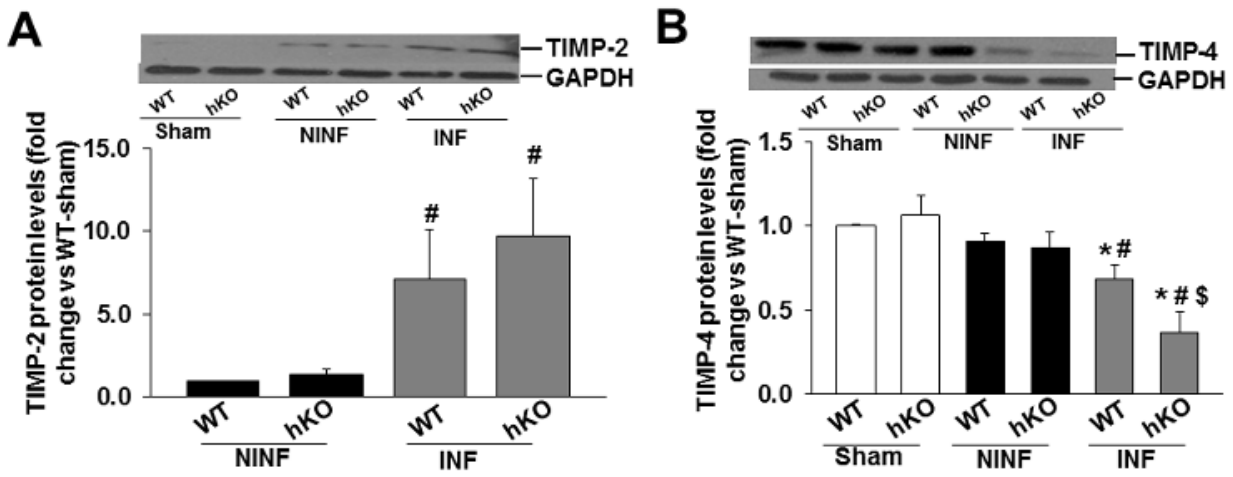

Figure 3.7. Expression of TIMPs. Total LV lysates (50 µg), prepared from sham and non-infarct (NINF) and infarct (INF) LV regions, were analyzed by western blot using anti-TIMP-2 (A) and anti-TIMP-4 (B) antibodies. The upper panels show autoradiograms indicating immunostaining for TIMP-2, TIMP-4, and GAPDH. The lower panels exhibit quantitative analyses of TIMP-2, TIMP-4 normalized to GAPDH. *$p<0.05$ vs sham; $^{\#}p<0.05$ vs NINF; $^{\$}p<0.05$ vs WT-INF; n=7.

Expression and phosphorylation of apoptosis-related proteins

ATM phosphorylates p53 (serine-15) following DNA damage [25]. Western blot analyses of LV lysates using anti-p53 antibodies showed no immunostaining for p53 in the sham or non-infarct LV regions of WT or hKO groups. Phosphorylation of p53 (serine-15) was only observed in the infarct regions with a greater increase in the hKO-MI group (Fig 3.8A).

Deficiency of ATM is suggested to associate with increased oxidative stress [26]. Intrinsic mitochondrial abnormalities are also reported in thymocytes lacking ATM [27]. Western blot analysis of mitochondrial antioxidant protein manganese superoxide dismutase (SOD-2) demonstrated no change in SOD-2 protein levels in the sham and non-infarct LV regions of the heart in both groups. MI significantly decreased SOD-2 protein levels in the infarct LV of both groups. However, the decrease in SOD-2 protein levels was significantly higher in hKO group vs WT (Fig 3.8B).

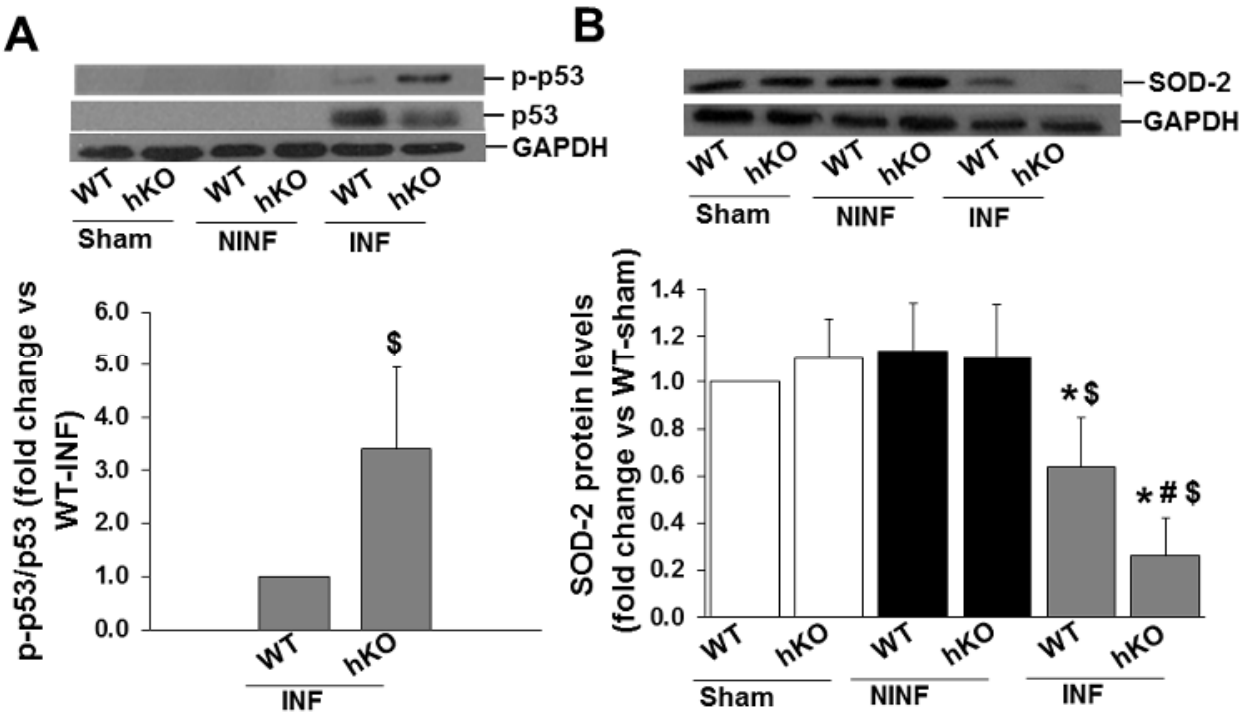

Figure 3.8. Expression and phosphorylation of apoptosis-related proteins. A. Total LV lysates were analyzed by western blot using phospho-specific (serine-15) p53 or total p53 antibodies. Protein loading in each lane is indicated by GAPDH immunostaining. $p<0.05 vs WT-INF; n=7. B. Total LV lysates were analyzed by western blot using anti-SOD-2 antibodies. Protein loading in each lane is indicated by GAPDH. *p<0.05 vs sham; $p<0.05 vs NINF; #p<0.05 vs WT-INF; n=7.

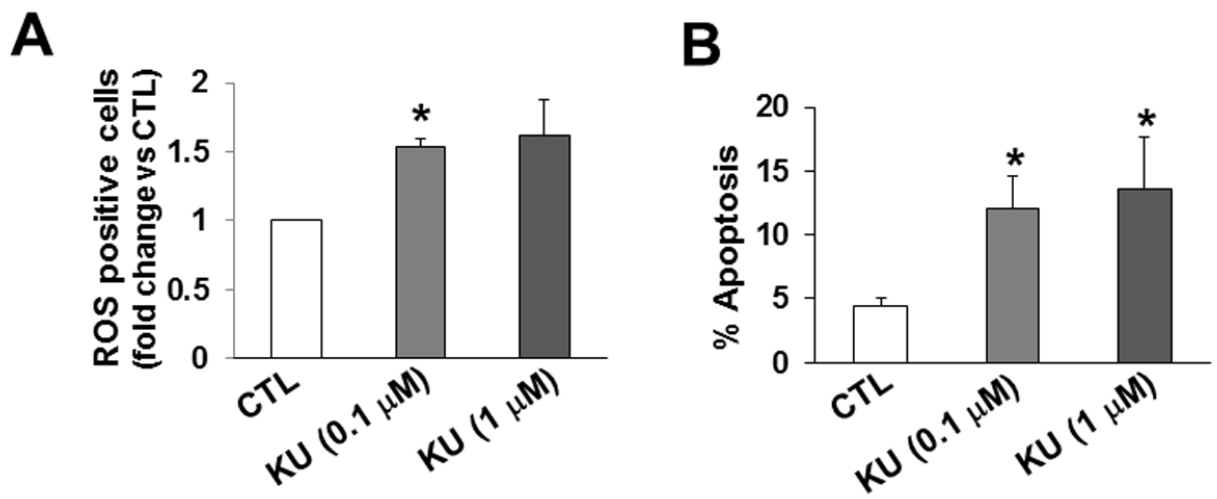

Figure 3.9. Inhibition of ATM increases the number of ROS-positive ARVMs and induces apoptosis. ARVMs were treated with KU-55933 (KU) for 3 h (A) or 24 h (B). A. Cells were stained using ROS-detection kit and ROS-positive cells were counted using fluorescent microscopy. *p<0.05 vs control (CTL); n=3. B. TUNEL-assay was used to count the number of apoptotic ARVMs. *p<0.05 vs CTL; n=3.

Oxidative stress and apoptosis in ARVMs

Inhibition of ATM using KU-55933 (KU) is shown to increase reactive oxygen species (ROS) in cancer cells [28]. To investigate if inhibition of ATM also increases ROS in myocytes, ARVMs were treated with KU (0.1 μM and 1 μM) for 3 h. Analysis of ROS-positive ARVMs using fluorescent microscopy showed increased number of ROS-positive ARVMs at both concentrations of KU (Fig 9A). To investigate if inhibition of ATM induces apoptosis, ARVMs were treated with KU (0.1 μM and 1 μM) for 24 h. Measurement of apoptosis using TUNEL-assay showed that KU at 0.1 μM and 1 μM concentrations significantly increases the number of apoptotic ARVMs (Fig 3.9B).

Discussion

Previous studies from our lab have shown that lack of ATM induces structural and functional changes in the heart [10,11]. A major finding of this study is that deficiency of ATM attenuates LV dysfunction and dilatation 7 days post-MI. Although infarct size were comparable between the WT and hKO mice, infarct thickness was greater in the hKO mice. Deficiency of ATM associated with increased expression of α-SMA and fibrosis. Cardiac cell apoptosis was lower in the infarct LV region of ATM deficient mice. However, apoptosis was significantly higher in the border area of the infarct in ATM deficient mice. ATM deficiency also associated with changes in the expression of fibrosis- and apoptosis-related proteins. In vitro, inhibition of ATM increased the number of ROS-positive ARVMs and induced apoptosis. The results presented here suggest that ATM plays a multifaceted role in remodeling pathways following myocardial infarction.

Systolic dysfunction is characterized by decreased cardiac contractility and pumping capacity of the heart. In general, MI results in severe LV dilation and systolic dysfunction [29]. The data presented here demonstrate that ATM deficient mice suffer to a lesser degree from impaired systolic function following MI. The study also provides evidence that deficiency of ATM affects the infarct scar. We observed that the infarct size remained unchanged between WT and ATM deficient mice. However, infarct thickness was greater in the ATM deficient mice. Fibrosis and expression of α-SMA, a marker of myofibroblasts, was significantly higher in the ATM deficient heart after MI. Our findings suggest that myofibroblasts, a major cell type involved in the deposition of fibrosis, may escape the apoptotic death during the granulation phase and contribute to the increase in infarct wall thickness in the ATM deficient mice. This may in turn decrease LV dilation and dysfunction. Of note, cardiac cell apoptosis in the infarct

LV region of ATM deficient mice was lower when compared to that in the WT. Increased infarct thickness with reduced apoptosis in granulation tissue cells is previously described in Angiotensin II type 1A receptor KO (AT1AKO) 7 days post-MI [30]. Expression of soluble transforming growth factor-β (TGF-β) type II receptor, a competitive inhibitor of TGF-β, led to a greater infarct thickness and smaller LV circumference [31]. Therefore, it is conceivable that ATM signaling may involve Angiotensin II and/or TGF-β axis for its effect on infarct thickness, LV circumference and apoptosis. Further investigations are warranted to clarify the role of these molecules in ATM signaling.

Cardiac structure consists of various cell types whose function is to promote contractility of the heart. Following injury, macrophages and other immune cells initiate a healing process. Once the damaged cells have been removed, activation of myofibroblasts helps promote scar tissue formation. This response is suggested to be associated with increases in α-SMA [21,32]. We observed greater increase in α-SMA expression in the infarct region of ATM deficient mice. Increased α-SMA may help explain the presence of increased fibrosis in the infarct region of ATM deficient mice.

Cardiac cell apoptosis increases in the infarct and border areas and to a smaller extent in the non-infarcted areas of the heart after MI [6,33]. Early activation of apoptosis is a necessary step in remodeling as it allows room for entry of immune repair cells following injury [1,34,35]. The infarct region is a predictor of post-MI prognosis as it can relate to infarct expansion. ATM deficient mice exhibited a greater increase in apoptosis in the border region. This may lead to a greater infarct expansion and worse prognosis late post-MI [1,3,36]. Likewise, increased granulation tissue cell apoptosis in WT-MI hearts may reflect timely removal of unhealthy cells, thereby enhancing the repair process.

The matrix metalloproteinases (MMPs) are endopeptidases that are present within the myocardium. Changes in MMP abundance is shown to be associated with changes in extracellular matrix deposition (ECM) and LV remodeling post-MI, including increased LV dilation and cardiac rupture [37–41]. The ECM is a critical component in the restructuring of the heart after MI. Using promoter reporter constructs, Mukherjee et. al. showed that MMP-2 promoter activation peaks in the MI region 7 days post-MI, while MMP-9 promoter activation was highest in the border region at 7 and 14 days post-MI [42]. Consistent with these findings, we observed increased MMP-2 protein levels in the MI regions of both groups when compared to their respective sham groups. No difference in MMP-2 protein levels and activity in the infarct LV region suggest that increased fibrosis in hKO mice occurs via MMP-2-independent mechanism. MMP-9 protein levels were significantly higher in the non-infarct LV region of WT group when compared to sham. However, we observed decreased MMP-9 protein levels in the infarct LV region of WT group. No such changes in MMP-9 protein levels were observed in the hKO group. MMP-9 activity was higher in the infarct LV region of hKO when compared to WT. Higher MMP-9 protein levels and activity suggest involvement of MMP-9 in ECM deposition and LV remodeling during ATM deficiency. The decreased MMP-9 protein levels observed in this study in the WT infarct region may reflect localization and/or timing of the remodeling events. [43]. Tao *et al.* has shown that MMP-9 activity increases as early as 1 day post-MI and reaches a maximum by 2 days, then gradually decreases. MMP-2 activity starts to increase 4 days post-MI, reaching a maximum by 7 days [41].

TIMP's are traditionally believed to function solely as inhibitors of active MMPs [4]. TIMP-2 is suggested to have maximum affinity for MMP-2 [44]. In the heart, MMP-9 and TIMP-4 are suggested to play a key in the myocardial remodeling. In cardiac myocytes, the

effects of MMP-9 on voltage-induced contraction can be reversed by TIMP-4 [45]. We observed increased TIMP-2 expression in the infarct region of both groups to a similar extent. However, TIMP-4 protein levels were significantly lower in the ATM deficient mice. ATM deficient mice also exhibited increased MMP-9 protein levels and activity in the infarct region when compared to their WT counterparts. Increased MMP-9 activity is expected to correlate with decreased fibrosis in ATM deficient mice. However, we observed increased fibrosis in the infarct and remote regions of ATM deficient mice. Recent evidence suggests additional roles for TIMPs independent of their function as MMP inhibitors [36]. Therefore, it is plausible that changes in TIMP protein levels observed in the infarct region of WT and ATM deficient mice could function in the remodeling processes of the heart independent of MMP-2 and -9.

ATM deficiency results in impaired repair of double-stranded DNA breaks and increased oxidative stress [26,46]. Deceased SOD levels impair the cell's response to handle reactive oxygen species following myocardial injury [47,48]. ATM is also known to phosphorylate p53 on serine-15 resulting in its stabilization. Stabilization of p53 increases its transcriptional activity, leading to increased apoptosis [49]. Here we observed greater increase in phosphorylation of p53 in the infarct region of ATM deficient hearts. On the other hand, SOD-2 protein levels were lower in ATM deficient hearts, suggesting enhanced oxidative stress during ATM deficiency. Enhanced oxidative stress and apoptosis was also observed in ARVMs during inhibition of ATM using KU-55933. It can be argued that increased p53 phosphorylation and oxidative stress should increase apoptosis in the infarct region of ATM deficient mice. We did observe increased apoptosis in the border area of ATM deficient mice. However, apoptosis was lower in the infarct region of ATM deficient mice. Inhibition of ATM and ATR failed to prevent H_2O_2-induced phosphorylation of p53 in neonatal cardiac myocytes [50]. In addition, graded

increases in the level of oxidative stress induce a graded phenotype shift in cardiac myocytes, from hypertrophy at low levels of oxidative stress, to apoptosis at high levels of oxidative stress [51]. Therefore, it is conceivable that p53 phosphorylation during ATM deficiency involves signaling pathways independent of ATM, and increased oxidative stress during ATM deficiency promotes cell growth in the infarct LV region at this time point.

Conclusion and study limitations

The data presented here provide evidence that ATM has the potential to modulate infarct tissue dynamics. It alters the infarct structure by affecting apoptosis, fibrosis, and expression of α-SMA. It should be emphasized that our data on investigating the role of ATM in myocardial remodeling post-MI are obtained 7 days post-MI. Changes in the size and thickness of infarct scar can eventually affect infarct expansion and contribute to the diastolic dysfunction. Therefore, it is possible that increased fibrosis (stiffness) and apoptosis (in the border area) in ATM deficient mice may associate with earlier diastolic dysfunction if the study time points are extended beyond 7 days post-MI.

Funding Statement

This work is supported by National Institutes of Health (Grant numbers R21HL-091405 and R21HL-092459), a Merit Review award (number BX000640) from the Biomedical Laboratory Research and Development Service of the VA Office of Research and Development, and institutional Research and Improvement funds. The funders had no role in study design, data collection and analysis, decision to publish, or preparation of the manuscript.

References

1. Frantz S, Bauersachs J, Ertl G (2009) Post-infarct remodelling: contribution of wound healing and inflammation. Cardiovasc Res 81: 474-481.

2. Hori M, Nishida K (2009) Oxidative stress and left ventricular remodelling after myocardial infarction. Cardiovasc Res 81: 457-464.

3. Kempf T, Zarbock A, Vestweber D, Wollert KC (2012) Anti-inflammatory mechanisms and therapeutic opportunities in myocardial infarct healing. J Mol Med (Berl) 90: 361-369.

4. Li YY, McTiernan CF, Feldman AM (2000) Interplay of matrix metalloproteinases, tissue inhibitors of metalloproteinases and their regulators in cardiac matrix remodeling. Cardiovasc Res 46: 214-224.

5. Spinale FG (2002) Matrix metalloproteinases: regulation and dysregulation in the failing heart. Circ Res 90: 520-530.

6. Abbate A, Narula J (2012) Role of apoptosis in adverse ventricular remodeling. Heart Fail Clin 8: 79-86.

7. Khanna KK, Lavin MF, Jackson SP, Mulhern TD (2001) ATM, a central controller of cellular responses to DNA damage. Cell Death Differ 8: 1052-1065.

8. Lavin MF, Khanna KK, Beamish H, Spring K, Watters D et al. (1995) Relationship of the ataxia-telangiectasia protein ATM to phosphoinositide 3-kinase. Trends Biochem Sci 20: 382-383.

9. Su Y, Swift M (2000) Mortality rates among carriers of ataxia-telangiectasia mutant alleles. Ann Intern Med 133: 770-778.

10. Foster CR, Singh M, Subramanian V, Singh K (2011) Ataxia telangiectasia mutated kinase plays a protective role in beta-adrenergic receptor-stimulated cardiac myocyte apoptosis and myocardial remodeling. Mol Cell Biochem 353: 13-22.

11. Foster CR, Zha Q, Daniel LL, Singh M, Singh K (2012) Lack of ataxia telangiectasia mutated kinase induces structural and functional changes in the heart: role in beta-adrenergic receptor-stimulated apoptosis. Exp Physiol 97: 506-515.

12. Yan M, Kuang X, Qiang W, Shen J, Claypool K et al. (2002) Prevention of thymic lymphoma development in Atm-/- mice by dexamethasone. Cancer Res 62: 5153-5157.

13. Barlow C, Hirotsune S, Paylor R, Liyanage M, Eckhaus M et al. (1996) Atm-deficient mice: a paradigm of ataxia telangiectasia. Cell 86: 159-171.

14. Krishnamurthy P, Subramanian V, Singh M, Singh K (2006) Deficiency of beta1 integrins results in increased myocardial dysfunction after myocardial infarction. Heart 92: 1309-1315.

15. Krishnamurthy P, Peterson JT, Subramanian V, Singh M, Singh K (2009) Inhibition of matrix metalloproteinases improves left ventricular function in mice lacking osteopontin after myocardial infarction. Mol Cell Biochem 322: 53-62.

16. Trueblood NA, Xie Z, Communal C, Sam F, Ngoy S et al. (2001) Exaggerated left ventricular dilation and reduced collagen deposition after myocardial infarction in mice lacking osteopontin. Circ Res 88: 1080-1087.

17. Krishnamurthy P, Subramanian V, Singh M, Singh K (2007) Beta1 integrins modulate beta-adrenergic receptor-stimulated cardiac myocyte apoptosis and myocardial remodeling. Hypertension 49: 865-872.

18. Daniels CR, Foster CR, Yakoob S, Dalal S, Joyner WL et al. (2012) Exogenous ubiquitin modulates chronic β-adrenergic receptor-stimulated myocardial remodeling: role in Akt activity and matrix metalloproteinase expression. Am J Physiol Heart Circ Physiol 303: H1459-68

19. Dalal S, Foster CR, Das BC, Singh M, Singh K (2012) Beta-adrenergic receptor stimulation induces endoplasmic reticulum stress in adult cardiac myocytes: role in apoptosis. mol Cell Biochem 364:59-70.

20. Zakikhani M, Bazile M, Hashemi S, Javesghani S, Avizonis D et al. (2012). Alterations in cellular energy metabolism associated with the antiproliferative effects of the ATM inhibitor KU-55933 and with metformin. PLoS One 7:e49513

21. Chen W, Frangogiannis NG (2012) Fibroblasts in post-infarction inflammation and cardiac repair. Biochim Biophys Acta .

22. Frangogiannis NG, Michael LH, Entman ML (2000) Myofibroblasts in reperfused myocardial infarcts express the embryonic form of smooth muscle myosin heavy chain (SMemb). Cardiovasc Res 48: 89-100.

23. Willems IE, Havenith MG, De Mey JG, Daemen MJ (1994) The alpha-smooth muscle actin-positive cells in healing human myocardial scars. Am J Pathol 145: 868-875.

24. Greene J, Wang M, Liu YE, Raymond LA, Rosen C et al. (1996) Molecular cloning and characterization of human tissue inhibitor of metalloproteinase 4. J Biol Chem 271: 30375-30380.

25. Banin S, Moyal L, Shieh S, Taya Y, Anderson CW et al. (1998) Enhanced phosphorylation of p53 by ATM in response to DNA damage. Science 281: 1674-1677.

26. Barzilai A, Rotman G, Shiloh Y (2002) ATM deficiency and oxidative stress: a new dimension of defective response to DNA damage. DNA Repair (Amst) 1: 3-25.

27. Valentin-Vega YA, Maclean KH, Tait-Mulder J, Milasta S, Steeves M et al. (2012) Mitochondrial dysfunction in ataxia-telangiectasia. Blood 119: 1490-1500.

28. Lin CS, Wang YC, Huang JL, Hung CC, Chen JY (2012) Autophagy and reactive oxygen species modulate cytotoxicity induced by suppression of ATM kinase activity in head and neck cancer cells. Oral Oncol. 48:1152-8

29. Yang XP, Liu YH, Rhaleb NE, Kurihara N, Kim HE et al. (1999) Echocardiographic assessment of cardiac function in conscious and anesthetized mice. Am J Physiol 277: H1967-H1974.

30. Li Y, Takemura G, Okada H, Miyata S, Kanamori H et al. (2007) ANG II type 1A receptor signaling causes unfavorable scar dynamics in the postinfarct heart. Am J Physiol Heart Circ Physiol 292: H946-H953.

31. Okada H, Takemura G, Kosai K, Li Y, Takahashi T et al. (2005) Postinfarction gene therapy against transforming growth factor-beta signal modulates infarct tissue dynamics and attenuates left ventricular remodeling and heart failure. Circulation 111: 2430-2437.

32. Chen W, Frangogiannis NG (2010) The role of inflammatory and fibrogenic pathways in heart failure associated with aging. Heart Fail Rev 15: 415-422.

33. Bialik S, Geenen DL, Sasson IE, Cheng R, Horner JW et al. (1997) Myocyte apoptosis during acute myocardial infarction in the mouse localizes to hypoxic regions but occurs independently of p53. J Clin Invest 100: 1363-1372.

34. Colucci WS (1997) Molecular and cellular mechanisms of myocardial failure. Am J Cardiol 80: 15L-25L.

35. Frangogiannis NG (2012) Regulation of the inflammatory response in cardiac repair. Circ Res 110: 159-173.

36. Lovelock JD, Baker AH, Gao F, Dong JF, Bergeron AL et al. (2005) Heterogeneous effects of tissue inhibitors of matrix metalloproteinases on cardiac fibroblasts. Am J Physiol Heart Circ Physiol 288: H461-H468.

37. Cleutjens JP, Kandala JC, Guarda E, Guntaka RV, Weber KT (1995) Regulation of collagen degradation in the rat myocardium after infarction. J Mol Cell Cardiol 27: 1281-1292.

38. Creemers EE, Cleutjens JP, Smits JF, Daemen MJ (2001) Matrix metalloproteinase inhibition after myocardial infarction: a new approach to prevent heart failure? Circ Res 89: 201-210.

39. Ducharme A, Frantz S, Aikawa M, Rabkin E, Lindsey M et al. (2000) Targeted deletion of matrix metalloproteinase-9 attenuates left ventricular enlargement and collagen accumulation after experimental myocardial infarction. J Clin Invest 106: 55-62.

40. Sutton MG, Sharpe N (2000) Left ventricular remodeling after myocardial infarction: pathophysiology and therapy. Circulation 101: 2981-2988.

41. Tao ZY, Cavasin MA, Yang F, Liu YH, Yang XP (2004) Temporal changes in matrix metalloproteinase expression and inflammatory response associated with cardiac rupture after myocardial infarction in mice. Life Sci 74: 1561-1572.

42. Mukherjee R, Snipes JM, Saunders SM, Zavadzkas JA, Spinale FG (2012) Discordant activation of gene promoters for matrix metalloproteinases and tissue inhibitors of the metalloproteinases following myocardial infarction. J Surg Res 172: 59-67.

43. Mukherjee R, Mingoia JT, Bruce JA, Austin JS, Stroud RE et al. (2006) Selective spatiotemporal induction of matrix metalloproteinase-2 and matrix metalloproteinase-9 transcription after myocardial infarction. Am J Physiol Heart Circ Physiol 291: H2216-H2228.

44. Goldberg GI, Marmer BL, Grant GA, Eisen AZ, Wilhelm S et al. (1989) Human 72-kilodalton type IV collagenase forms a complex with a tissue inhibitor of metalloproteases designated TIMP-2. Proc Natl Acad Sci U S A 86: 8207-8211.

45. Mishra PK, Metreveli N, Tyagi SC (2010) MMP-9 gene ablation and TIMP-4 mitigate PAR-1-mediated cardiomyocyte dysfunction: a plausible role of dicer and miRNA. Cell Biochem Biophys 57: 67-76.

46. Tanaka T, Halicka HD, Huang X, Traganos F, Darzynkiewicz Z (2006) Constitutive histone H2AX phosphorylation and ATM activation, the reporters of DNA damage by endogenous oxidants. Cell Cycle 5: 1940-1945.

47. Chen Y, Hou M, Li Y, Traverse JH, Zhang P et al. (2005) Increased superoxide production causes coronary endothelial dysfunction and depressed oxygen consumption in the failing heart. Am J Physiol Heart Circ Physiol 288: H133-H141.

48. Obal D, Dai S, Keith R, Dimova N, Kingery J et al. (2012) Cardiomyocyte-restricted overexpression of extracellular superoxide dismutase increases nitric oxide bioavailability and reduces infarct size after ischemia/reperfusion. Basic Res Cardiol 107: 305.

49. Meulmeester E, Jochemsen AG (2008) p53: a guide to apoptosis. Curr Cancer Drug Targets 8: 87-97.

50. Long X, Goldenthal MJ, Marin-Garcia J (2007) Oxidative stress enhances phosphorylation of p53 in neonatal rat cardiomyocytes. Mol Cell Biochem 303: 167-174.

51. Siwik DA, Tzortzis JD, Pimental DR, Chang DL, Pagano PJ et al. (1999) Inhibition of copper-zinc superoxide dismutase induces cell growth, hypertrophic phenotype, and apoptosis in neonatal rat cardiac myocytes in vitro. Circ Res 85: 147-153.

CHAPTER 4

ATAXIA TELAGIECTASIA MUTATED KINASE DEFICIENCY EXACERBATES CARDIAC REMODELING 28 DAYS FOLLOWING MYOCARDIAL INFARCTION

Laura L. Daniel, BS[1]; Cerrone R. Foster, PhD[1,2]; Christopher R. Daniels, PhD[1]; Stephanie LC Scofield B.A. [1]; Mahipal Singh, PhD[1]; Krishna Singh, PhD[1,3]

[1]Department of Biomedical Sciences, James H Quillen College of Medicine
[2]Department of Biological Sciences
[3]James H Quillen Veterans Affairs Medical Center
East Tennessee State University
Johnson City, TN 37614

Running title: ATM and myocardial infarction

Total number of figures: 10

Number of Tables: 1

Key words: ATM, ataxia telangiectasia mutated kinase, cardiac remodeling, fibrosis, apoptosis, hypertrophy, myocardial infarction, senescence,

*__Correspondence__: Krishna Singh, Ph.D.
Department of Biomedical Sciences
James H Quillen College of Medicine
East Tennessee State University
PO Box 70582, Johnson City, TN 37614
Ph: 423-439-2049
Fax: 423-439-2052
E-mail: singhk@etsu.edu

Abstract

BACKGROUND: Ataxia telangiectasia mutated kinase (ATM) is a serine/threonine kinase that phosphorylates several proteins in response to cellular stressors such as DNA damage and oxidative stress. We have previously shown that deficiency of ATM associates with increased apoptosis, increased fibrosis and attenuation of cardiac dysfunction 1, 3 and 7 days following myocardial infarction (MI). Here we investigated the role of ATM in cardiac remodeling 14 and 28 days post-MI. **METHODS AND RESULTS:** Left ventricle (LV) structure and function were measured in wild-type (WT) and ATM heterozygous knock (hKO) mice 14 and 28 days post-MI. Biochemical parameters were measured 28 days post-MI. MI resulted in cardiac dysfunction in both genotypes, as measured by a decrease in percent fractional shortening (%FS) and ejection fraction (EF). However, the decrease in %FS and EF was greater in the hKO-MI group versus the WT-MI group. ATM deficiency had no effect on infarct size or infarct thickness. However, the hKO group exhibited a tendency towards decreased survival post-MI. Fibrosis and expression of α-smooth muscle actin was greater in the hKO-MI infarct region, while apoptosis was greater in the WT-MI infarct region. MI-induced increases in myocyte cross-sectional area were greater in the hKO-MI group versus the WT-MI. Activation of glycogen synthase kinase-3β (GSK-3β) was significantly lower in the infarct region of the hKO-MI group versus the WT-MI group. Activation of extracellular signal-regulated kinases (ERK1/2) were significantly lower in the non-infarct region of the hKO-MI group versus WT-MI group. Expression of Beclin-1, a marker for autophagy, was greater in the hKO-sham as well as the non-infarct region of the hKO-MI. Matrix metalloprotesase-2 (MMP-2) expression was not different between the two genotypes. However, MMP-9 expression was significantly lower in the non-infarct region of the hKO-MI group versus the WT-MI group. The hKO-MI sham group

exhibited increased levels of cell senescence marker p16 when compared to the WT-sham group. However, the hKO-MI group exhibited decreased expression of p16 in the infarct region versus the WT-MI group. **CONCLUSION:** ATM deficiency worsened cardiac remodeling late post-MI with increased cardiac dysfunction, fibrosis and myocyte hypertrophy. It also associated with decreased cardiac cell apoptosis and senescence, which may have resulted in enhanced survival of myofibroblasts leading to increased fibrosis and cardiac dysfunction.

Introduction

Following myocardial infarction (MI), the heart undergoes a remodeling process whereby the architecture and composition of the left ventricle (LV) changes. Factors affecting these changes include myocyte hypertrophy, myocyte apoptosis, myofibroblast proliferation and interstitial fibrosis (Konstam et al., 2011). During the early stages of LV repair, there is differentiation of fibroblasts into myofibroblasts. The myofibroblast is a very proliferative cell type that secretes the majority of the collagen that ultimately forms the post-MI scar (Turner & Porter, 2013). Increases in autophagy can act as a source of ATP during the ischemia-induced energy shortage (Nishida et al., 2009). The early changes in LV architecture include formation of a scar and thinning of the infarct region (Konstam et al., 2011). During the later stages of cardiac remodeling, cross-linking of the newly formed scar occurs resulting in a reduction of myofibroblasts from the infarct region. This reduction of myofibroblasts from the wound can occur as a result of apoptosis (Y Sun & Weber, 1996; Willems et al., 1994) and/or senescence. Senescence of myofibroblasts inhibits their ability to proliferate and also signals for their removal by natural killer (NK) cells. However, mice deficient in p16, a regulator of senescence, exhibit increased fibrosis in the heart (Jun & Lau, 2010). The resulting scar is composed of the remaining myofibroblasts which continue to turn over type I and type III fibrillar collagen long after the scar has restored structural integrity to the infarcted myocardium (Yao Sun et al., 2002). MI-induced increases in autophagy during the later stages of remodeling often results in the accumulation of autophagosomes and is considered to be a contributing factor leading to myocyte death, hypertrophy and heart failure (Nishida et al., 2009). The later stages of structural remodeling are predominated by myocyte elongation in the non-infarcted zone, increased septal wall mass, chamber enlargement and a shift from an elliptical to a more spherical configuration

of the LV chamber. The changes in myocyte size as well as increases in interstitial fibrosis ultimately result in a progressive decline in ventricular performance eventually leading to heart failure (Konstam et al., 2011).

Ataxia telangiectasia mutated kinase (ATM) is activated in response to DNA damage. Following DNA damage, ATM phosphorylates several proteins involved in cell cycle arrest, DNA repair and apoptosis (Nowak-Wegrzyn, et al., 2004). Mutations in the ATM gene cause the autosomal recessive disorder known as ataxia-telangiectasia (AT). AT individuals exhibit neuronal degeneration and are at increased risk for developing cancer (Taylor & Byrd, 2005). Carriers of only one mutated allele do not exhibit neuronal degeneration but are predisposed to cancer and ischemic heart disease, and die earlier than non-carriers as a result (Su & Swift, 2000). Previously, we examined the role of ATM in cardiac remodeling during the inflammatory and proliferative phases of the post-MI healing process. ATM deficiency was shown to attenuate cardiac dysfunction. In addition, ATM deficiency was associated with increased cardiac cell apoptosis and fibrosis post-MI (Daniel et al., 2014; Foster et al., 2013). Although, early increase in fibrosis post-MI is suggested to help maintain heart function, it can ultimately result in cardiac dysfunction (See et al., 2013). Apoptosis also associates with a negative post-MI outcome while inhibition of cardiac cell apoptosis is shown to reduce infarct size and preserve ventricular function (Holly et al., 1999; Rivard et al., 2007; Zhao et al., 2003). Here, we tested the hypothesis that enhanced fibrosis and apoptosis, as observed early post-MI during ATM deficiency, would result in greater cardiac dysfunction late post-MI in the ATM deficient group. These data presented here demonstrate that ATM deficiency exacerbates cardiac remodeling 28 days post-MI with effects on LV function, fibrosis, apoptosis and myocyte hypertrophy. ATM

deficiency also affected the expression and/or activation of proteins involved in apoptosis, fibrosis, hypertrophy, senescence and autophagy.

Methods

Vertebrate Animals:

This investigation conforms to The Guide for the Care and Use of Laboratory Animals published by the US National Institutes of Health (NIH Publication No. 85-23, revised 1996). The East Tennessee State University Animal Care and Use Committee approved all animal protocols. ATM transgenic mice (129xblack Swiss hybrid background) were originally purchased from Jackson Laboratory and created as previously described (Barlow et al., 1996). Aged-matched (~ 4-month-old) male and female mice were used for this study. ATM heterozygous knockout (hKO) mice were used in this study because homozygous (KO) mice die at approximately 2 months of age, mainly due to thymic lymphomas (Barlow et al., 1996). Genotyping was performed by PCR using primers suggested by Jackson Laboratory.

Myocardial infarction MI:

MI was performed as previously described (Daniel et al., 2014). In brief, mice were anesthetized using 2% isoflurane inhalation and oxygen (0.5 L/min) and ventilated using a rodent ventilator. Body temperature was maintained at ~ 37ºC using a warmed platform. Hearts were exposed by a left thoracotomy followed by ligation of the left anterior descending artery (LAD) with a 7-0 polypropylene suture. Mice in the sham group underwent the same procedure without ligation of the LAD. At the end of the study period (28 days) hearts were used for either histology or molecular analysis.

Echocardiography:

Echocardiographic measurements were recorded 14 days and 28 days post-MI using a Toshiba Aplio 80 Imaging System (Tochigi, Japan) equipped with a 12 MHz linear transducer as previously described (Daniel et al., 2014). An individual blinded to the experimental groups recorded the images, while a second individual assessed the images and calculated the functional parameters of the heart.

Morphometric analyses:

Following MI, hearts were perfused with Krebs buffer and stopped in diastole using KCL (30 mmol/L). Hearts were then fixed using 10% buffered formalin. Each heart was divided into 3 transverse sections (base, mid and apex) and embedded in paraffin. Tissue sections were stained using Masson's Trichrome stain in order to determine infarct size. Percent infarct size was determined by summing the midline infarct lengths of 3 histological sections and dividing them by the sum of the midline LV circumference and multiplying by 100 (Nascimento et al., 2011). Masson's Trichrome-stained sections were also used to determine percent fibrosis. For this, images were obtained from at least five frames of the infarcted LV. Percent fibrosis was calculated by dividing total fibrosis by total tissue area and multiplying by 100.

Terminal deoxynucleotidyl transferase nick end labeling (TUNEL) assay:

TUNEL staining was carried out according to manufacturer's instruction (Cell death detection assay; Roche). Sections (4 µm thick) were stained with Hoechst 33258 (Sigma) to identify nuclei and with rhodamine-conjugated wheat germ agglutinin (WGA) to identify myocytes. Apoptosis

was calculated as the total number of apoptotic cells divided by the total number of nuclei and multiplied by 100.

Immunohistochemistry:

Cross-sections of the heart (4 μm thick) were deparaffinized with xylene then rehydrated with graded ethanol rinses. Immunohistochemical staining for myofibroblasts was performed using anti-α-smooth muscle actin (α-sma) antibodies (Sigma). All images were acquired using a Nikon TE-2000 microscope with an Andor Zyla sCMOS camera. Quantitative analysis was carried out using Nikon's NIS-Elements software.

Myocyte Cross-Sectional Area

Cross-sections of the heart (4 μm thick) were stained with rhodamine-conjugated WGA to measure myocyte cross-sectional area. Images were acquired using fluorescent microscopy and recorded using an Andor Zyla sCMOS camera. Suitable area of the section was defined as myocytes with nearly circular profiles. Myocyte cross-sectional areas were measured using Nikon's NIS-Elements software as described (Daniel et al., 2014).

Western Blot Analysis:

LV lysates were prepared in RIPA buffer, separated by SDS-PAGE and transferred to a PVDF membrane. Following an initial blocking using either 5% non-fat milk or 2% BSA in TBST, the membranes were then incubated overnight with antibodies against p16, Beclin-1, MMP-2, MMP-9 (Santa Cruz), p-GSK-3β (Ser9) and p-ERK1/2 (Thr202, Tyr204) (Cell Signaling). GAPDH

(Santa Cruz) immunostaining was used as a protein loading control. Band intensities were quantified using Kodak photo documentation system.

Statistical Analyses:

Data are represented as mean ± SEM. Data were tested for normality using a Shapiro-Wilk test. Multiple comparisons were analyzed using either one-way ANOVA or a Kruskal-Wallis test. All pairwise comparisons were carried out using either a one-tailed student's t-test or a Mann-Whitney U-test. Survival analysis was performed using log rank test. Probability (P) values of <0.05 were considered to be significant.

Results

Survival and Morphological Analyses

There was no significant difference in infarct size (% infarct-size; WT 38.8 ± 3.5; hKO 38.0 ± 3.8; p = ns; n = 7- 9) or infarct width (WT 48.9 ± 11.1 µm; hKO 43.2 ± 4.1 µm; p = ns; n = 7- 9) between the two groups 28 days post-MI. The survival rate between the two genotypes was not different 1-7 days post-MI. At 7 days post-MI survival in WT and hKO group was 55.2% (WT, 37/67) and 52.9% (hKO, 37/70), respectively. Interestingly, Kaplan-Meier analysis showed survival rates of 52.2% in the WT-MI and 40.0% in hKO 28 days post-MI (Fig 4.1; p=0.228).

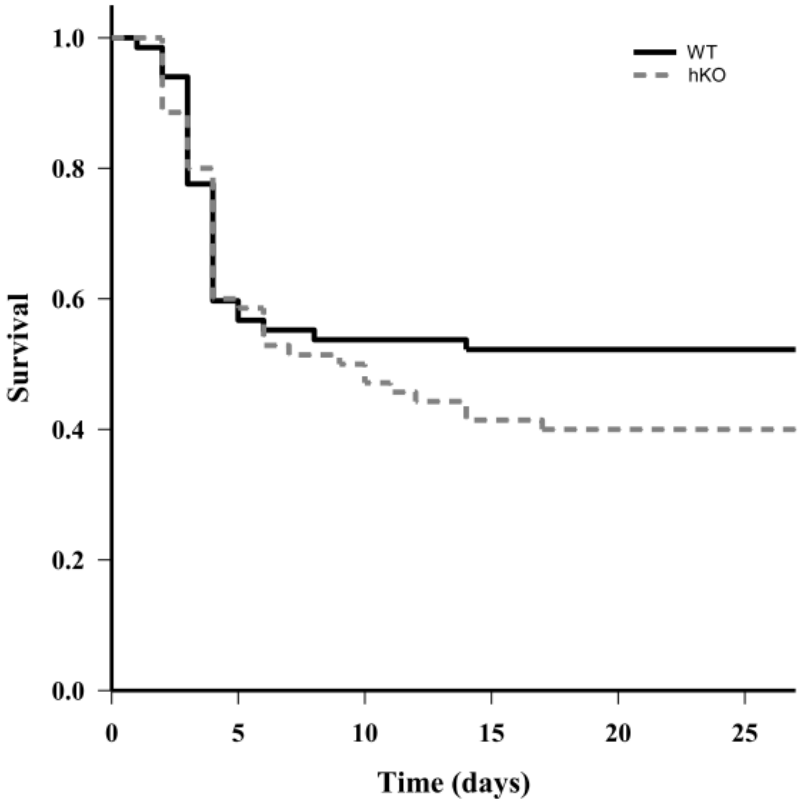

Figure 4.1. Kaplan Meyer survival curve. WT, wild-type mice; hKO heterozygous knockout mice

There was no significant difference in the body weight (BW) between the two genotypes. Both MI groups had a significant increase in heart weight (HW) and HW/BW ratio when compared to their respective sham groups, with no significant difference between the two genotypes (Table 4.1).

Table 4.1. Morphometric Measurements 28 Days Post-MI

	Body Weight	Heart Weight	HW/BW
WT-Sham (N=8)	25.89 ± 0.60	107.66 ± 3.21	4.16 ± 0.05
hKO-Sham (N=9)	28.90 ± 1.57	119.29 ± 13.68	4.57 ± 0.21
WT-MI (N=21)	25.36 ± 0.73	158.27 ± 9.90 #	6.67 ± 0.46 #
hKO-MI (N=22)	26.03 ± 0.67	158.92 ± 6.00 #	6.13 ± 0.20 #

Values are mean ±SEM; #P<0.05 vs sham. WT, wild-type; hKO, heterozygous; MI, myocardial infarction

Echocardiographic studies

There was no significant difference in ejection fraction (EF) between the two sham groups. However, the WT-sham group exhibited slightly higher percent fractional shortening (%FS) when compared with the hKO-sham group. Percent FS and EF decreased in both MI groups when compared to their respective sham group 14 and 28 days post-MI. Interestingly, the decrease in %FS and EF was significantly greater in the hKO-MI group when compared to the WT-MI group at both time points (Fig 4.2).

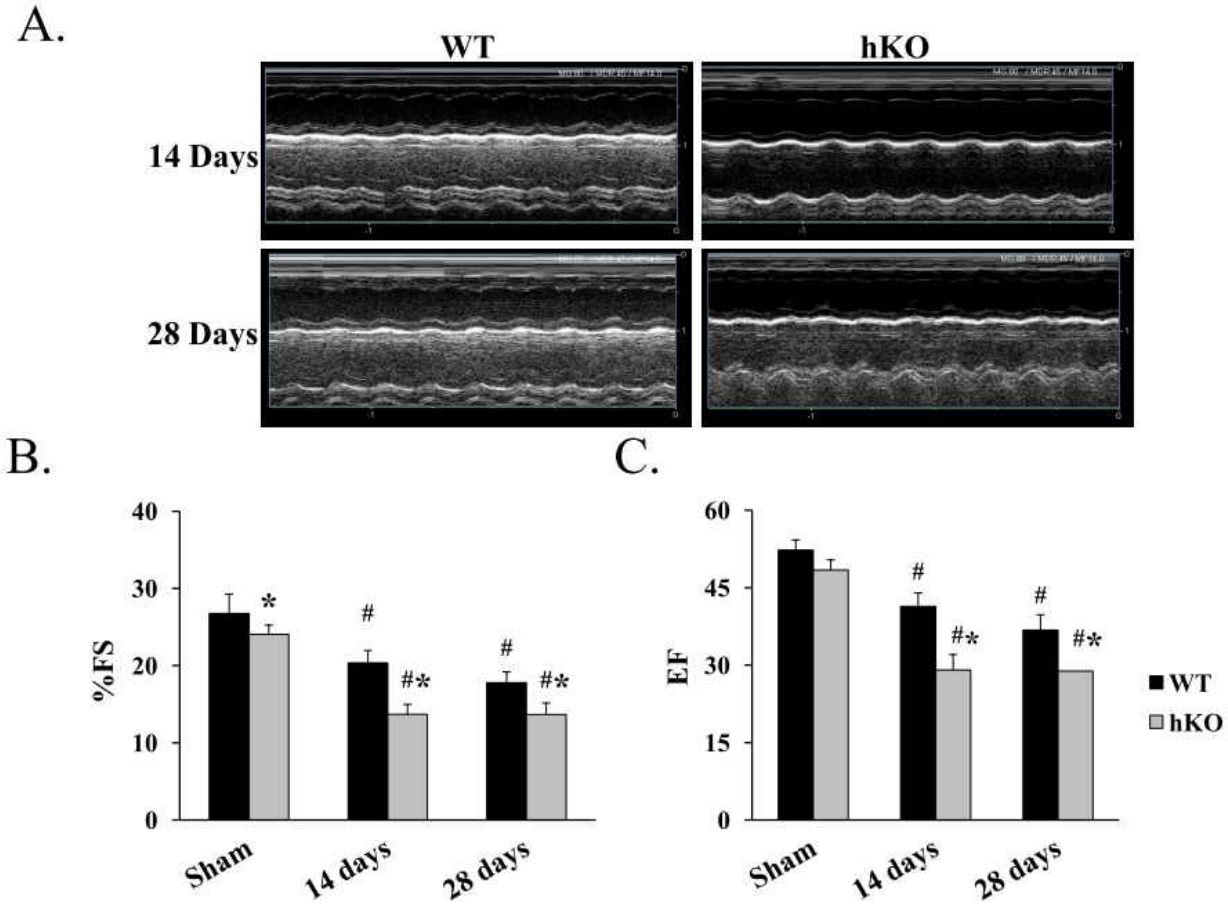

Figure 4.2. ATM deficiency worsens LV function post-MI. A. M-mode echocardiographic images. B. Indices of cardiac function percent fractional shortening (%FS) and ejection fraction (EF) were calculated using echocardiographic images 14 and 28 days post-MI. $^{\#}P<0.001$ vs Sham, $^{*}P<0.05$ vs WT; n=7-11.

Quantitative measurement of fibrosis using Mason's Trichrome-stained sections showed that the hKO-sham group exhibited increased fibrosis in the infarct region when compared to the WT-sham group. At 28 days post-MI, there was a significant increase in fibrosis in the non-infarct and infarct region of both genotypes when compared to their respective sham groups. However, the increased infarct fibrosis was significantly greater in the hKO-MI group when compared to the WT-MI group. There was no significant difference in fibrosis in the non-infarct region between the two genotypes (Fig 4.3).

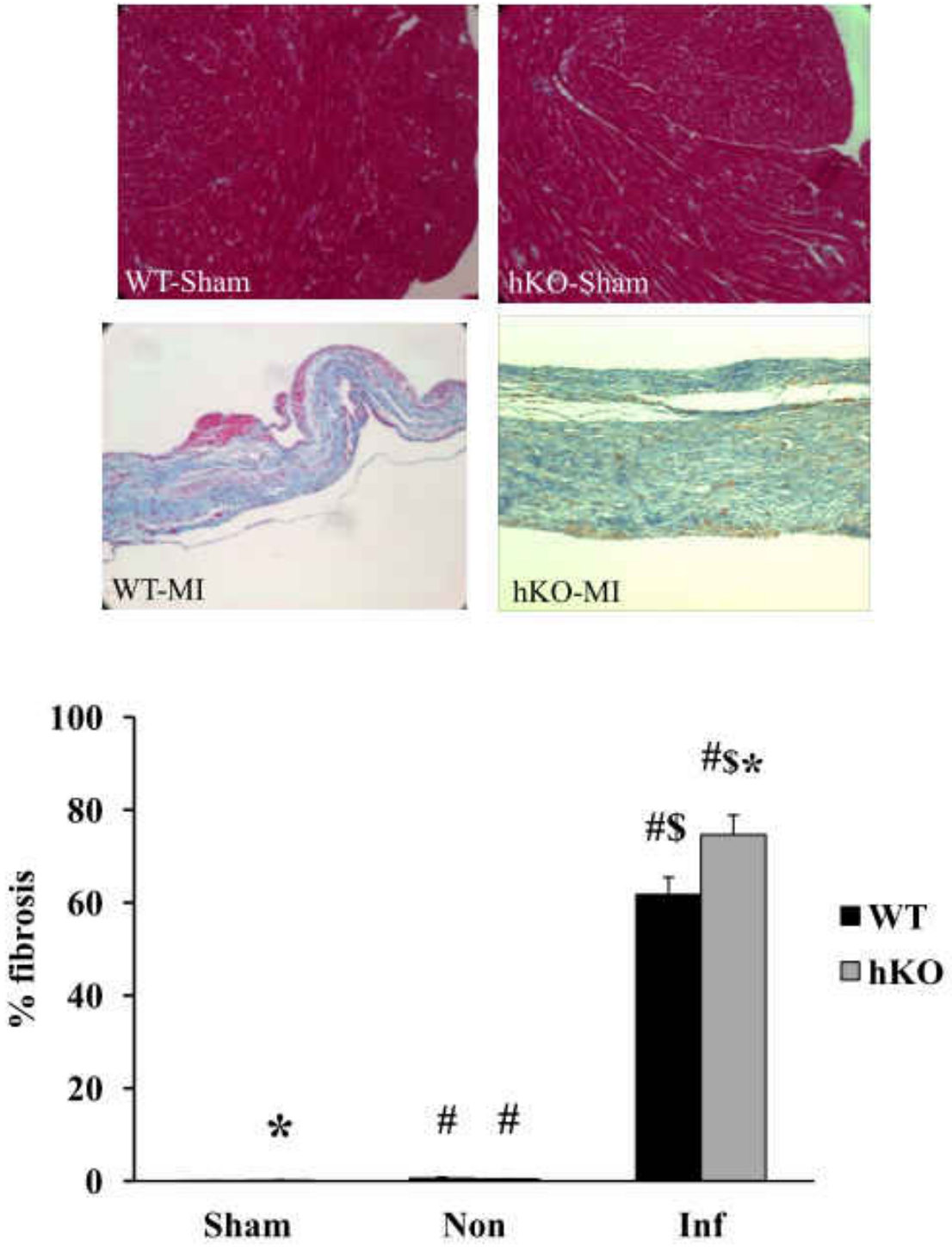

Figure 4.3. ATM deficiency results in increased fibrosis. The upper panels depict Masson's trichrome-stained heart sections of WT and hKO (sham and infarct region 28 days post-MI). Lower panel exhibits quantitative analysis of fibrosis. $^{\#}P<0.05$ vs Sham, $^{\$}P<0.05$ vs non-infarct; $^{*}P<0.05$ vs WT-MI; n=6-8. Non, non-infarct; Inf, infarct.

There was no significant difference in the total cardiac cell apoptosis between the two sham groups. Apoptosis was significantly higher in the non-infarct and infarct regions of both genotypes at 28 days post-MI when compared to their respective sham groups. There was no significant difference in apoptosis between the two genotypes in the non-infarct region. However, apoptosis was significantly higher in the infarct region of the WT-MI group when compared to the hKO-MI group (Fig 4.4). Myocyte apoptosis was not significantly different between the two genotypes in the sham groups or in the non-infarct regions (data not shown).

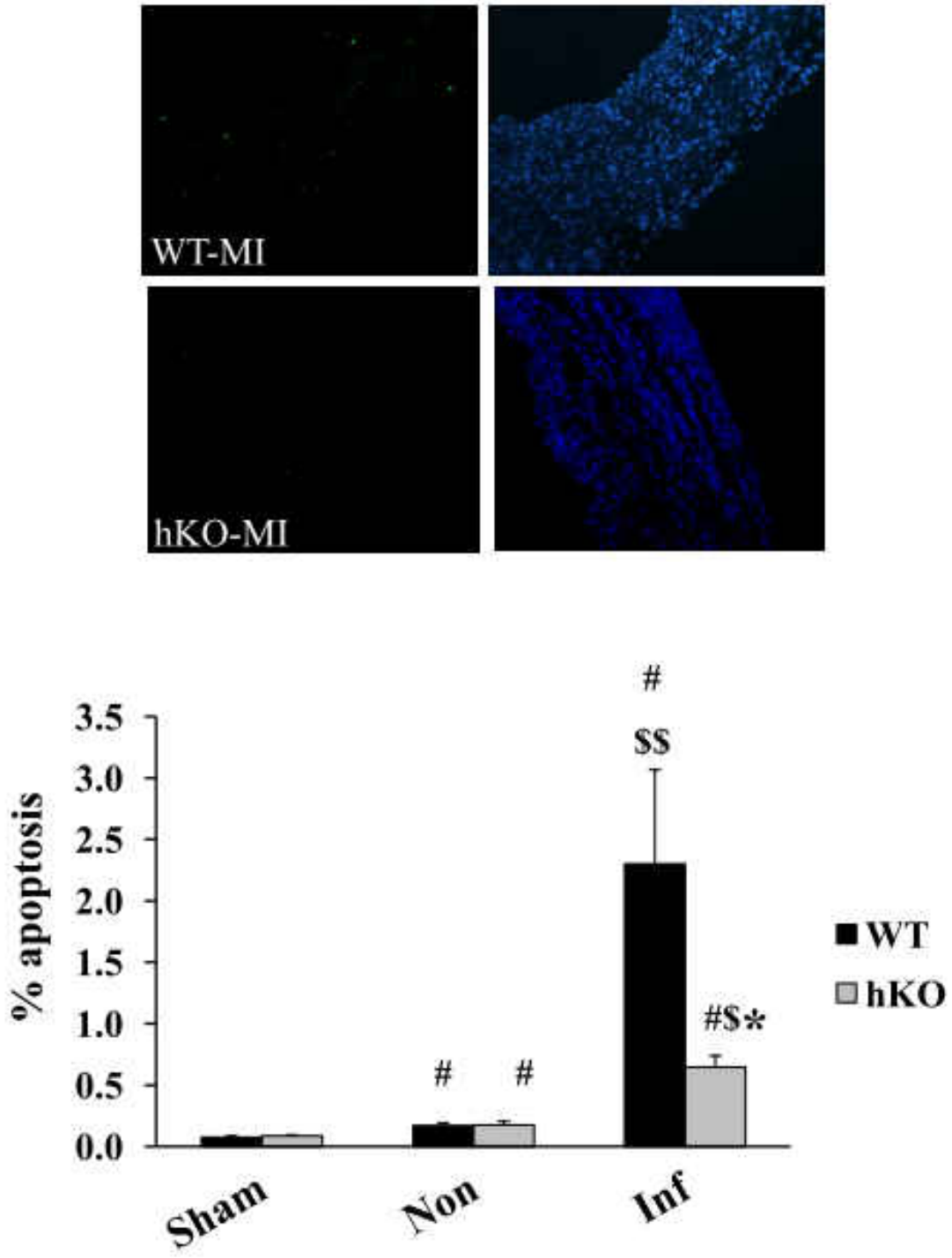

Figure 4.4. ATM deficiency decreases apoptosis in the infarct region 28 days post-MI. Upper panels depict TUNEL-stained (left) and Hoechst-stained (right) images obtained from WT (top) and hKO (bottom) hearts post-MI. Green fluorescent staining indicates TUNEL-positive (apoptotic) nuclei, while blue fluorescent staining indicates total number of nuclei. The lower panel exhibits quantitative analysis. $^{\#}P<0.05$ vs Sham, $^{*}P<0.05$ vs WT, $^{\$}P<0.05$ vs Non; n=5-8.

Myocyte cross-sectional area was greater in the hKO-sham group when compared to the WT-sham group. Following MI, there was a significant increase in myocyte cross-sectional area in both genotypes when compared to their respective sham groups. However, myocyte cross-sectional area in the non-infarct region was significantly larger in the hKO-MI group when compared to the WT-MI group (Fig 4.5).

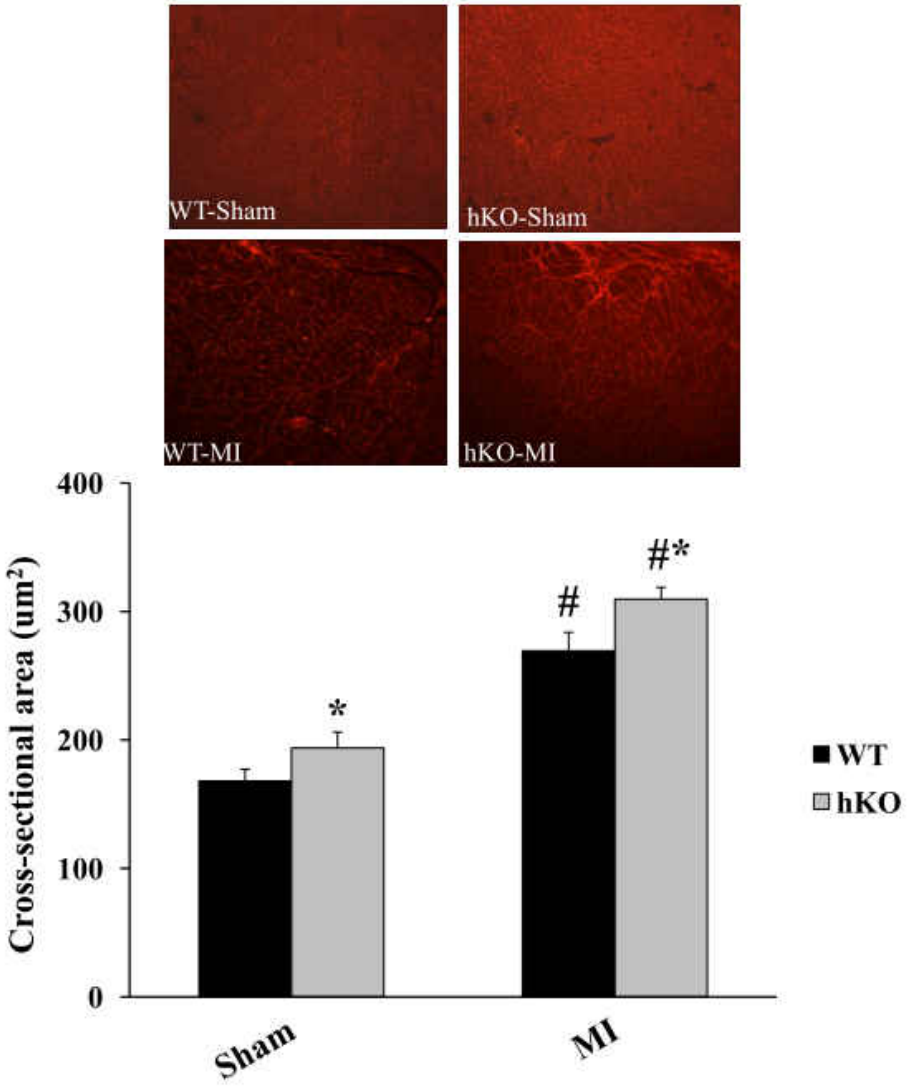

Figure 4.5. ATM deficiency increases myocyte cross-sectional area. Cross-sections of the heart were stained using rhodamine-conjugated anti-WGA. Upper panels depicts WGA-stained images from the sham (top) and the non-infarct regions (bottom) of WT (left) and hKO (right) hearts post-MI. Lower panel exhibits quantitative analysis of myocyte cross-sectional areas in the sham and the non-infarct regions 28 days post-MI. $^{\#}P<0.001$ vs Sham, $^{*}P<0.05$ vs WT; n=7-8.

Expression of α-Smooth Muscle Actin (α-sma)

Myofibroblasts are the main producers of collagen post-MI. Expression of α-sma is commonly used to identify myofibroblasts (Eddy, Petro, & Tomasek, 1988). There was no significant difference in α-sma expression between the two sham groups. Twenty-eight days post-MI, α-sma expression was significantly greater in the infarct region of both genotypes when compared to their respective sham groups or their non-infarct regions. However, α-sma expression was significantly higher in the infarct region of the hKO-MI group versus the WT-MI group (Fig 4.6).

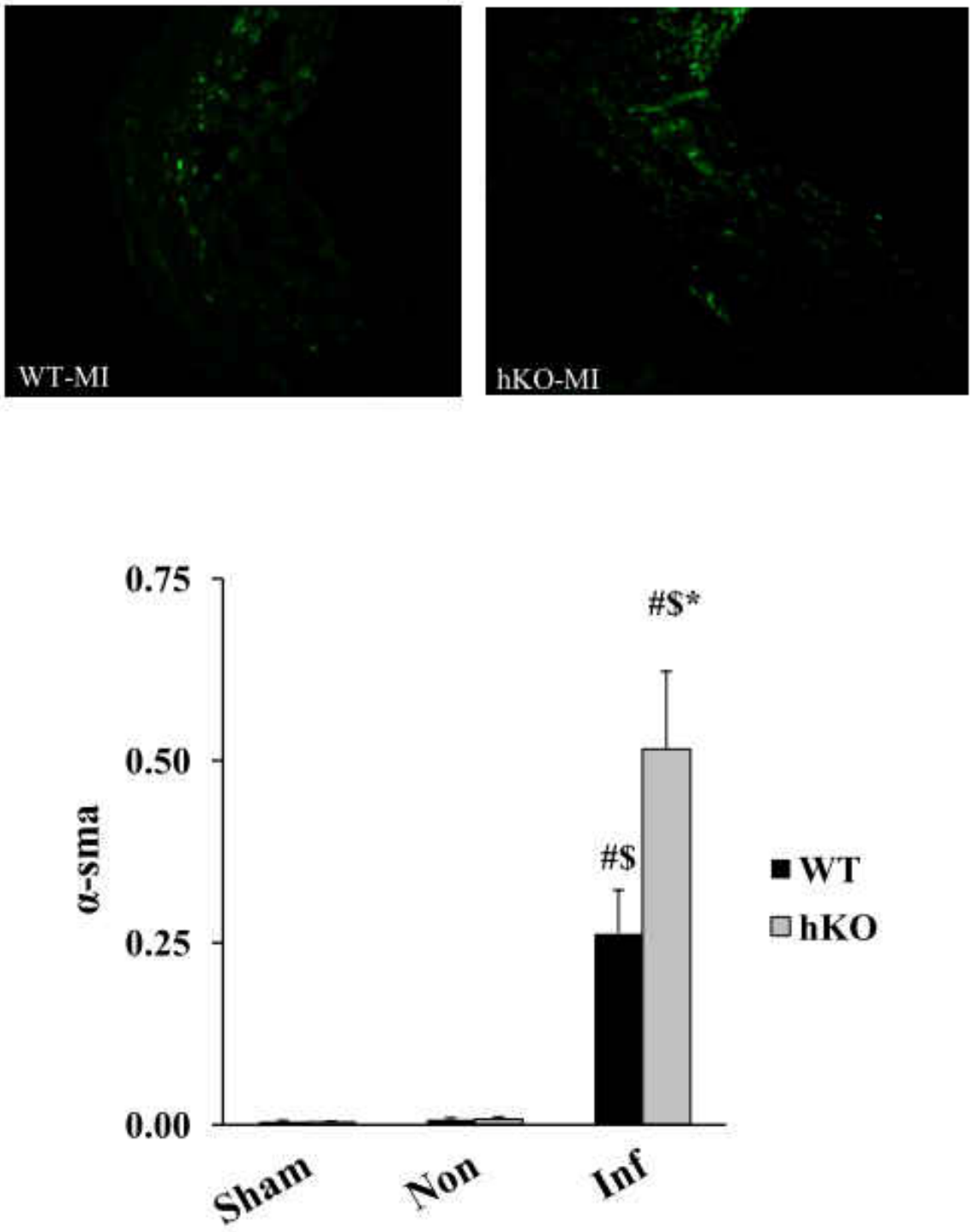

Figure 4.6. ATM deficiency increases α-sma expression 28 days post-MI. Cross-sections of the hearts were immunostained using anti-α-sma antibodies. Upper panel depicts α-sma-stained images from the infarct regions of WT and hKO hearts 28 days post-MI. Lower panel exhibits quantitative Immunohistochemical analysis of α-sma expression. $^{\#}P<0.01$ vs Sham, $^{\$}P<0.01$ vs Non-infarct, $^{*}P<0.05$ vs WT; n=6-7.

Phosphorylation of GSK-3β and ERK1/2.

Glycogen synthase kinase-3β (GSK-3β) is a pro-apoptotic kinase that is inactivated by phosphorylation at serine-9 (Sutherland et al., 1993). This inactivation of GSK-3β by phosphorylation remained unchanged between the sham groups and non-infarct regions of the two groups 28 days post-MI. However, GSK-3β phosphorylation was significantly lower in the infarct region of the WT-MI group when compared to the infarct region of the hKO-MI, suggesting enhanced activation of GSK-3β in the WT-MI groups (Fig 4.7A).

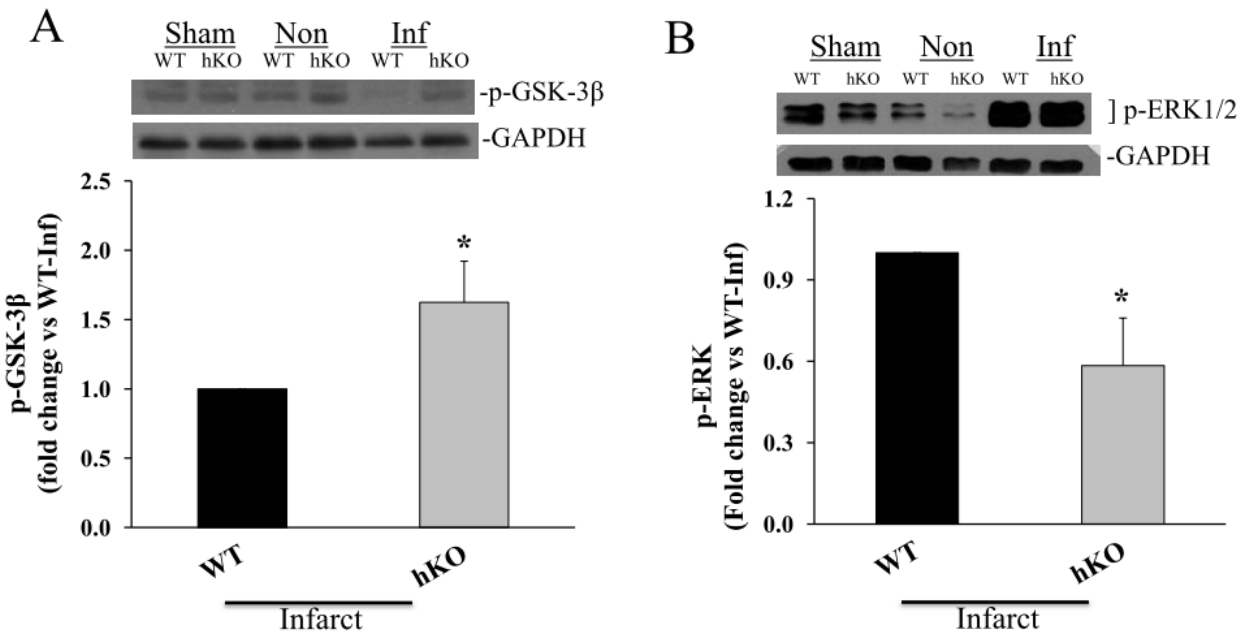

Figure 4.7. ATM deficiency decreases GSK-3β and ERK1/2 activities 28 days post-MI. Total LV lysates, prepared from sham and non-infarct and infarct LV regions post-MI, were analyzed by western blot using phospho-specific antibodies for GSK-3β (Ser9) and ERK1/2 (Thr202, Tyr204). The upper panels depict autoradiograms immunostained for p-GSK-3β, p-ERK1/2 and GAPDH. The lower panels exhibit quantitative analyses of p-GSK-3β (n=8) and p-ERK1/2 (n=8) normalized to GAPDH.*P<0.05 vs WT-Inf.

Activation of ERK1/2 plays a role in cell proliferation, differentiation, apoptosis and cardiac hypertrophy (Bueno et al., 2000; Lin et al., 2013). ERK1/2 phosphorylation (activation) remained unchanged between the sham groups. At twenty-eight days post-MI, there was a significant increase in ERK1/2 activation in the infarct region of both genotypes with no difference between the two genotypes. However, phosphorylation of ERK1/2 was significantly lower in the non-infarct region of the hKO-MI group when compared to the WT-MI group (Figure 4.7B).

Expression of Beclin-1 and p16

Increased Beclin-1 expression associates with increased autophagy. Mice deficient in Beclin-1 exhibit decreased autophagy and attenuated pathological remodeling following myocardial ischemia/reperfusion injury and aortic banding (Matsui et al., 2007; Zhu et al., 2007). Beclin-1 protein levels were significantly higher in the hKO-sham group when compared to the WT-sham group. Following MI, Beclin-1 protein levels stayed higher in the non-infarct region of the hKO-MI group when compared to the WT-MI group (Figure 4.8). However, no significant difference in Beclin-1 expression was observed in the infarct region between the two genotypes.

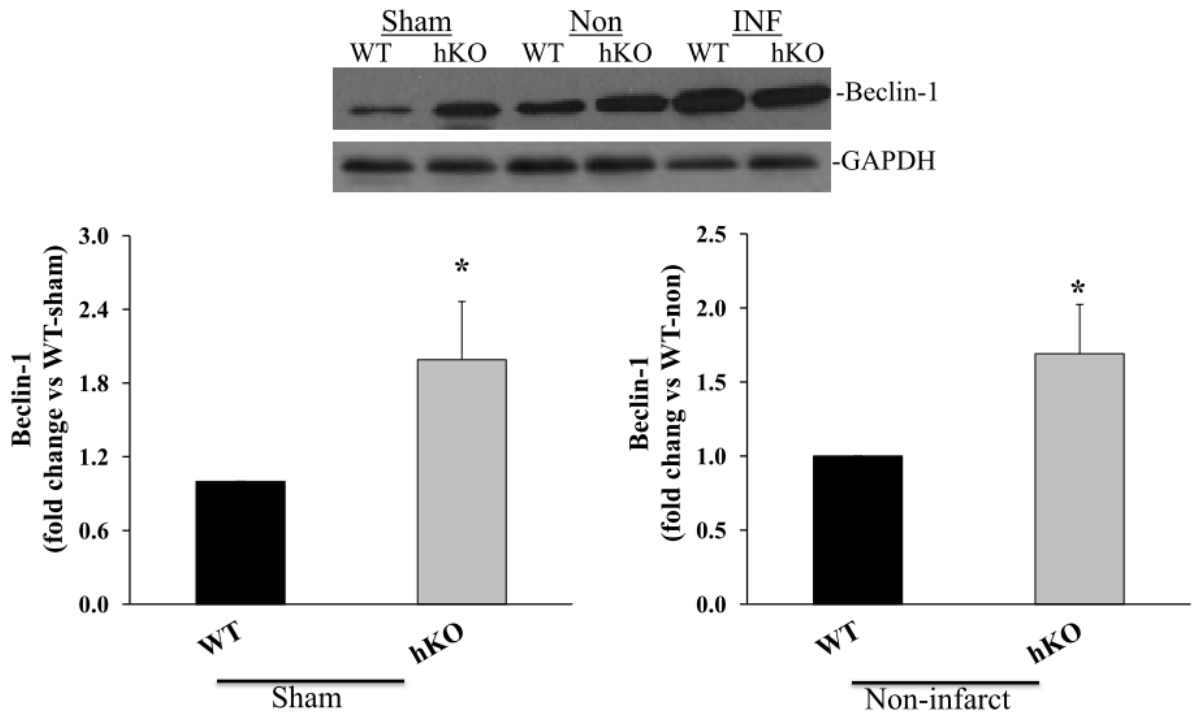

Figure 4.8. ATM deficiency increases expression of Beclin-1. Total LV lysates, prepared from the sham and non-infarct and infarct LV regions 28 days post-MI, were analyzed by western blot using anti-Beclin-1 antibodies. The upper panels depict autoradiograms immunostained for Beclin-1 and GAPDH. The lower panels exhibit quantitative analyses of Beclin-1 normalized to GAPDH. *P<0.05 vs WT; n=6-8.

The protein p16 is expressed by most senescent cells (Rodier & Campisi, 2011). Expression of p16 was higher in the hKO-sham group when compared to the WT-sham group. Following MI, no significant difference in p16 protein levels was observed between the two genotypes in the non-infarct regions. However, the infarct region of the hKO-MI group exhibited decreased protein levels of p16 when compared to the WT-MI group (Fig 4.9).

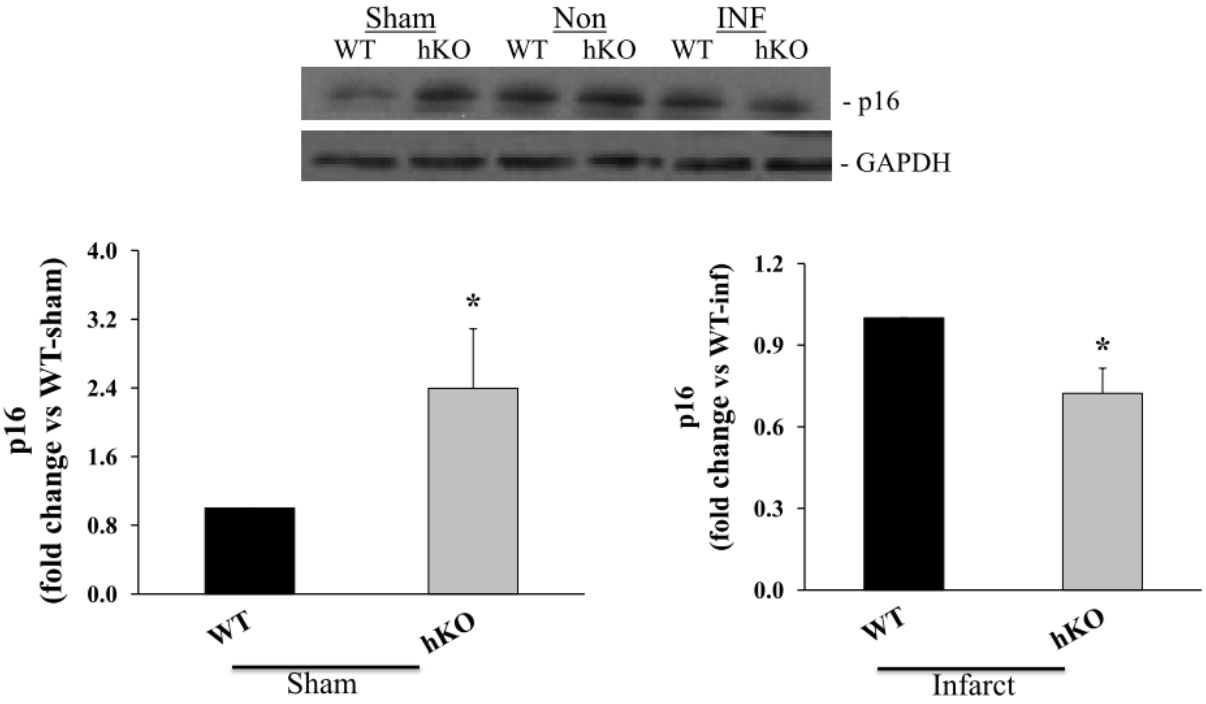

Figure 4.9. ATM deficiency alters p16 expression. Total LV lysates, prepared from sham and non-infarct and infarct LV regions 28 days post-MI, were analyzed by western blot using anti-p16 antibodies. The upper panels depict autoradiograms immunostained for p16 and GAPDH. The lower panels exhibit quantitative analyses of p16 normalized to GAPDH. *P<0.05 vs WT; n=6-7.

Expression of MMP-2 and MMP-9.

Matrix metalloproteinases (MMP-2 and -9) play an important role in the fibrotic response following MI (Lindsey & Zamilpa, 2012). MMP-2 expression and activity increase in the infarct region following MI peaking 7 days post-MI and decreasing thereafter. MMP-9 is activated following MI and its activity remains elevated until 14 days post-MI (Cleutjens et al., 1995). MMP-2 expression was significantly lower in the infarct region of both MI groups when compared to their respective sham group with no significant differences in MMP-2 expression between the two genotypes (data not shown). There was a significant decrease in MMP-9 expression in the infarct region of both genotypes when compared to their respective sham

groups. However, no significant differences were observed between the two genotypes in either the sham group or the infarct region. Interestingly, MMP-9 protein levels were significantly lower in the non-infarct region of the hKO-MI group when compared to that of the WT-MI group (Figure 10).

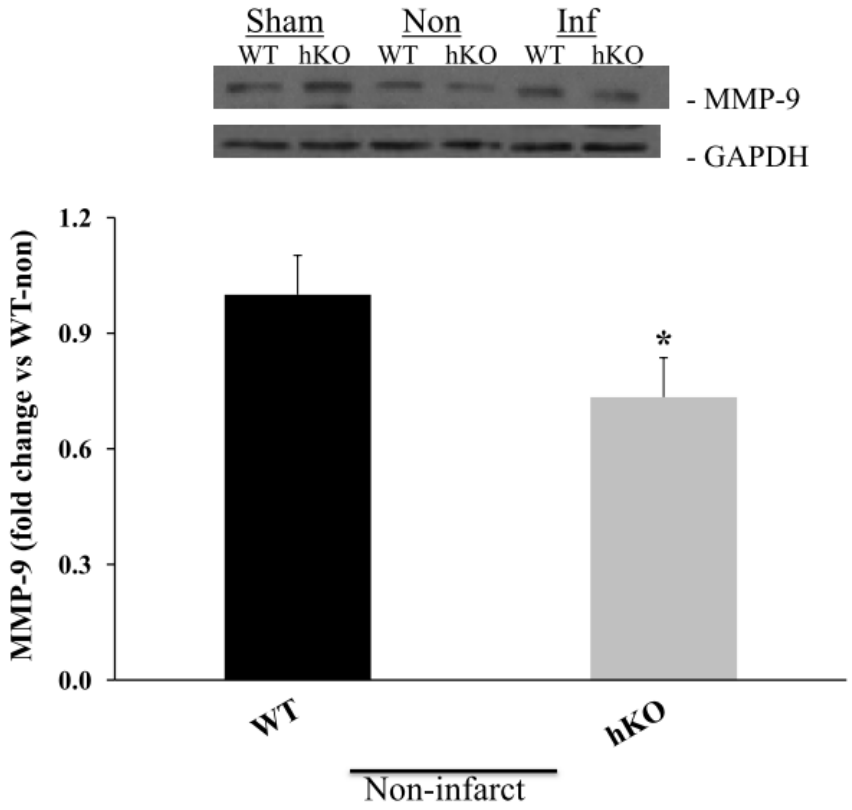

Figure 4.10. ATM deficiency decreases expression of MMP-9 in the non-infarct region 28 days post-MI. Total LV lysates, prepared from sham and non-infarct and infarct LV regions 28 days post-MI, were analyzed by western blot using anti-MMP-9 antibodies. The upper panels depict autoradiograms immunostained for MMP-9 and GAPDH. The lower panels exhibit quantitative analyses of MMP-9 normalized to GAPDH. *P<0.05 vs WT; n=8.

Discussion

The data presented here demonstrate that ATM deficiency associates with LV dysfunction, increased expression of p16 and Beclin-1, increased myocyte cross-sectional area and increased fibrosis in the sham group. Twenty-eight days post-MI, ATM deficiency associated with a greater decline in LV function. Post-MI survival tended to be lower in the ATM deficient group. Myocardial fibrosis and expression of α-sma was higher in the ATM deficient group, while apoptosis was higher in the WT group 28 days post-MI. Myocyte cross-sectional area was greater in the ATM deficient group. Beclin-1 expression remained higher in the hKO-MI group when compared to the WT-group, but only in the non-infarcted region. ATM deficiency associated with lower activity of ERK1/2 in the non-infarct region and lower GSK-3β activity in the infarct region. It was also associated with lower p16 expression in the infarct region. ATM deficiency associated with lower MMP-9 expression in the non-infarct region. Thus, ATM deficiency affects heart function and molecular parameters of the heart associated with apoptosis, fibrosis, autophagy and senescence 28 days post-MI.

In the sham group, ATM deficiency associated with reduced cardiac function, increased fibrosis and myocyte hypertrophy. ATM deficiency also associated with increased expression of p16 and Beclin-1. p16 is a marker for cellular senescence and has been shown to be elevated in the myocytes of aged diseased hearts. The presence of p16 is also associated with myocyte hypertrophy and myocyte apoptosis (Chimenti et al., 2003; Nadal-Ginard, 2003; Urbanek et al., 2003). The aged heart is shown to exhibit increased expression of the autophagy-related protein, Beclin-1 (Wohlgemuth et al., 2007) as well as increased cardiac fibrosis (Shinmura et al., 2011). Therefore, the observation of increased fibrosis, myocyte hypertrophy and increased

expression of p16 and Beclin-1 suggest that ATM deficiency may result in the premature aging of the heart.

Fourteen and 28 days post-MI, ATM deficiency associated with exacerbated cardiac dysfunction as determined by decreased %FS and EF. Cardiac fibrosis following MI occurs primarily as a result of collagen secretion by myofibroblasts (Turner & Porter, 2013). Inhibition of myofibroblast apoptosis has been linked to the progression of cardiac fibrosis (Li et al., 2004). An increase in cardiac fibrosis following MI has been suggested to cause cardiac dysfunction (See et al., 2013). Here, we observed decreased apoptosis, increased fibrosis and increased expression of α-sma in the infarct region of ATM deficient hearts. Although not indentified here, we speculate that the observed decrease in apoptosis in the infarct region during ATM deficiency is due to the decrease in myofibroblast apoptosis. It is interesting to note that myofibroblasts are identified as the major cell type undergoing apoptosis in the infarct region at this time point (W. Zhao, Lu, Chen, & Sun, 2004). This increase in fibrosis may be a contributing factor towards the observed LV dysfunction during ATM deficiency 28 days post-MI.

ATM deficiency also associated with increased expression of Beclin-1, an autophagy-related protein, in the non-infarct region following MI. During energy deprivation, such as an ischemic event, a cell uses autophagy to generate ATP. This is done by degrading cytosolic proteins and organelles (Levine & Kroemer, 2008). In this regard, increased autophagy can be beneficial following MI (Kanamori et al., 2011). However, when autophagy levels are too high, the volume occupied by the autophagic vacuoles can become too large leading to apoptosis (Maiuri, Zalckvar, Kimchi, & Kroemer, 2007). Of note, Beclin-$1^{+/-}$ mice exhibit a reduction in

autophagosome formation and a reduction in infarct size following myocardial ischemia/reperfusion injury (Matsui et al., 2007). Lack of ATM results in mitochondrial dysfunction in thymocytes *in vivo*. However, allelic loss of Beclin-1 in these mice attenuated these abnormalities (Valentin-Vega et al., 2012). Thus, increased expression of Beclin-1 is likely deleterious during ATM deficiency. This may provide another explanation as to why ATM deficiency presents itself with exaggerated cardiac dysfunction 14 and 28 days post-MI.

ATM deficiency also associated with increased myocyte cross-sectional area. Cardiac hypertrophy is induced following myocardial infarction in order to maintain cardiac output during myocyte loss (Gould et al., 2002). However, increases in myocyte size can often result in cardiac dysfunction late post-MI (Konstam et al., 2011). This increased myocyte size could be a contributing factor to the increased cardiac dysfunction in ATM deficient mice. Induction of hypertrophic signaling often converges on MAPK signaling pathway, which includes ERK1/2, Jun N-terminal kinase (JNK) and p38 (Wakatsuki, Schlessinger, & Elson, 2004). Activation of ERK1/2 is shown to induce cardiac hypertrophy. However, this induction is thought to be compensatory, not pathological, as is the case during the later stages of post-MI infarct healing. Similar pathways that are involved in ERK1/2 activation also activate JNK. Recent work using JNK transgenic mice suggest an anti-hypertrophic role for JNK (reviewed in (Liang, 2003)). Activation of ERK1/2 is reduced in the non-infarct region of the hKO-MI group, which suggests that ERK1/2 is not likely involved in the modulation of myocyte size at this time point. Previously, our lab has shown that β-AR stimulation activates JNK in WT mice but not in ATM KO mice (Foster, Singh, Subramanian, & Singh, 2011). Therefore, the increased hypertrophic response observed during ATM deficiency may in part be due to alterations in the activity of

JNK. Alternatively, the increased expression of Beclin-1 may result in increased hypertrophy via the accumulation of autophagic vesicles.

Activation of ERK1/2 is also shown to result in an increased fibroblast proliferation (Bueno et al., 2000; Lin et al., 2013). However, there was no difference in ERK1/2 activation between the two genotypes in the infarct region. This suggests that the increase in expression of α-sma during ATM deficiency occurs independently of ERK1/2 pathway. However, the increase in fibrosis during ATM deficiency could be a result of decreased GSK-3β activity and/or increased expression of p16, both of which can lead to increased cell proliferation.

Changes in MMP expression can result in changes in fibrosis (Matsui, Morimoto, & Uede, 2010). There was no difference in MMP-2 expression between the two genotypes. ATM deficiency associated with a reduction in MMP-9 expression in the non-infarct region. However, there were no differences in fibrosis between the two genotypes in the non-infarct region. Differences in fibrosis were only observed in the infarct region. These data suggest that changes in MMP-9 expression may not be a major contributing factor toward fibrosis late post-MI.

This study is a continuation of a project in which we examined how ATM deficiency affected cardiac remodeling during the inflammatory phase of infarct healing (1 and 3 days post-MI) and during the proliferative phase of healing (7 days post-MI) (Daniel et al., 2014; Foster et al., 2013). An important finding of those studies was that early post-MI infarct healing appeared to benefit from ATM deficiency in terms of cardiac function. However, this deficiency ultimately had negative consequences on cardiac function, which might be attributed to increased cardiac fibrosis as well as increased myocyte apoptosis. At this time, future investigations are

needed to clarify the role of ATM in cell survival and growth in different cell types of the heart post-MI.

Funding

This work was supported by a Merit Review award (number BX000640) from the Biomedical Laboratory Research and Development Service of the Veterans Affairs Office of Research and Development, grants from The National Heart, Lung, and Blood Institute (Grant numbers R21HL-091405 and R21HL-092459), and funds from Institutional Research and Improvement account (KS).

Acknowledgement

Technical help received from Barbara A. Connelly is appreciated.

Conflict of Interest/Disclosure: None

References

Barlow C, Hirotsune S, Paylor R, Liyanage M, Eckhaus M, Collins F, Shiloh Y, Crawley JN, Ried T, Tagle D, et al. 1996. Atm - Deficient Mice□: A Paradigm of Ataxia Telangiectasia. 86:159–71.

Bueno OF, De Windt LJ, Tymitz KM, Witt SA, Kimball TR, Klevitsky R, Hewett TE, Jones SP, Lefer DJ, Peng CF, et al. 2000. The MEK1-ERK1/2 signaling pathway promotes compensated cardiac hypertrophy in transgenic mice. EMBO J. 19:6341–50.

Chimenti C, Kajstura J, Torella D, Urbanek K, Heleniak H, Colussi C, Di Meglio F, Nadal-Ginard B, Frustaci A, Leri A, et al. 2003. Senescence and death of primitive cells and myocytes lead to premature cardiac aging and heart failure. Circ. Res. 93:604–13.

Cleutjens JP, Kandala JC, Guarda E, Guntaka R V, Weber KT. 1995. Regulation of collagen degradation in the rat myocardium after infarction. J. Mol. Cell. Cardiol. 27:1281–92.

Daniel LL, Daniels CR, Harirforoosh S, Foster CR, Singh M, Singh K. 2014. Deficiency of ataxia telangiectasia mutated kinase delays inflammatory response in the heart following myocardial infarction. J. Am. Heart Assoc. 3:e001286.

Eddy RJ, Petro JA, Tomasek JJ. 1988. Evidence for the nonmuscle nature of the “myofibroblast” of granulation tissue and hypertropic scar. An immunofluorescence study. Am. J. Pathol. 130:252–60.

Foster CR, Daniel LL, Daniels CR, Dalal S, Singh M, Singh K. 2013. Deficiency of ataxia telangiectasia mutated kinase modulates cardiac remodeling following myocardial infarction: involvement in fibrosis and apoptosis. PLoS One 8:e83513.

Foster CR, Singh M, Subramanian V, Singh K. 2011. Ataxia telangiectasia mutated kinase plays a protective role in β-adrenergic receptor-stimulated cardiac myocyte apoptosis and myocardial remodeling. Mol. Cell. Biochem. 353:13–22.

Gould KE, Taffet GE, Michael LH, Christie RM, Konkol DL, Pocius JS, Zachariah JP, Chaupin DF, Daniel SL, Sandusky GE, et al. 2002. Heart failure and greater infarct expansion in middle-aged mice: a relevant model for postinfarction failure. Am. J. Physiol. Heart Circ. Physiol. 282:H615–21.

Holly TA, Drincic A, Byun Y, Nakamura S, Harris K, Klocke FJ, Cryns VL. 1999. Caspase inhibition reduces myocyte cell death induced by myocardial ischemia and reperfusion in vivo. J. Mol. Cell. Cardiol. 31:1709–15.

Jun I, Lau LF. 2010. Cellular senescence controls fibrosis in wound healing. Aging. 2:627–31.

Kanamori H, Takemura G, Goto K, Maruyama R, Ono K, Nagao K, Tsujimoto A, Ogino A, Takeyama T, Kawaguchi T, et al. 2011. Autophagy limits acute myocardial infarction induced by permanent coronary artery occlusion. Am. J. Physiol. Heart Circ. Physiol. 300:H2261–71.

Konstam MA, Kramer DG, Patel AR, Maron MS, Udelson JE. 2011. Left ventricular remodeling in heart failure: current concepts in clinical significance and assessment. JACC. Cardiovasc. Imaging 4:98–108.

Levine B, Kroemer G. 2008. Autophagy in the pathogenesis of disease. Cell 132:27–42.

Li Y, Takemura G, Kosai K, Takahashi T, Okada H, Miyata S, Yuge K, Nagano S, Esaki M, Khai NC, et al. 2004. Critical roles for the Fas/Fas ligand system in postinfarction ventricular remodeling and heart failure. Circ. Res. 95:627–36.

Liang Q. 2003. Redefining the roles of p38 and JNK signaling in cardiac hypertrophy: dichotomy between cultured myocytes and animal models. J. Mol. Cell. Cardiol. 35:1385–94.

Lin X, Yan J, Tang D. 2013. ERK kinases modulate the activation of PI3 kinase related kinases (PIKKs) in DNA damage response. Histol. Histopathol. 28:1547–54.

Lindsey ML, Zamilpa R. 2012. Temporal and spatial expression of matrix metalloproteinases and tissue inhibitors of metalloproteinases following myocardial infarction. Cardiovasc. Ther. 30:31–41.

Maiuri MC, Zalckvar E, Kimchi A, Kroemer G. 2007. Self-eating and self-killing: crosstalk between autophagy and apoptosis. Nat. Rev. Mol. Cell Biol. 8:741–52.

Matsui Y, Morimoto J, Uede T. 2010. Role of matricellular proteins in cardiac tissue remodeling after myocardial infarction. World J. Biol. Chem. 1:69–80.

Matsui Y, Takagi H, Qu X, Abdellatif M, Sakoda H, Asano T, Levine B, Sadoshima J. 2007. Distinct roles of autophagy in the heart during ischemia and reperfusion: roles of AMP-activated protein kinase and Beclin 1 in mediating autophagy. Circ. Res. 100:914–22.

Nadal-Ginard B. 2003. Myocyte Death, Growth, and Regeneration in Cardiac Hypertrophy and Failure. Circ. Res. 92:139–50.

Nascimento DS, Valente M, Esteves T, de Pina M de F, Guedes JG, Freire A, Quelhas P, Pinto-do-Ó P. 2011. MIQuant--semi-automation of infarct size assessment in models of cardiac ischemic injury. PLoS One 6:e25045.

Nishida K, Kyoi S, Yamaguchi O, Sadoshima J, Otsu K. 2009. The role of autophagy in the heart. Cell Death Differ. 16:31–8.

Nowak-Wegrzyn A, Crawford TO, Winkelstein JA, Carson KA, Lederman HM. 2004. Immunodeficiency and infections in ataxia-telangiectasia. J. Pediatr. 144:505–11.

Rivard AL, Steer CJ, Kren BT, Rodrigues CMP, Castro RE, Bianco RW, Low WC. 2007. Administration of tauroursodeoxycholic acid (TUDCA) reduces apoptosis following myocardial infarction in rat. Am. J. Chin. Med. 35:279–95.

Rodier F, Campisi J. 2011. Four faces of cellular senescence. J. Cell Biol. 192:547–56.

See F, Watanabe M, Kompa AR, Wang BH, Boyle AJ, Kelly DJ, Gilbert RE, Krum H. 2013. Early and delayed tranilast treatment reduces pathological fibrosis following myocardial infarction. Heart. Lung Circ. 22:122–32.

Shinmura K, Tamaki K, Sano M, Murata M, Yamakawa H, Ishida H, Fukuda K. 2011. Impact of long-term caloric restriction on cardiac senescence: caloric restriction ameliorates cardiac diastolic dysfunction associated with aging. J. Mol. Cell. Cardiol. 50:117–27.

Su Y, Swift M. 2000. Mortality rates among carriers of ataxia-telangiectasia mutant alleles. Ann. Intern. Med. 133:770–8.

Sun Y, Kiani MF, Postlethwaite AE, Weber KT. 2002. Infarct scar as living tissue. Basic Res. Cardiol. 97:343–7.

Sun Y, Weber KT. 1996. Angiotensin converting enzyme and myofibroblasts during tissue repair in the rat heart. J. Mol. Cell. Cardiol. 28:851–8.

Sutherland C, Leighton IA, Cohen P. 1993. Inactivation of glycogen synthase kinase-3 beta by phosphorylation: new kinase connections in insulin and growth-factor signalling. Biochem. J. 296:15–9.

Taylor AMR, Byrd PJ. 2005. Molecular pathology of ataxia telangiectasia. J. Clin. Pathol. 58:1009–15.

Turner NA, Porter KE. 2013. Function and fate of myofibroblasts after myocardial infarction. Fibrogenesis Tissue Repair 6:5.

Urbanek K, Quaini F, Tasca G, Torella D, Castaldo C, Nadal-Ginard B, Leri A, Kajstura J, Quaini E, Anversa P. 2003. Intense myocyte formation from cardiac stem cells in human cardiac hypertrophy. Proc. Natl. Acad. Sci. U. S. A. 100:10440–5.

Valentin-Vega YA, Maclean KH, Tait-Mulder J, Milasta S, Steeves M, Dorsey FC, Cleveland JL, Green DR, Kastan MB. 2012. Mitochondrial dysfunction in ataxia-telangiectasia. Blood 119:1490–500.

Wakatsuki T, Schlessinger J, Elson EL. 2004. The biochemical response of the heart to hypertension and exercise. Trends Biochem. Sci. 29:609–17.

Willems IE, Havenith MG, De Mey JG, Daemen MJ. 1994. The alpha-smooth muscle actin-positive cells in healing human myocardial scars. Am. J. Pathol. 145:868–75.

Wohlgemuth SE, Julian D, Akin DE, Fried J, Toscano K, Leeuwenburgh C, Dunn WA. 2007. Autophagy in the heart and liver during normal aging and calorie restriction. Rejuvenation Res. 10:281–92.

Zhao W, Lu L, Chen SS, Sun Y. 2004. Temporal and spatial characteristics of apoptosis in the infarcted rat heart. Biochem. Biophys. Res. Commun. 325:605–11.

Zhao ZQ, Morris CD, Budde JM, Wang NP, Muraki S, Sun HY, Guyton RA. 2003. Inhibition of myocardial apoptosis reduces infarct size and improves regional contractile dysfunction during reperfusion. Cardiovasc. Res. 59:132–42.

Zhu H, Tannous P, Johnstone JL, Kong Y, Shelton JM, Richardson JA, Le V, Levine B, Rothermel BA, Hill JA. 2007. Cardiac autophagy is a maladaptive response to hemodynamic stress. J. Clin. Invest. 117:1782–93.

CHAPTER 5

CONCLUSION

Carriers of ATM exhibit enhanced susceptibility towards ischemic heart disease. Here, we observed that MI increased expression of ATM in the infarct and non-infarct LV regions of the heart. Using ATM deficient mice, this study investigated the role of ATM in different phases of infarct healing post-MI. A major finding of this study was that ATM modulated cardiac structure and function post-MI by affecting myocardial fibrosis, apoptosis and myocyte hypertrophy. Early post-MI (1, 3 and 7 days), ATM deficiency associated with increased fibrosis which correlated with attenuated dilative remodeling and cardiac dysfunction. However, late post-MI (14 and 28 days post-MI), ATM deficiency associated with greater cardiac dysfunction which we attributed to increased myocardial fibrosis and myocyte hypertrophy. At each stage of infarct healing, there is a different cell type predominately undergoing apoptosis. Early post-MI, the predominant cell type undergoing apoptosis is myocytes. After the majority of myocytes have been lost from the infarct region, inflammatory cells become the predominant cell type undergoing apoptosis. During the last stages of infarct healing, myofibroblasts become the primary cell type undergoing apoptosis in the infarct region. On the other hand, the primary cell type undergoing apoptosis, during the later stages of remodeling, in the non-infarct region is myocytes (Zhao et al. 2004). The data presented here suggest that ATM deficiency increased the susceptibility of myocytes towards apoptosis, while decreasing the susceptibility of fibroblasts towards apoptosis.

ATM and Inflammatory Phase

During the inflammatory phase of post-MI healing (1 and 3 days post-MI) ATM deficiency delayed the inflammatory response post-MI and resulted in decreased dilative

remodeling. In the infarct region, ATM deficiency resulted in enhanced fibrosis and expression of α-sma (myofibroblast marker). However, cardiac cell apoptosis was higher during ATM deficiency. Activation of the anti-apoptotic kinase Akt and inactivation of pro-apoptotic kinase GSK-3β were lower, while the expression of the pro-apoptotic protein Bax was higher in the infarct region during ATM deficiency.

MI causes cardiac cell death via necrosis and apoptosis. Necrosis leads to inflammatory response via the release of chemokines which attract neutrophils. Leukocytes extravasation primarily occurs in post-capillary venules (Ma et al. 2013). The retina of mice lacking ATM is shown to have decreased vasculature when compared to the retina of WT mice (Raz-Prag et al. 2011). Although not investigated here, the reduced inflammatory response observed during ATM deficiency could be, at least in part, due to decreased vasculature in the heart. Increased apoptosis can also affect the inflammatory response post-MI. Apoptotic cells release signals such as lactoferrin and annexin 1 which can inhibit neutrophil recruitment (Hayhoe et al. 2006; Bournazou et al. 2009). Therefore, increased apoptosis during ATM deficiency post-MI can cause inhibitory effects on neutrophil migration.

Cardiac cell death following MI leads to an increase in wall stress resulting in dilative remodeling and decreased survival post-MI. However, an early increase in collagen fibers can prevent dilative remodeling (White et al. 1987; Sutton and Sharpe 2000). Here, we observed decreased dilative remodeling and increased fibrosis during ATM deficiency post-MI. Therefore, increased fibrosis may contribute to the decreased dilative remodeling during ATM deficiency post-MI. Myofibroblasts are the main producers of collagen in the infarct region. The collagen being produced in the non-infarcted region originates from undifferentiated fibroblasts (Cleutjens, Verluyten, et al. 1995). In the uninjured heart fibroblasts are inactive. Following MI,

fibroblasts experience mechanical stress due to myocyte death, resulting in their activation and differentiation into myofibroblasts (Li et al. 1997; Turner and Porter 2013). The differentiation of fibroblast is also aided by biochemical stimuli, such as TGF-β1 and fibronectin splice form ED-A (Turner and Porter 2013). TGF-β1 is secreted as a latent protein and associates with the latency-associated peptide (LAP). It remains inactive until it is activated by either proteolytic cleavage or mechanical force (Buscemi et al. 2011). Three days post-MI, ATM deficiency resulted in higher expression of α-sma and fibrosis. However, levels of active TGF-β1 were lower in the infarct region during ATM deficiency. These data suggest that activation of TGF-β1 may not be solely responsible for differentiation of fibroblasts into myofibroblasts during ATM deficiency. Increased mechanical stress and/or ED-A splice variant of fibronectin may play a role in fibroblast differentiation during ATM deficiency.

ATM deficiency associated with increased apoptosis 1 and 3 days post-MI when compared to WT. During this time point, myocytes and inflammatory cells are the predominant cell types undergoing apoptosis (Zhao et al. 2004). Therefore, the increased apoptosis could be attributed to either one of these two cell types. Activation of Akt plays an anti-apoptotic role in cardiac myocytes, in part by acting upstream in the phosphorylation and inactivation GSK-3β (Sutherland et al. 1993). Akt has also been shown to inhibit Bax (a pro-apoptotic protein) by phosphorylating it on Ser-184 (Gardai et al. 2004). One day post-MI, ATM deficiency associated with decreased activation of Akt and an enhanced activation of GSK-3β. Also, expression of Bax was higher in the infarct region 3 days post-MI during ATM deficiency. Therefore, enhanced apoptosis, early post-MI, in the infarct region appears to be due to decreased survival signaling during ATM deficiency.

ATM and the Proliferative Phase

Seven days post-MI, ATM deficiency associated with attenuation of cardiac dysfunction and dilative remodeling as well as increased infarct thickness, fibrosis and expression of α-sma. ATM deficient mice exhibited lower total cardiac cell apoptosis in the infarct region. The two main cell types undergoing apoptosis at this time point, in the infarct region, are macrophages and myofibroblasts. ATM deficiency associated with enhanced expression of α-sma and fibrosis in the infarct region post-MI. Therefore, it can be argued that the decreased apoptosis in the infarct region during ATM deficiency may be due to decreased myofibroblast apoptosis. The increased fibrosis may have contributed to the increased infarct wall thickness leading to decreased LV dilation and dysfunction.

Another interesting finding of this study was that ATM deficient mice exhibited increased myocyte apoptosis in the border region, when compared to WT. Increased myocyte apoptosis in the border region is predicative of infarct expansion, resulting in a worse outcome late post-MI (Frantz et al. 2009; Kempf et al. 2012). Therefore, it is possible that increased fibrosis and apoptosis in the border region during ATM deficiency may associate with cardiac dysfunction if the study time points are extended beyond 7 days post-MI. Although there was higher myocyte apoptosis in the border area during ATM deficiency, the attenuated cardiac dysfunction as well as the increased infarct thickness might be attributed to increased infarct fibrosis.

ATM and the Maturation Phase

Fourteen and 28 days post-MI, ATM deficient mice exhibited greater cardiac dysfunction. We also saw a trend towards enhanced mortality in ATM deficient mice 28 days post-MI. Fibrosis and expression of α-sma in the infarct region remained higher in ATM

deficient mice 28 days post-MI. Therefore, it appears that the increased fibrosis during ATM deficiency only delays dilative remodeling resulting in an initial attenuation of cardiac dysfunction. Cross-linking of the collagen matrix, which occurs during the maturation phase of cardiac remodeling, leads to increases in passive stiffness resulting in cardiac dysfunction (Kato et al. 1995; Badenhorst et al. 2003). The increased fibrosis during ATM deficiency could be contributing to exacerbated cardiac dysfunction 14 and 28 days post-MI.

ATM deficiency associated with decreased apoptosis in the infarct region. At this time point, the majority of cells undergoing apoptosis are most likely myofibroblasts. In addition, expression of α-sma was higher in ATM deficient hearts, supporting our hypothesis that ATM deficiency may be anti-apoptotic for myofibroblasts. Levels of active GSK-3β were lower in the infarct region of ATM deficient hearts. Active GSK-3β can inhibit cell cycle and lead to apoptosis (Alt et al. 2000; Hall et al. 2001; Antos et al. 2002). Therefore, decreased GSK-3β activity during ATM deficiency could have contributed to not only decreased myofibroblast apoptosis, but also to increased myofibroblast proliferation. Induction of senescence in myofibroblasts is an important step to inhibit fibrosis (Jun and Lau 2010). In streptozotocin-induced model of diabetes, ATM deficiency is shown to inhibit endothelial senescence (Zhan et al. 2010). Here, we observed decreased expression of p16 in the infarct region of ATM deficient hearts. Therefore, decreased myofibroblast senescence may also explain increased expression of α-sma in the infarct region during ATM deficiency. Of note, expression of p16 was higher in ATM deficient sham hearts. Expression of Beclin-1, an autophagy-related protein, was also higher in ATM deficient sham hearts. Expression of autophagy-related proteins is shown to be impaired in the aged heart (Wohlgemuth et al. 2007). The increased expression of p16 and

Beclin-1 during ATM deficiency points toward premature aging of the myocytes and possible predisposition to myocyte apoptosis post-MI.

Future Directions

Future directions of the study are numerous. We showed that MI increases the expression of the ATM gene in the heart in both the infarct and non-infarct LV regions. Therefore, it would be interesting to identify the cell-type involved in the increased expression of ATM post-MI. Mitogenic signals have also been shown to increase expression of ATM in peripheral blood mononuclear cells (Fukao et al. 1999). In addition ,we have previously shown, that β-AR stimulation increased ATM expression in the heart and in cardiac myocytes (Foster et al. 2011). In certain neuronal cell types, expression of ATM is shown to decrease when the cell differentiates into a non-dividing phenotype, at which point ATM moves from the nucleus into the cytoplasm. Here it can play an anti-apoptotic role, protecting the cell from serum starvation (Allen et al. 2001; Boehrs et al. 2007). Therefore, it is possible that a differential expression of ATM and/or differential cellular localization of ATM may influence the apoptotic response differently in myocytes versus fibroblasts. However, further investigations are needed to identify factors and cell types involved in the increased ATM expression in the heart post-MI.

The data presented here suggest that ATM deficiency decreased heart function and worsened survival late post-MI. As discussed, different phases of the infarct healing process involve different cell types of the heart undergoing apoptosis. Previous work from our lab showed cardiac myocyte apoptosis and myocardial fibrosis was greater in the myocardium of ATM deficient mice 28 days following β-AR stimulation (Foster et al. 2011). The previous study in combination with the work presented here leads us to hypothesize that ATM deficiency predisposes cardiac myocytes to apoptosis while either protecting myofibroblasts against

apoptosis and/or resulting in increased proliferation of the myofibroblasts. A major limitation of this study is that we did not identify the cell types undergoing apoptosis. Identification of the cell types undergoing apoptosis may help explain the healing process of the heart during ATM deficiency. Post-MI healing is a complex process involving various cytokines, chemokines and growth factors. Signals such as lactoferrin and annexin 1 can inhibit recruitment of neutrophils to the injury site. Chemokines and cytokines present at different phases of infarct healing can influence the fibrotic and apoptotic response. Future investigations are needed to determine if ATM deficiency influences the production of cytokines, chemokines and growth factors in the heart post-MI.

Another interesting observation is that the increased fibrosis during ATM deficiency only delayed dilative remodeling resulting in an initial attenuation of cardiac dysfunction. However, increased fibrosis may have ultimately led to exacerbated heart dysfunction late post-MI. Deposition of fibrotic tissue is a complex process involving synthesis and degradation of ECM that relies on various MMPs and TIMPs. The current study mainly investigated the protein levels of MMP-2 and -9. A thorough analysis of different components leading to fibrosis may provide insight into the modulation of heart function during ATM deficiency post-MI.

Likewise, apoptosis is complex process involving a variety of signaling molecules. Using mice lacking ATM and acute β-AR stimulation as a model, we have previously provided evidence that the signaling pathway involved in myocyte apoptosis was different in the presence or absence of ATM. In WT hearts, β-AR-stimulated apoptosis occurred via the involvement of p53 and JNKs pathway. However, decreased Akt activity may have played a role in β-AR-stimulated myocyte apoptosis in the absence of ATM (Foster et al. 2012). The study done here points towards the involvement of ATM in cell senescence and autophagy. Future investigations

are required to understand the signaling mechanism and organelles involved in this process and whether the changes in these mechanisms are beneficial or detrimental.

REFERENCES

Ahmet I, Krawczyk M, Zhu W, Woo AY, Morrell C, Poosala S, Xiao RP, Lakatta EG, Talan MI. 2008. Cardioprotective and survival benefits of long-term combined therapy with beta2 adrenoreceptor (AR) agonist and beta1 AR blocker in dilated cardiomyopathy postmyocardial infarction. J. Pharmacol. Exp. Ther. 325:491–9.

Allen DM, van Praag H, Ray J, Weaver Z, Winrow CJ, Carter TA, Braquet R, Harrington E, Ried T, Brown KD, et al. 2001. Ataxia telangiectasia mutated is essential during adult neurogenesis. Genes Dev. 15:554–66.

Alpert JS, Thygesen K, Antman E, Bassand JP. 2000. Myocardial infarction redefined--a consensus document of The Joint European Society of Cardiology/American College of Cardiology Committee for the redefinition of myocardial infarction. J. Am. Coll. Cardiol. 36:959–69.

Alt JR, Cleveland JL, Hannink M, Diehl JA. 2000. Phosphorylation-dependent regulation of cyclin D1 nuclear export and cyclin D1-dependent cellular transformation. Genes Dev. 14:3102–14.

Antos CL, McKinsey TA, Frey N, Kutschke W, McAnally J, Shelton JM, Richardson JA, Hill JA, Olson EN. 2002. Activated glycogen synthase-3 beta suppresses cardiac hypertrophy in vivo. Proc. Natl. Acad. Sci. U. S. A. 99:907–12.

Badenhorst D, Maseko M, Tsotetsi OJ, Naidoo A, Brooksbank R, Norton GR, Woodiwiss AJ. 2003. Cross-linking influences the impact of quantitative changes in myocardial collagen on cardiac stiffness and remodelling in hypertension in rats. Cardiovasc. Res. 57:632–41.

Bakkenist CJ, Kastan MB. 2003. DNA damage activates ATM through intermolecular autophosphorylation and dimer dissociation. Nature 421:499–506.

Barzilai A, Rotman G, Shiloh Y. 2002. ATM deficiency and oxidative stress: a new dimension of defective response to DNA damage. DNA Repair (Amst). 1:3–25.

Vanden Berghe T, Kalai M, Denecker G, Meeus A, Saelens X, Vandenabeele P. 2006. Necrosis is associated with IL-6 production but apoptosis is not. Cell. Signal. 18:328–35.

Berkovich E, Monnat RJ, Kastan MB. 2007. Roles of ATM and NBS1 in chromatin structure modulation and DNA double-strand break repair. Nat. Cell Biol. 9:683–90.

Boehrs JK, He J, Halaby M-J, Yang D-Q. 2007. Constitutive expression and cytoplasmic compartmentalization of ATM protein in differentiated human neuron-like SH-SY5Y cells. J. Neurochem. 100:337–45.

Bournazou I, Pound JD, Duffin R, Bournazos S, Melville LA, Brown SB, Rossi AG, Gregory CD. 2009. Apoptotic human cells inhibit migration of granulocytes via release of lactoferrin. J. Clin. Invest. 119:20–32.

Brouckaert G, Kalai M, Krysko D V, Saelens X, Vercammen D, Ndlovu M, Haegeman G, D'Herde K, Vandenabeele P. 2004. Phagocytosis of necrotic cells by macrophages is phosphatidylserine dependent and does not induce inflammatory cytokine production. Mol. Biol. Cell 15:1089–100.

Brown RD, Ambler SK, Mitchell MD, Long CS. 2005. The cardiac fibroblast: therapeutic target in myocardial remodeling and failure. Annu. Rev. Pharmacol. Toxicol. 45:657–87.

Buscemi L, Ramonet D, Klingberg F, Formey A, Smith-Clerc J, Meister JJ, Hinz B. 2011. The single-molecule mechanics of the latent TGF-β1 complex. Curr. Biol. 21:2046–54.

Cadenas E, Davies KJ. 2000. Mitochondrial free radical generation, oxidative stress, and aging. Free Radic. Biol. Med. 29:222–30.

Chen YR, Zweier JL. 2014. Cardiac mitochondria and reactive oxygen species generation. Circ. Res. 114:524–37.

Cleutjens JP, Blankesteijn WM, Daemen MJ, Smits JF. 1999. The infarcted myocardium Simply dead tissue, or a lively target for therapeutic interventions. Cardiovasc. Res. 44:232–41.

Cleutjens JP, Kandala JC, Guarda E, Guntaka RV, Weber KT. 1995. Regulation of collagen degradation in the rat myocardium after infarction. J. Mol. Cell. Cardiol. 27:1281–92.

Cleutjens JP, Verluyten MJ, Smiths JF, Daemen MJ. 1995. Collagen remodeling after myocardial infarction in the rat heart. Am. J. Pathol. 147:325–38.

Cocco RE, Ucker DS. 2001. Distinct modes of macrophage recognition for apoptotic and necrotic cells are not specified exclusively by phosphatidylserine exposure. Mol. Biol. Cell 12:919–30.

Cochain C, Channon KM, Silvestre JS. 2013. Angiogenesis in the infarcted myocardium. Antioxid. Redox Signal. 18:1100–13.

Colucci WS, Sawyer DB, Singh K, Communal C. 2000. Adrenergic overload and apoptosis in heart failure: implications for therapy. J. Card. Fail. 6:1–7.

Cosentino C, Grieco D, Costanzo V. 2011. ATM activates the pentose phosphate pathway promoting anti-oxidant defence and DNA repair. EMBO J. 30:546–55.

Dobaczewski M, Gonzalez-Quesada C, Frangogiannis NG. 2010. The extracellular matrix as a modulator of the inflammatory and reparative response following myocardial infarction. J. Mol. Cell. Cardiol. 48:504–11.

Downing SE, Chen V. 1985. Myocardial injury following endogenous catecholamine release in rabbits. J. Mol. Cell. Cardiol. 17:377–87.

Etoh T, Joffs C, Deschamps A, Davis J, Dowdy K, Hendrick J, Baicu S, Mukherjee R, Manhaini M, Spinale F. 2001. Myocardial and interstitial matrix metalloproteinase activity after acute myocardial infarction in pigs. Am. J. Physiol. Hear. Circ Physiol 281:H987–H994.

Eyre D. 1980. Collagen: molecular diversity in the body's protein scaffold. Science. 207:1315–22.

Farina L, Uggetti C, Ottolini A, Martelli A, Bergamaschi R, Sibilla L, Zappoli F, Egitto MG, Lanzi G. 1994. Ataxia-telangiectasia: MR and CT findings. J. Comput. Assist. Tomogr. 18:724–7.

Fliss H, Gattinger D. 1996. Apoptosis in ischemic and reperfused rat myocardium. Circ. Res. 79:949–56.

Foster CR, Singh M, Subramanian V, Singh K. 2011. Ataxia telangiectasia mutated kinase plays a protective role in β-adrenergic receptor-stimulated cardiac myocyte apoptosis and myocardial remodeling. Mol. Cell. Biochem. 353:13–22.

Foster CR, Zha Q, Daniel LL, Singh M, Singh K. 2012. Lack of ataxia telangiectasia mutated kinase induces structural and functional changes in the heart: role in β-adrenergic receptor-stimulated apoptosis. Exp. Physiol. 97:506–15.

Frangogiannis NG. 2008. The immune system and cardiac repair. Pharmacol. Res. 58:88–111.

Frangogiannis NG, Mendoza LH, Ren G, Akrivakis S, Jackson PL, Michael LH, Smith CW, Entman ML. 2003. MCSF expression is induced in healing myocardial infarcts and may regulate monocyte and endothelial cell phenotype. Am. J. Physiol. Heart Circ. Physiol. 285:H483–92.

Frantz S, Bauersachs J, Ertl G. 2009. Post-infarct remodelling: contribution of wound healing and inflammation. Cardiovasc. Res. 81:474–81.

Fukao T, Kaneko H, Birrell G, Gatei M, Tashita H, Yoshida T, Cross S, Kedar P, Watters D, Khana KK, et al. 1999. ATM is upregulated during the mitogenic response in peripheral blood mononuclear cells. Blood 94:1998–2006.

Gardai SJ, Hildeman DA, Frankel SK, Whitlock BB, Frasch SC, Borregaard N, Marrack P, Bratton DL, Henson PM. 2004. Phosphorylation of Bax Ser184 by Akt regulates its activity and apoptosis in neutrophils. J. Biol. Chem. 279:21085–95.

Go AS, Mozaffarian D, Roger VL, Benjamin EJ, Berry JD, Blaha MJ, Dai S, Ford ES, Fox CS, Franco S, et al. 2014. Heart disease and stroke statistics--2014 update: a report from the American Heart Association. Circulation 129:e28–e292.

Goodarzi AA, Noon AT, Deckbar D, Ziv Y, Shiloh Y, Löbrich M, Jeggo PA. 2008. ATM signaling facilitates repair of DNA double-strand breaks associated with heterochromatin. Mol. Cell 31:167–77.

Gumy-Pause F, Wacker P, Sappino AP. 2004. ATM gene and lymphoid malignancies. Leukemia 18:238–42.

Guo Z, Kozlov S, Lavin MF, Person MD, Paull TT. 2010. ATM activation by oxidative stress. Science 330:517–21.

Hall JL, Chatham JC, Eldar-Finkelman H, Gibbons GH. 2001. Upregulation of glucose metabolism during intimal lesion formation is coupled to the inhibition of vascular smooth muscle cell apoptosis. Role of GSK3beta. Diabetes 50:1171–9.

Hayhoe RPG, Kamal AM, Solito E, Flower RJ, Cooper D, Perretti M. 2006. Annexin 1 and its bioactive peptide inhibit neutrophil-endothelium interactions under flow: indication of distinct receptor involvement. Blood 107:2123–30.

Hill JH, Ward PA. 1971. The phlogistic role of C3 leukotactic fragments in myocardial infarcts of rats. J. Exp. Med. 133:885–900.

Hinz B, Mastrangelo D, Iselin CE, Chaponnier C, Gabbiani G. 2001. Mechanical tension controls granulation tissue contractile activity and myofibroblast differentiation. Am. J. Pathol. 159:1009–20.

James TN. 1998. The variable morphological coexistence of apoptosis and necrosis in human myocardial infarction: significance for understanding its pathogenesis, clinical course, diagnosis and prognosis. Coron. Artery Dis. 9:291–307.

Jiang D, Liang J, Fan J, Yu S, Chen S, Luo Y, Prestwich GD, Mascarenhas MM, Garg HG, Quinn DA, et al. 2005. Regulation of lung injury and repair by Toll-like receptors and hyaluronan. Nat. Med. 11:1173–9.

Jun I, Lau LF. 2010. Cellular senescence controls fibrosis in wound healing. Aging. 2:627–31.

Kabe Y, Ando K, Hirao S, Yoshida M, Handa H. 2005. Redox regulation of NF-kappaB activation: distinct redox regulation between the cytoplasm and the nucleus. Antioxid. Redox Signal. 7:395–403.

Kamsler A, Daily D, Hochman A, Stern N, Shiloh Y, Rotman G, Barzilai A. 2001. Increased Oxidative Stress in Ataxia Telangiectasia Evidenced by Alterations in Redox State of Brains from Atm-deficient Mice. Cancer Res. 61:1849–54.

Kato S, Spinale FG, Tanaka R, Johnson W, Cooper, G. 4th, Zile MR. 1995. Inhibition of collagen cross-linking: effects on fibrillar collagen and ventricular diastolic function. Am J Physiol Hear. Circ Physiol 269:H863–8.

Kawai K, Qin F, Shite J, Mao W, Fukuoka S, Liang C-S. 2004. Importance of antioxidant and antiapoptotic effects of beta-receptor blockers in heart failure therapy. Am. J. Physiol. Heart Circ. Physiol. 287:H1003–12.

Kempf T, Zarbock A, Vestweber D, Wollert KC. 2012. Anti-inflammatory mechanisms and therapeutic opportunities in myocardial infarct healing. J. Mol. Med. (Berl). 90:361–9.

Kozlov S V, Graham ME, Jakob B, Tobias F, Kijas AW, Tanuji M, Chen P, Robinson PJ, Taucher-Scholz G, Suzuki K, et al. 2011. Autophosphorylation and ATM activation: additional sites add to the complexity. J. Biol. Chem. 286:9107–19.

Kozlov S V, Graham ME, Peng C, Chen P, Robinson PJ, Lavin MF. 2006. Involvement of novel autophosphorylation sites in ATM activation. EMBO J. 25:3504–14.

Krysko DV, Denecker G, Festjens N, Gabriels S, Parthoens E, D'Herde K, Vandenabeele P. 2006. Macrophages use different internalization mechanisms to clear apoptotic and necrotic cells. Cell Death Differ. 13:2011–22.

Lavin MF, Gueven N, Bottle S, Gatti RA. 2007. Current and potential therapeutic strategies for the treatment of ataxia-telangiectasia. Br. Med. Bull. 81-82:129–47.

Lefton-Greif MA, Crawford TO, Winkelstein JA, Loughlin GM, Koerner CB, Zahurak M, Lederman HM. 2000. Oropharyngeal dysphagia and aspiration in patients with ataxia-telangiectasia. J. Pediatr. 136:225–31.

Li Q, Li B, Wang X, Leri A, Jana KP, Liu Y, Kajstura J, Baserga R, Anversa P. 1997. Overexpression of insulin-like growth factor-1 in mice protects from myocyte death after infarction, attenuating ventricular dilation, wall stress, and cardiac hypertrophy. J. Clin. Invest. 100:1991–9.

Lozano R, Naghavi M, Foreman K, Lim S, Shibuya K, Aboyans V, Abraham J, Adair T, Aggarwal R, Ahn SY, et al. 2012. Global and regional mortality from 235 causes of death for 20 age groups in 1990 and 2010: a systematic analysis for the Global Burden of Disease Study 2010. Lancet 380:2095–128.

Ma Y, Yabluchanskiy A, Lindsey ML. 2013. Neutrophil roles in left ventricular remodeling following myocardial infarction. Fibrogenesis Tissue Repair 6:11.

Matsui Y, Morimoto J, Uede T. 2010. Role of matricellular proteins in cardiac tissue remodeling after myocardial infarction. World J. Biol. Chem. 1:69–80.

McKinnon PJ. 2004. ATM and ataxia telangiectasia. EMBO Rep. 5:772–6.

Nakayama H, Chen X, Baines CP, Klevitsky R, Zhang X, Zhang H, Jaleel N, Chua BHL, Hewett TE, Robbins J, et al. 2007. Ca2+- and mitochondrial-dependent cardiomyocyte necrosis as a primary mediator of heart failure. J. Clin. Invest. 117:2431–44.

Nowak-Wegrzyn A, Crawford TO, Winkelstein JA, Carson KA, Lederman HM. 2004. Immunodeficiency and infections in ataxia-telangiectasia. J. Pediatr. 144:505–11.

Olivetti G, Abbi R, Quaini F, Kajstura J, Cheng W, Nitahara JA, Quaini E, Di Loreto C, Beltrami CA, Krajewski S, et al. 1997. Apoptosis in the failing human heart. N. Engl. J. Med. 336:1131–41.

Ouyang L, Shi Z, Zhao S, Wang FT, Zhou TT, Liu B, Bao JK. 2012. Programmed cell death pathways in cancer: a review of apoptosis, autophagy and programmed necrosis. Cell Prolif. 45:487–98.

Pinckard RN, Olson MS, Giclas PC, Terry R, Boyer JT, O'Rourke RA. 1975. Consumption of classical complement components by heart subcellular membranes in vitro and in patients after acute myocardial infarction. J. Clin. Invest. 56:740–50.

Proskuryakov SY, Konoplyannikov AG, Gabai VL. 2003. Necrosis: a specific form of programmed cell death? Exp. Cell Res. 283:1–16.

Quick KL, Dugan LL. 2001. Superoxide stress identifies neurons at risk in a model of ataxia-telangiectasia. Ann. Neurol. 49:627–635.

Raz-Prag D, Galron R, Segev-Amzaleg N, Solomon AS, Shiloh Y, Barzilai A, Frenkel D. 2011. A role for vascular deficiency in retinal pathology in a mouse model of ataxia-telangiectasia. Am. J. Pathol. 179:1533–41.

Rotman G. 1998. ATM: from gene to function. Hum. Mol. Genet. 7:1555–63.

Sandoval N, Platzer M, Rosenthal A, Dörk T, Bendix R, Skawran B, Stuhrmann M, Wegner RD, Sperling K, Banin S, et al. 1999. Characterization of ATM gene mutations in 66 ataxia telangiectasia families. Hum. Mol. Genet. 8:69–79.

Schömig A. 1990. Catecholamines in myocardial ischemia. Systemic and cardiac release. Circulation 82:II13–22.

Serini G, Bochaton-Piallat ML, Ropraz P, Geinoz A, Borsi L, Zardi L, Gabbiani G. 1998. The fibronectin domain ED-A is crucial for myofibroblastic phenotype induction by transforming growth factor-beta1. J. Cell Biol. 142:873–81.

Shiloh Y, Ziv Y. 2013. The ATM protein kinase: regulating the cellular response to genotoxic stress, and more. Nat. Rev. Mol. Cell Biol. 14:197–210.

Shizukuda Y, Buttrick PM, Geenen DL, Borczuk AC, Kitsis RN, Sonnenblick EH. 1998. beta-adrenergic stimulation causes cardiocyte apoptosis: influence of tachycardia and hypertrophy. Am. J. Physiol. 275:H961–8.

Singh K, Xiao L, Remondino A, Sawyer DB, Colucci WS. 2001. Adrenergic regulation of cardiac myocyte apoptosis. J. Cell. Physiol. 189:257–65.

Squires CE, Escobar GP, Payne JF, Leonardi RA, Goshorn DK, Sheats NJ, Mains IM, Mingoia JT, Flack EC, Lindsey ML. 2005. Altered fibroblast function following myocardial infarction. J. Mol. Cell. Cardiol. 39:699–707.

Stancovski I, Baltimore D. 1997. NF-κB Activation: The IκB Kinase Revealed? Cell 91:299–302.

Stewart GS, Last JI, Stankovic T, Haites N, Kidd AM, Byrd PJ, Taylor AM. 2001. Residual ataxia telangiectasia mutated protein function in cells from ataxia telangiectasia patients, with 5762ins137 and 7271T-->G mutations, showing a less severe phenotype. J. Biol. Chem. 276:30133–41.

Stracker TH, Roig I, Knobel PA, Marjanović M. 2013. The ATM signaling network in development and disease. Front. Genet. 4.

Su Y, Swift M. 2000. Mortality rates among carriers of ataxia-telangiectasia mutant alleles. Ann. Intern. Med. 133:770–8.

Sutherland C, Leighton IA, Cohen P. 1993. Inactivation of glycogen synthase kinase-3 beta by phosphorylation: new kinase connections in insulin and growth-factor signalling. Biochem. J. 296:15–19.

Sutton MGSJ, Sharpe N. 2000. Left Ventricular Remodeling After Myocardial Infarction□: Pathophysiology and Therapy. Circulation 101:2981–8.

Tavani F, Zimmerman RA, Berry GT, Sullivan K, Gatti R, Bingham P. 2003. Ataxia-telangiectasia: the pattern of cerebellar atrophy on MRI. Neuroradiology 45:315–9.

Termeer C, Benedix F, Sleeman J, Fieber C, Voith U, Ahrens T, Miyake K, Freudenberg M, Galanos C, Simon JC. 2002. Oligosaccharides of Hyaluronan Activate Dendritic Cells via Toll-like Receptor 4. J. Exp. Med. 195:99–111.

Timmers L, Pasterkamp G, de Hoog VC, Arslan F, Appelman Y, de Kleijn DPV. 2012. The innate immune response in reperfused myocardium. Cardiovasc. Res. 94:276–83.

Tomasek JJ, Gabbiani G, Hinz B, Chaponnier C, Brown RA. 2002. Myofibroblasts and mechano-regulation of connective tissue remodelling. Nat. Rev. Mol. Cell Biol. 3:349–63.

Tonnesen MG, Feng X, Clark RA. 2000. Angiogenesis in wound healing. J Investig Dermatol Symp Proc. 5:40–6.

Turner NA, Porter KE. 2013. Function and fate of myofibroblasts after myocardial infarction. Fibrogenesis Tissue Repair 6:5.

Turpie AG. 2006. Burden of disease: medical and economic impact of acute coronary syndromes. Am. J. Manag. Care 12:S430–4.

Valentin-Vega YA, Maclean KH, Tait-Mulder J, Milasta S, Steeves M, Dorsey FC, Cleveland JL, Green DR, Kastan MB. 2012. Mitochondrial dysfunction in ataxia-telangiectasia. Blood 119:1490–500.

Villarreal F, Omens J, Dillmann W, Risteli J, Nguyen J, Covell J. 2004. Early degradation and serum appearance of type I collagen fragments after myocardial infarction. J. Mol. Cell. Cardiol. 36:597–601.

Virag JI, Murry CE. 2003. Myofibroblast and endothelial cell proliferation during murine myocardial infarct repair. Am. J. Pathol. 163:2433–40.

Ward AJ, Olive PL, Burr AH, Rosin MP. 1994. Response of fibroblast cultures from ataxia-telangiectasia patients to reactive oxygen species generated during inflammatory reactions. Environ. Mol. Mutagen. 24:103–11.

Weber KT. 1989. Cardiac Interstitium in Health and Disease□: The Fibrillar Collagen Network. J Am. Coll. Cardiol. 13:1637–52.

White HD, Norris RM, Brown MA, Brandt PW, Whitlock RM, Wild CJ. 1987. Left ventricular end-systolic volume as the major determinant of survival after recovery from myocardial infarction. Circulation 76:44–51.

Williams MR, Azcutia V, Newton G, Alcaide P, Luscinskas FW. 2011. Emerging mechanisms of neutrophil recruitment across endothelium. Trends Immunol. 32:461–9.

Wohlgemuth SE, Julian D, Akin DE, Fried J, Toscano K, Leeuwenburgh C, Dunn WA. 2007. Autophagy in the heart and liver during normal aging and calorie restriction. Rejuvenation Res. 10:281–92.

Yi M, Rosin MP, Anderson CK. 1990. Response of fibroblast cultures from ataxia-telangiectasia patients to oxidative stress. Cancer Lett. 54:43–50.

Zhan H, Suzuki T, Aizawa K, Miyagawa K, Nagai R. 2010. Ataxia telangiectasia mutated (ATM)-mediated DNA damage response in oxidative stress-induced vascular endothelial cell senescence. J. Biol. Chem. 285:29662–70.

Zhao W, Lu L, Chen SS, Sun Y. 2004. Temporal and spatial characteristics of apoptosis in the infarcted rat heart. Biochem. Biophys. Res. Commun. 325:605–11.

VITA

LAURA LYNN DANIEL

Education:

Ph.D., Biomedical Sciences, James H. Quillen College of Medicine, East Tennessee State University, Johnson City, Tennessee, 2015

B.S Biology, University of Tennessee at Martin, Martin, TN, 2005

Professional Experience:

Graduate Assistant, James H. Quillen College of Medicine, East Tennessee State University, Department of Biomedical Sciences August 2010 – May 2015

Environmental Technologist, Laboratory Management Partners (LMP), Memphis, TN, March 2009 - June 2010

Technologist – Toxicology extractions and confirmations, LabCorp, Southaven, MS, October 2006 – February 2009

Publications:

Daniel LL, Daniels CR, Harirforoosh S, Singh M, and Singh K. Deficiency of Ataxia Telangiectasia Mutated Kinase Decreases Inflammatory Response in the Heart Following Myocardial Infarction. J Am Heart Assoc. 2014 Dec; 3(6)e001286. Published with an editorial; Ataxia-telangiectasia mutated kinase: a potential new target for suppressing inflammation in heart failure? J Am Heart Assoc. 2014 Dec;3(6):e001591

Foster CR, **Daniel LL**, Daniels CR, Dalal S, Singh M, and Singh K. Deficiency of ataxia telangiectasia mutated kinase modulates cardiac remodeling following myocardial infarction: involvement in fibrosis and apoptosis. PLoS One. 2013 Dec;16;8(12)e83513

Foster CR, Zha Q, **Daniel LL**, Singh M, Singh K. Lack of ataxia telangiectasia mutated kinase induces structural and functional changes in the heart: role in β-adrenergic receptor-stimulated apoptosis. Exp Physiol. 2012 Apr;97(4):506-515. Published with a view point; Ataxia telangiectasia mutated kinase in the heart: currency for myocyte apoptosis. Exp Physiol. 2012 Apr; 97(4):476.

Daniel LL, Joyner WL, Singh M, and Singh K. Aging and Heart Failure: Mechanisms and Management. By Bodh I. Jugdutt. *Chapter 27*: Integrins:

Implications for Aging in heart failure Therapy. Springer Publishing Co. 2014; 401-410.

Honors:

Appalachian Research Forum, Poster presentation 2012. **1st place** poster in graduate research category

Summa Cum Laude graduate, University of Tennessee at Martin, 2006

Dean's List 2001-2005, University of Tennessee at Martin